NASA CR-132747

MATERIALS SCIENCES CORPORATION

(MSC/TFR/7501)

FATIGUE OF NOTCHED FIBER COMPOSITE LAMINATES
PART I: ANALYTICAL MODEL

by

P. V. McLaughlin, Jr., S. V. Kulkarni,
S. N. Huang, and B. Walter Rosen

March, 1975

Prepared under Contract No. NAS1-12967

for

NATIONAL AERONAUTICS AND SPACE ADMINISTRATION

FATIGUE OF NOTCHED FIBER COMPOSITE LAMINATES
PART I: ANALYTICAL MODEL

By P. V. McLaughlin, Jr., S. V. Kulkarni,
S. N. Huang, and B. Walter Rosen

Prepared under Contract No. NAS1 - 12967 by

MATERIALS SCIENCES CORPORATION
Blue Bell, PA. 19422

for

NATIONAL AERONAUTICS AND SPACE ADMINISTRATION

TABLE OF CONTENTS

	Page
LIST OF SYMBOLS	v
SUMMARY	1
INTRODUCTION	3
ANALYTICAL AND EXPERIMENTAL OBSERVATIONS	6
STATIC FAILURE MODEL	8
Axial and Transverse Crack Propagation Model	9
Analysis procedure and typical results for axial and transverse cracking	11
Discussion	12
Off-Axis Crack Propagation Model	13
Notch inclination and combined stress effects	14
Procedure for off-axis failure analysis	15
Static Failure Analysis Procedure	16
Discussion	16
FATIGUE MODEL	18
Notch Region Material Degradation	19
Axial/Transverse Fatigue Crack Modes	21
Off-Axis Fatigue Crack Mode	23
Stresses in the Notch Region	24
Laminate stress state near notch	24
Combined stress effects on lamina fatigue	25
Fatigue Analysis Procedure	26
Nonuniform Fatigue Loading	28
CONCLUDING REMARKS	30
FIGURES	33
APPENDIX A - GOVERNING EQUATIONS FOR FAILURE MODEL	47
APPENDIX B - COMBINED STRESS EFFECTS ON LAMINATE STATIC AXIAL CRACKING	60
APPENDIX C - STATIC FAILURE ANALYSIS EXAMPLES	62
APPENDIX D - NOTCH ROOT STRESS STATE CONSIDERATIONS	74
APPENDIX E - OFF-AXIS LAMINATE COMBINED STRESS STATE IN FATIGUE	81
APPENDIX F - INTERACTION EFFECTS OF LAYER STRESS COMPONENTS IN FATIGUE	83
APPENDIX G - FATIGUE FAILURE ANALYSIS EXAMPLES	88
REFERENCES	110

SYMBOLS

a	- half length of notch
c	- superscript indicating compressive failure stress
E_x	- tensile modulus of laminate
E_{11}, E_{22}	- tensile moduli of lamina in fiber and transverse directions, respectively
G_{xy}	- axial shear modulus of laminate in xy coordinate system
$G_{x'y'}$	- axial shear modulus of laminate in x'y' off-axis coordinate system
G_{12}	- axial shear modulus of lamina
H	- laminate thickness
h	- lamina thickness
k	- empirical constant used in Equations (3) and (4)
m	- size of overstressed intact region
N	- number of cycles
N_f	- fatigue lifetime
n	- superscript indicating notch stress
R	- $\sigma_{min}/\sigma_{max}$, stress ratio
S	- cyclic maximum stress/static failure strength
S_{12}	- cyclic maximum shear stress/static failure shear strength
S_{12}^e	- effective S_{12} due to combined stress state
t	- superscript indicating tensile failure stress
u_0, U_0	- non-dimensional and dimensional axial displacement inside the core region, respectively
u_1, U_1	- non-dimensional and dimensional axial displacement in the overstressed region, respectively
u_2, U_2	- non-dimensional and dimensional axial displacement in the average uniformly stressed region, respectively

x	- direction of load in laminate
y	- transverse direction to the load
x',y'	- direction of and transverse direction to an off-axis crack in a laminate
α	- non-dimensional axial "crack" length (including plastic zone), inelastic length
γ_{ult}	- axial shear failure strain
ζ	- non-dimensional axial crack length
θ	- lamina orientation
σ	- applied gross laminate stress in x direction
σ_A	- applied laminate stress at which axial crack propagates to infinity
σ_A°	- initial static σ_A
$\sigma_{A'}$	- axial tensile strength in x'y' coordinate system
σ_C	- applied laminate stress at which axial crack is initiated at notch tip
σ_M	- applied laminate stress when material adjacent to the notch reaches σ_{SCFM}
σ_{max}	- maximum tensile cyclic stress
σ_{min}	- minimum tensile cyclic stress
σ_r	- residual strength
σ_{SCFM}	- maximum composite overstress in material adjacent to notch
σ_T	- applied laminate stress at which transverse crack propagates from notch tip
σ_T°	- initial static σ_T
σ_{xy}	- laminate axial shear stress
σ_x^t	- unnotched laminate tensile strength
σ_x^c	- unnotched laminate compressive strength

$\sigma_{x'}, \sigma_{y'}, \sigma_{x'y'}$ - laminate stress components in x'y' coordinate system

σ_Y - applied stress at which axial plasticity is initiated at the notch tip

$\sigma^c_{y'}, \sigma^t_{y'}$ - compressive and tensile strengths of the unnotched laminate in y' direction, respectively

$\sigma^d_{y'}$, $\sigma^p_{y'}$ - $1/2(\sigma^c_{y'} - \sigma^t_{y'})$ and $1/2(\sigma^c_{y'} + \sigma^t_{y'})$, respectively

σ^n - notch root tensile stress in xy coordinate system due to σ_{max}

$\sigma_{11}, \sigma_{22}, \sigma_{12}$ - stress components in lamina

σ_θ - laminate strength for off-axis crack failure mode

τ_{max} - maximum cyclic shear stress level

τ° - shear yield stress and strength of the unnotched laminate in the xy coordinate system

τ°_{12} - layer axial static shear strength

$\tau^{\circ\prime}$ - shear yield stress and strength of the unnotched laminate in the x'y' coordinate system

$\tau^{\circ\prime}_e$ - effective laminate shear yield stress and strength due to the combined stress state in the x'y' coordinate system

τ^n - notch root shear stress in xy coordinate system due to σ_{max}

$\tau^{n'}$ - notch root shear stress in x'y' coordinate system due to $\sigma_{x'}$ only

$\tau^{n'}_e$ - effective laminate notch shear stress

$\tau^{\prime d}$ - reduced shear strength at notch root used in Eq. (1)

$\tau^{\prime p}$ - increased notch shear stress used in Eq. (5)

$\tau^\circ_{\sigma max}$ - laminate axial shear strength which correlates with axial crack propagation failure at σ_{max} in a notched laminate

FATIGUE OF NOTCHED FIBER COMPOSITE LAMINATES
PART I: ANALYTICAL MODEL

By P. V. McLaughlin, Jr., S. V. Kulkarni,
S. N. Huang and B. Walter Rosen
Materials Sciences Corporation

SUMMARY

This report describes a semi-empirical, deterministic analysis for prediction and correlation of fatigue crack growth, residual strength, and fatigue lifetime for fiber composite laminates containing notches (holes). The failure model used for the analysis is based upon composite heterogeneous behavior and experimentally observed failure modes under both static and fatigue loading. The analysis is consistent with the wearout philosophy.

During fatigue loading of a notched laminate, high axial shear stresses exist near the notch root. These high shear stresses will cause the material in the vicinity of the notch to be degraded much more rapidly than throughout the rest of the laminate. As the properties of laminae change in the notch region due to cyclic loading, the strength of the notched laminate will alter. Residual strength of a notched composite is therefore treated as a static failure utilizing fatigue-degraded lamina properties in the notch region. A fatigue failure occurs when the residual strength of the notched composite falls to the level of applied maximum cyclic stress.

Laminate axial shear behavior governs notched composite fatigue behavior. The fatigue analysis method therefore consists of the following:

(1) Estimating the notch root stress state for a given laminate tensile stress.
(2) Performing a laminate analysis to obtain lamina stresses.
(3) Computing fatigue-induced material property changes in each layer.

(4) Predicting new laminate properties in axial shear.

(5) Calculating the changed residual strength properties of the notched composite.

The process is repeated as necessary utilizing convenient increments of number of cycles.

The modes of failure treated by the present analysis are:

(1) Axial cracking in the load direction.

(2) Transverse cracking across the specimen.

(3) Cracking at an angle to the load axis along a fiber direction.

Axial cracking and transverse cracking failure modes are treated together in the analysis. Cracking off-axis is handled by making a modification to the axial cracking analysis.

The analysis predicts notched laminate failure from unidirectional material fatigue properties using constant strain laminate analysis techniques. For multidirectional laminates, it is necessary to know lamina fatigue behavior under axial normal stress, transverse normal stress and axial shear stress.

Examples of the analysis method are given for [0] and $[0_2/\pm 45]$ boron/epoxy laminates with varying notch sizes. Results show that static failure and fatigue failure modes need not be the same. This fact suggests that the often-made assumption of one-to-one correlation between static and fatigue failure distributions should be critically reexamined.

The present model has not been experimentally verified for fatigue loading, although good correlation has been obtained for static failure. Also, the present model does not include the effects of stacking sequence or interlaminar debonding. Further work should concentrate in these areas.

INTRODUCTION

The utilization of any material for primary aerospace structural applications requires adequate safety margins under all anticipated environments and an adequate structural lifetime. This requires a sound understanding of the fracture and fatigue behavior of the structural material. Over the years, a great body of empirical data and analytical techniques have been generated for metallic alloys. In contrast, relatively little is known about the fatigue behavior and residual strengths of composite materials, particularly when the material has a notch or other source of stress concentration. Furthermore, for any composite material (e.g., boron/epoxy), there are many aspects of the internal material geometry which can be varied, such as amounts of fibers oriented in different directions. Thus, the development of a broad experimental data base to completely characterize one material system is a costly undertaking. For this reason, an analytical model of the fatigue behavior of composite laminates is desirable for the design engineer.

Until recently, fatigue analysis took the form of empirical generation of standard S - N curves and perhaps residual stress information for specific materials and particular composite layups. An important addition to fatigue thinking was made with the conception of a "wearout" philosophy of composite material degradation under cyclic loading (Reference 1). This philosophy treats fatigue damage as the growth of preexisting flaws or discontinuities in a material. As these flaws are made larger due to the action of cyclic stresses, there is a generally greater tendency to failure and a lower residual strength. When residual strength drops to the level of maximum cyclic stress, fatigue failure ensues. If a model can be developed for the growth of these flaws and their effect upon static strength, then residual strength and lifetime of materials can be predicted.

This report presents a semi-empirical analysis for prediction

and correlation of fatigue crack growth, residual strength, and fatigue lifetime of fiber composite laminates containing notches. The analysis utilizes a material model which treats physically realistic failure modes. The approach is consistent with the wearout fatigue philosophy, in that the layered material properties degrade with cyclic loading and cause reduced residual strength and eventual fatigue failure of a notched composite material. A major difference between the current analysis and that of Reference 1 is the mechanics of crack propagation employed. Reference 1 treats crack propagation in composite materials using concepts of classical fracture mechanics which have been developed for homogeneous materials. The present work, on the other hand, incorporates the main physical characteristics and failure mechanisms of fiber composite materials which have been observed during static and fatigue tests (see, for example, Reference 2). This topic is given further discussion in the next section.

The philosophy behind the present fatigue analysis is that cyclic loading of a notched composite causes localized property degradation in the vicinity of the notch. This combination of reduced properties and stress concentrations due to static loading causes localized damage in the vicinity of the notch. This damage results in a redistribution of local stresses and hence a change in strength. When these fatigue-induced changes cause a decrease in residual strength with number of cycles N, the fatigue lifetime N_f is the number of cycles at which the residual strength has reduced to the applied stress. Implicit in this philosophy is the notion that a static failure model will always be able to determine strength and stress-strain behavior if the instantaneous properties of the material are known at any given N. Therefore, the two main ingredients in this fatigue analysis model are a valid static failure model plus a method for determining the degradation of material properties and growth of flaws with number of cycles. The approaches taken to these two topics under the present research program are described

following a discussion of analytical and experimental considerations essential to the fatigue analysis model. The body of this report contains material which is judged essential to understanding the analysis. Mathematical details are presented in appendices.

ANALYTICAL AND EXPERIMENTAL OBSERVATIONS

The behavior of notched fiber composite laminates under static and fatigue loading exhibits many features which are not observed for homogeneous materials such as metals (Ref. 2, 5, 6). For example:

(i) Frequently, the direction of crack growth in a fiber composite laminate is not perpendicular to the applied load, even for perpendicular slit notches.

(ii) Static failure modes may be completely different from the mode of failure observed during or after a program of cyclic loading.

(iii) The residual tensile static strength of certain notched composite laminates subjected to fatigue loading can be greater than the initial static strength of those laminates.

Due to these observed inconsistencies with homogeneous material fatigue and fracture mechanics theories, it is not expected that classical theories will have general application to composite laminates on the macroscale. Limited success has been obtained in applying classical fracture mechanics to composites when the mode of failure is a collinear crack growth from a preexisting notch (Reference 3). Unfortunately, composites exhibit several types of non-collinear crack growth which cannot be treated by classical means. Several attempts have been made to utilize classical fracture mechanics by treating fiber and matrix as distinct homogeneous materials and analyzing details of stress and strain around cracks or flaws in the separate phases (e.g., Reference 4). While these studies provide insight into the mechanisms of crack growth in heterogeneous materials, they are not well developed and appear to be too complicated for inclusion in an overall analysis of composite laminate fatigue behavior.

Tests of many fiber composite material systems (e.g., see

References 2 and 5) have shown that there are primarily three modes of failure in a notched fiber composite laminate under tension. All three failure modes have been experimentally observed in both static and fatigue tests. The failure modes are illustrated in Figure 1 which contains photographs from Reference 2 of failed boron/epoxy laminates that have undergone fatigue cycling. An axial crack propagation mode (Figure 1a) occurs when the central portion of the laminate near the notch pulls out of the remaining material due to high shear stresses in the notch vicinity. The axial crack propagates to the grips, ultimately causing specimen failure. A transverse or collinear crack propagation mode is shown in Figure 1b. Here, material immediately adjacent to the notch has been overstressed to the point where an unstable crack continues to grow perpendicular to the load direction. If there are fiber families oriented at an angle to the direction of loading (Figure 1c), a crack may initiate and extend parallel to these off-axis fibers, resulting in an off-axis crack propagation failure mode. As shown in Figure 1d, failure can occur by several of these modes in the same laminate.

In all failures, it has been observed that cracks propagate either along a fiber direction or transversely across the specimen perpendicular to the direction of tensile loading. The mode of failure can be different for fatigue or static loading of the same laminate. In addition, different notch sizes can trigger different failure modes in the same laminate. Other factors which can affect failure mode are ply orientation and constituent material properties.

Any fatigue failure model of a fiber composite laminate must exhibit the above described failure modes, preferably through a built-in recognition of the key aspects of fiber composite material heterogeneity. The model described in this report has attempted to do this in a way which is sufficiently general to apply to all fiber composite laminates.

STATIC FAILURE MODEL

The primary modes of both static and fatigue failure of notched composites are:

(a) Propagation of a crack parallel to one of the fiber directions (either axial or off-axis).

(b) Propagation of a crack transversely across the specimen normal to the direction of applied tensile stress.

The basic static model for axial and transverse failure of notched composites was developed in Reference 6. Modifications to the basic model and addition of off-axis cracking was performed during the present program. Because of its importance to the fatigue analysis, a discussion of the static failure model and examples for all modes of failure will be given here.

The basic model for static failure of notched composites treats axial and transverse crack propagation. Axial failure is caused by the tendency of the material separated by the notch to "pull out". This causes high shear stresses in the direction of load and may result in propagation of an axial crack. Transverse crack propagation is caused by the stress concentration effect of the notch. Material adjacent to the notch may be overstressed to failure, causing a crack to run perpendicular to the load.

When a crack propagates at an angle between 0° and 90° to the load direction, it does so under the action of combined shear and normal stresses along the crack. The off-axis phenomenon has been judged to be physically similar to axial crack propagation, but with the added complexity of a combined stress state. The off-axis crack propagation model has, therefore, been developed from the axial crack propagation model by the inclusion of combined stress effects.

The analysis uses the same model to treat axial and transverse crack propagation, and a modified model to treat off-axis crack propagation. In the following subsections, the axial/transverse

failure model and the off-axis failure modification are summarized. Mathematical details can be found in Appendix D.

Axial and Transverse Crack Propagation Model

The model for static failure of a notched composite laminate is illustrated in Figure 2, and coordinate system conventions are shown in Figure 3. The laminate is assumed (Figure 2) to be under a tensile load σ_x in the x direction. A notch of width 2a is centered in the specimen at x = 0. The coordinate y lies in the laminate plane transverse to the direction of applied tensile load. Reference 2 has shown that notch shape is not as important to failure as the size (width) of the notch. Hence, a slit, circular hole, or square hole of width 2a will all be modeled in a y direction discontinuity in the laminate of 2a. Unless specifically noted to the contrary, the word "notch" will apply to any through-the-thickness hole of any shape.

In the central core region (Figure 2), the core wants to "pull out" from the notch area due to the applied tensile loading. This core, however, is restrained by shear stresses between the core and the adjacent intact material. These shear stresses generally result in a region of high shear strain parallel to the loading direction along the 0° fibers. Immediately adjacent to the notch core, there is a region of width m which is overstressed due to presence of the notch. It is assumed that this region bears the full stress concentration effects. Everywhere outside the core and overstressed regions, the laminate is uniformly strained. This uniformly strained region is called "average material", because there are no overall average stress or strain gradients and the laminate is assumed to behave as a homogeneous anisotropic material.

Shear strain due to core pullout is assumed to be effective over a region three times the size of the overstressed fiber regions. This shear strain region extends a distance m into the

region of uniformly strained average material which lies adjacent to the overstressed region. The total thickness of the laminate is H, and the thickness of each layer in the laminate is h.

Due to the high axial shear strain region near the notch, description of the behavior of the laminate in axial shear, σ_{xy}, is very important. The shear stress-strain curve can vary anywhere from nearly linearly elastic, as would occur for a $[0_i/\pm45_j/90_k]$ laminate to one which is highly nonlinear, such as would occur for a [0] laminate. The axial shear stress-strain curve is therefore approximated as linear elastic-perfectly plastic (Figure 4). The shear yield stress is assumed equal to the shear strength, $\tau°$. The axial shear modulus, G_{xy}, is chosen to obtain the best fit to the actual laminate shear stress-strain curve.

As the gross laminate tensile stress σ is increased, the shear stresses at the notch tip will increase. When the yield stress in shear $\tau°$ is reached at the notch tip, continued loading will cause an inelastic region to form in the axial direction. As the axial shear strain at the notch tip continues to increase with increased stress, the axial shear failure strain γ_{ult} will be exceeded and a crack will begin to grow in the axial or x direction. When this crack grows very large (mathematically, to infinity)the notched laminate is considered to have failed in an axial crack propagation mode. If, however, material in the overstressed region adjacent to the notch is stressed past the tensile strength of the unnotched laminate, a crack will propagate in the transverse or y direction. In this latter case, the laminate is considered to have failed in a transverse or collinear crack propagation mode.

Appendix A fully describes the static failure model and resulting stress and deformation analysis for axial and transverse crack propagation modes. It is, in essence, an inelastic shear lag analysis with the axial shear behavior of the laminate playing

an extremely important role.

In the analysis, ζ is a nondimensional axial crack half-length extending from the notch tip (x = 0) to the bottom of the plastic zone. The non-dimensional distance from the notch to the beginning of the elastic zone is α, and includes axial crack and plastic zones (see Appendix A for details of the non-dimensionalization). For this reason, α is called the "inelastic length" and is a good measure of the extent of damage in the axial direction from the notch tip.

The analysis has the capability of computing both the inelastic length and maximum overstress in material adjacent to the notch for a given applied laminate tensile stress so that tendency to axial or transverse crack propagation modes can be monitored. Typical results of the analysis and a demonstration of the procedure to be followed in computing axial and transverse failure stresses are presented below.

Analysis procedure and typical results for axial and transverse cracking.- Typical results of the static failure analysis for a notched laminate are shown in Figure 5. Figure 5a illustrates the growth of the damaged region with increased applied tensile stress σ. Until the yield stress of the laminate in shear is exceeded at the notch tip, α will be zero. When the yield shear stress τ° is exceeded at the notch tip, the inelastic length α will begin to grow. The applied stress at which plasticity is initiated at the notch tip is called σ_y. At some higher stress level σ_c the shear strain in the laminate at the notch tip will exceed γ_{ult}, the laminate shear failure strain. An axial crack will then begin to grow from the notch tip. As loading progresses, the damage zone will increase without bound as the applied stress assymptotically approaches a level σ_A. This stress represents the failure stress of the notched composite in the axial crack propagation failure mode.

As stressing in the composite increases and as the inelastic length α grows, the region adjacent to the axial crack is overstressed by varying degrees (Figure 5b). As the applied stress is increased, it is possible that the maximum overstress in the adjacent material, σ_{SCFM}, will increase to the point where it exceeds the unnotched laminate strength, σ_x^t. In this case, transverse crack propagation ensues. The applied laminate stress at which transverse cracking occurs is called σ_T. It is also possible that, as the axial crack grows, a blunting of the stress concentration effects of the notch will occur. This could cause a decrease in stress in the adjacent material before it reaches failure levels, and remove any possibility of transverse crack propagation occurring.

The analysis is capable of computing both σ_A and σ_T assuming that neither failure mode has yet occurred. If the computed value of σ_A is lower than σ_T, axial cracking is the predicted mode of failure. In this case, σ_A is the notched composite failure stress. If, on the other hand, the computed σ_T is lower than σ_A, transverse cracking is the predicted mode of failure. The failure stress of the notched composite in this case is σ_T.

Discussion.- Two key ingredients to the failure predictions are the static stress-strain behavior in axial shear of the laminate and the unnotched axial tensile behavior of the laminate. These quantities can either be determined from laminate experimental data or from state-of-the-art laminate analysis techniques provided that layer data is available. In addition, the size of the shear transfer zone next to the notch, 3m, and the size of the stress concentration region, m, are of prime importance to the analysis. The basis for their selection is discussed in the following paragraphs.

The size of the shear transfer zone adjacent to the stress concentration region was chosen to be three times the size of the stress concentration region based on physical reasoning. There

the axial displacements inside the core region (U_0), in the overstressed region (U_1), and in the flanking uniformly strained material ($U_2 = \sigma/E_x$) are generally different from one another (see Figure 2). Shear stresses will therefore be developed between the core region and stress concentration region, and between the stress concentration region and the uniformly stressed regions. If the differences in displacements $U_0 - U_1$ and $U_1 - U_2$ are of the same order of magnitude, it is likely that shear strains will extend an equal distance into the core and into the average material. The choice of stress concentration region size m for these shear strain penetration distances was based on the stress concentration region size itself being a measure of stress perturbations near the notch.

The size of the overstressed region, m, is a parameter which must be experimentally determined for a given laminate. It is calculated from the static tensile strength of the laminate having a notch of a given size. The parameter m is chosen such that the analytical prediction for notched laminate strength and the mode of failure thereof match experimental data. Once the value m has been determined for one notch size in a particular laminate, it can be computed for any notch size from the equation $m/m_o=(a/a_o)^{1/2}$ where m_o is the experimentally determined value of m from tensile strength data on a laminate with notch width $2a_o$. This square root relationship is an experimentally determined correlation from tests on boron/epoxy laminates, and is described in Reference 6.

Off-Axis Crack Propagation Model

The preceding subsection has treated failure of notched laminates when the mode of cracking is either axial along the 0° fiber direction, or transverse to the specimen normal to the direction of loading. For some laminates, such as a [±45] boron/epoxy laminate, the mode of fatigue cracking is off-axis along a fiber direction (in this case, the ±45 degree direction). For this mode of failure, the preceding model and analysis are not

directly applicable without modification. This subsection describes modifications to the original model which were made to allow analysis of off-axis cracking.

Notch inclination and combined stress effects.- Figure 6 illustrates the stress state around a notch which is tending to develop a crack along the $\pm\theta$ fibers. Along the load axis the gross laminate stress state is axial tension. However, the crack is not growing in the direction of load. Suppose material axes x' and y' are selected in the θ direction (Figure 6). The crack will be growing in the direction of the x' axis tensile stress $\sigma_{x'}$. Due to the rotation of axes, the tensile stress $\sigma_{x'}$ will not be the same as the x direction stress σ. In addition, there will generally be substantial axial shear and transverse tensile stresses in the x'y' coordinate system. Also, the notch is now inclined at an angle θ to its original position. The following paragraphs describe how notch inclination and combined stress states are analyzed so that off-axis cracking can be handled directly by the original model referred to the x'y' coordinate system.

It has been shown (Reference 2) that the shape of the notch (slit, rectangular, circular, etc.) in a laminate does not greatly affect composite failure. The width of a notch perpendicular to the direction of loading is the only notch dimension which is of importance. Therefore, the slit notch configuration shown in the xy and x'y' coordinate systems (Figures 6a and b, respectively), can be treated for analysis purposes as shown in Figure 6c. In this case, the original notch has been replaced by an equivalent notch of size $2a \cos\theta$ in the y' direction. (Note that no change need be made for a circular hole, and that an increase or decrease in equivalent notch size may be necessary for a rectangular hole.)

Performing an exact analysis of axial cracking in the presence of a combined stress state is extremely difficult. Therefore,

combined stress effects are taken into account in an approximate fashion. Laminate gross transverse tension $\sigma_{y'}$ and axial shear $\sigma_{x'y'}$ are superimposed on the axial shear stress at the notch root which would be computed from the axial crack analysis due to only $\sigma_{x'}$ (see Figure 7). The main effect of this superposition will be to increase the likelihood of x'y' axial shear failure. Throughout the loading process, the axial shear stress $\sigma_{x'y'}$ reduces the stress required from the shear-lag analysis to cause axial cracking. The transverse normal stress $\sigma_{y'}$ is assumed to further reduce the shear strength.

The assumed effect of axial shear and transverse stresses is, therefore, to change the laminate axial shear strength inputted into the standard tensile strength analysis. One method of doing this is presented in Appendix B. The unnotched laminate shear strength $\tau^{\circ'}$ in the x'y' coordinate system is assumed to be directly reduced by applied shear $\sigma_{x'y'}$. A quadratic interaction is chosen for the reduction in $\tau^{\circ'}$ due to $\sigma_{y'}$. The result is a reduced, or effective, unnotched laminate shear strength $\tau_e^{\circ'}$ which depends upon the level of applied stress $\sigma_{x'}$ through $\sigma_{x'y'}$ and $\sigma_{y'}$. Figure 8 shows a typical variation in $\tau_e^{\circ'}$ with $\sigma_{x'}$.

Procedure for off-axis failure analysis.- If the effective shear strength were a constant, it could be used directly in the failure model to compute $\sigma_{A'}$, the value of $\sigma_{x'}$ which causes failure. The applied failure stress σ_θ required for off-axis failure could then be obtained from stress transformation equations with $\sigma_{x'} = \sigma_{A'}$ and the corresponding values of $\sigma_{y'}$ and $\sigma_{x'y'}$ at failure. However, $\tau_e^{\circ'}$ varies with applied load and a different procedure must be adopted.

First the x' crack failure stress $\sigma_{A'}$ is computed from the original model for a range of effective shear strength $\tau_e^{\circ'}$ which goes from near zero to $\tau^{\circ'}$ (the x' direction unnotched laminate shear strength). From this data, a curve of $\sigma_{A'}$ vs. $\tau_e^{\circ'}$ can be constructed as shown in Figure 8. Next, the variation in $\tau_e^{\circ'}$ as

a function of $\sigma_{x'}$, is computed from the Appendix B equations. This information is plotted on the same graph as the $\sigma_{A'}$ vs. $\tau_e°'$ curve in Figure 8 with $\sigma_{A'}$ and $\sigma_{x'}$ axes coincident. The intersection of the two curves defines both $\tau_e°'$ and the failure stress $\sigma_{A'}$.

Once $\sigma_{A'}$ has been determined, the corresponding stress state $\sigma_{x''}$, $\sigma_{y''}$, $\sigma_{x'y'}$ at failure is known. The stress transformation equations are then used to find the corresponding tensile failure stress σ_θ in the original xy coordinate system.

Static Failure Analysis Procedure

The static failure analysis procedure for notched composites which has been developed utilizing the axial/transverse model and the off-axis model is as follows:

1. The axial/transverse failure model is exercised to compute the laminate stresses causing axial crack failure (σ_A) and transverse crack failrue (σ_T).
2. The off-axis model is exercised to compute the laminate stress σ_θ which causes failure due to a crack running along θ-direction fibers.
3. The failure stresses σ_A, σ_T, and σ_θ are compared. The lowest is the predicted failure stress and represents the dominant failure mode.

Examples of the static failure analysis procedure are given in Appendix C for boron/epoxy unidirectional and multidirectional laminates. Figure 9 presents the procedure in more detail.

Discussion

It is noted that axial and off-axis crack propagation failure stresses may not be "ultimate" stress predictions in the usual sense for a uniaxial tensile specimen. This is especially true if there are elaborate load transfer devices at the grip. Once axial cracks have propagated to the grips during a tensile test, the specimen has become two smaller unnotched specimens. If the axial

crack is clean, loading may continue to be applied, and the specimen may fail at a load equal to the unnotched laminate strength times the net cross-sectional area. In a structure, however, large scale axial crack propagation would be considerably more serious because of the lack of crack arresting mechanisms such as the tabs on a tensile specimen and the grips of the testing machine. In addition, structural panels seldom, if ever, experience only uniaxial tensile loading. Under the presence of even small combined stresses, a large axial crack will precipitate catastrophic failure.

FATIGUE MODEL

Fatigue failure in notched fiber composite laminates occurs as a result of growth of cracks along preferred directions in the laminate as load cycling proceeds. This crack growth is influenced by local material properties which change as a result of the repeated loads. When the local material properties and the geometry of the damaged regions are defined after any number of cycles, the residual static strength of the material can be determined from the static model outlined in the preceding section. Thus, as a first requirement, it is necessary to determine the material properties of the laminate in the notch vicinity as functions of the number of load cycles. With this information, the growth of the damaged region can be defined.

The main modes of damage growth as discussed previously are: crack propagation along the load axis, crack propagation transverse to the loading direction, and crack propagation off-axis along a fiber direction. All of these crack and failure mechanisms are determined on a static basis by the analysis presented in the preceding chapter. The main inputs to the static failure analysis are the laminate elastic properties and the laminate failure stresses in axial tension and axial shear. As these properties change with cyclic loading, the static failure behavior of the notched composite will alter. If the properties are known at any given cycle, it is possible to perform a static analysis to determine the static residual strength of the notched composite. If the residual strength so computed is less than the maximum cyclic stress, the fatigue lifetime of the notched composite has been exceeded.

The main ingredients to the fatigue analysis, then, are:

(a) Determination of changes in material properties in the notch region with number of cycles, and

(b) Utilization of these properties in a static failure analysis to predict residual strength.

The approaches taken to these aspects are discussed in the following subsections.

Notch Region Material Degradation

In a notched composite, the main cause of crack growth is the tendency of the notched core region to pull out, generating stress concentrations in adjacent material and very high shear stresses in the axial direction. The remainder of the composite outside the notch region is generally not highly overstressed. Therefore, most fatigue degradation will occur due to shear and tensile stresses in the region immediately surrounding the notch, and the main result will be to alter the axial tensile and axial shear behavior. Specifically, it is anticipated that the axial Young's modulus, E_x, the unnotched tensile strength, σ_x^t, the shear modulus G_{xy}, the axial shear failure strength, $\tau°$, and the laminate axial shear failure strain γ_{ult} will be primary laminate properties which vary under cyclic loading. Due to the high shear stresses near the notch, the shear properties will degrade at a higher rate than the tensile properties. An assumption to this effect is not necessary, however, as will be seen later.

The most direct way to determine laminate tensile and shear behavior under cyclic loads is simply to perform fatigue tests on unnotched specimens. This method, though straightforward, would require a battery of tests for each laminate layup geometry in both the axial xy and off-axis x'y' systems. The results would only be applicable to the specific laminate tested; each new laminate would require its own battery of tests.

Clearly, if a method of generating laminate fatigue behavior from lamina properties can be derived, the number of basic property tests required can be reduced. Lamina properties so-generated would be applicable to laminates with any layup geometry and loaded in any coordinate direction. The method chosen for this analysis utilizes constant strain laminate analysis techniques, and is as follows:

1. The laminate stress state which exists in the notch vicinity (combined axial tension σ^n and axial shear τ^n) is determined. The method for so-doing is outlined later and presented in detail in Appendix D.
2. A constant strain laminate analysis is performed on the laminate under the stresses σ and τ utilizing initial static lamina properties. From this laminate analysis, the axial normal stress, σ_{11}, the axial shear stress σ_{12}, and the transverse normal stress, σ_{22} which exist in each layer of the laminate are computed. These stresses represent the maximum stress due to cyclic loading in each lamina.
3. From data on fatigue behavior of a unidirectional lamina, calculations are made of changes in lamina elastic properties and lamina residual failure stresses after some small increment in cycles. It is assumed that, over the range of cycles considered, the individual stresses in each lamina are not significantly changing. Therefore, the degradation which occurs in that cyclic loading interval does so under a constant stress state. This is an approximation, as it is expected that small changes will occur in each cycle. However, the error in such a "step function" approximation can be minimized by choosing very small increments of N for computation.
4. The changed lamina elastic properties and lamina strengths are re-introduced into the laminate analysis to predict new laminate elastic properties and failure stresses.
5. A second increment of cyclic loading is selected, and lamina stresses which are occurring in the notch vicinity are re-computed using the new lamina and laminate properties. The resulting lamina stresses are used with unidirectional material fatigue behavior to predict further changes in lamina properties which may have occurred over the second increment of cyclic loading. The new lamina properties from the second increment of

cyclic loading are then used in the laminate analysis to generate laminate elastic properties and residual failure strengths in the notch vicinity.

This procedure can be repeated enough times as is necessary to find the residual strength after a required number of cycles, or until the residual strength of the laminate reduces to the stress levels existing at the notch. When the latter occurs, the fatigue lifetime of the material near the notch has been reached.

Figure 10 illustrates the kind of lamina fatigue information which would be necessary to generate laminate fatigue properties in the notch vicinity. Only axial tensile strength, axial shear strength, and axial shear modulus are illustrated, although transverse Young's modulus information may also be necessary. This topic is given further discussion in later subsections of this report.

Figure 11 illustrates typical notch root material fatigue information which would be generated from lamina fatigue behavior using the above laminate analysis approach. Only axial shear information is shown, but axial tensile properties can also be computed. The following subsections outline the use of this information with the static failure model to perform fatigue analysis of notched composite laminates. The axial/transverse fatigue modes are discussed first, and the off-axis mode is discussed second.

Axial/Transverse Fatigue Crack Modes

Prediction of fatigue behavior of a notched laminate utilizes the static failure model in conjunction with laminate property degradation in the notch vicinity. Predicted fatigue behavior includes residual strength, crack propagation, and fatigue failure. Figure 12 illustrates the method for the axial and transverse fatigue crack propagation modes.

At N = 1 cycle, all material properties are at their initial

static values. As cyclic loading progresses, material behavior at the notch will change. These changes with N can be determined directly from lamina properties by methods described in the preceding subsection. The changed material properties after a given N are used as inputs to the static failure analysis model to predict the residual strength of the notched composite and the corresponding failure mode. In Figure 12, static behavior at several decades of N computed from the static failure analysis is shown. In the lower left are curves of axial "crack" length α (inelastic length) versus applied stress σ. The axial mode failure stresses σ_A are the values of σ at which the axial cracks extend to infinity. Overstress in material adjacent to the notch σ_{SCFM} versus the applied stress σ is plotted in the lower right. The transverse mode failure stresses σ_T are the applied stresses at which material adjacent to the notch fails in axial tension.

The resulting initial static failure prediction (N = 1) in Figure 12 is that the notched laminate will fail by transverse crack propagation at a stress $\sigma_r = \sigma_T^\circ$. After ten cycles has occurred, a similar situation is predicted. However, the transverse crack propagation failure strength $\sigma_T^{(1)}$ has now increased and the axial crack mode strength has decreased. The resulting residual failure stress is $\sigma_r = \sigma_T^{(1)}$. At 10^2 and all subsequent cycles, the reverse situation occurs. Either σ_T is greater than σ_A, as occurs for $N = 10^2$, or the maximum overstress in the material adjacent to the notch never exceeds the unnotched laminate strength. Therefore, for $N > 10^2$ cycles, the transverse crack propagation mode never occurs.

The information contained in Figure 12 for residual strength and axial crack growth can be utilized as shown in Figure 13 to predict the residual strength, the fatigue lifetime, and axial fatigue crack growth with N. In Figure 13a, residual strength by both the transverse crack propagation mode and the axial crack propagation mode are plotted versus number of cycles N. As seen in the figure, transverse cracking will occur until approximately 20

cycles at which time axial crack propagation becomes the mode of failure.. The notched composite residual strength is always determined by the lower of the two curves. In this hypothetical example, the composite residual strength increases until N = 20 cycles, then decreases until the strength of the composite becomes equal to the maximum cyclic stress. The composite will fail on the succeeding cycle, N_f, which is the resulting notched composite laminate lifetime.

The static axial crack length curves of Figure 12 may be utilized to calculate the axial fatigue crack growth with number of cycles. Initially, the cyclic stress level is below that for which any axial crack will form. Somewhere between 1 and 10 cycles an axial crack will begin to form. This occurs when the axial crack initiation stress drops to the cyclic stress level. At any given number of cycles, the axial crack length will grow to the length indicated by the intersection of the maximum cyclic stress level with the appropriate crack length curve. The intersection points of the maximum cyclic stress level and crack length curves for different N determine the axial fatigue crack growth curve. Figure 13b shows the results for this example.

Off-Axis Fatigue Crack Mode

In principle, the same procedure used for axial crack propagation can also be applied to the off-axis fatigue crack propagation mode. Special consideration is necessary, however, to treat the combined stress state in the off-axis x'y' coordinate system. A calculation must first be made of the stress state $\sigma_{x'}$, $\sigma_{y'}$, and $\sigma_{x'y'}$ around the notch root which occurs during fatigue loading. This is performed in a manner identical to that used to obtain the stress state around the notch for static loading.

With the combined stress state around the notch computed, it is necessary to determine how the laminate x'y' shear properties change under the combined cyclic loading. To do this, there are

two methods which may be utilized. The first method uses the laminate analysis technique discussed earlier to determine layer stresses which occur due to $\sigma_{x'}$, $\sigma_{y'}$, and $\sigma_{x'y'}$. The second method is completely empirical and utilizes an "effective" shear stress concept where the effects of combined stresses are all lumped into an increased value of shear stress at the notch root. Each method is described in more detail in Appendix E. It is expected that the laminate analysis technique will be the more accurate method. The effective shear stress method is an alternative which can be used if only laminate shear fatigue data is available (instead of lamina date) in the xy coordinate system.

Stresses in the Notch Region

Determination of the stress state in the vicinity of the notch is critical to performing the fatigue analysis. Also, once the lamina stresses have been determined in the notch region, it is necessary to have a method for determining the effects of the resulting combined stress state on lamina material property degradation. Therefore, discussions of these topics are presented here. More detail can be found in Appendices, D and F, respectively.

Laminate stress state near notch.- In a notched laminate, stresses and strains will vary with distance from the notch tip. The largest strains are expected to be at the notch, with decaying values as distance from the notch is increased. It would be beyond the resources of the present program to perform an exact determination of the degradation of laminate properties as a function of coordinates x and y. Therefore, an approximate average stress level in the notch root area is chosen, and it is assumed that all material in the notch vicinity degrades uniformly under this average stress state with fatigue cycling.

For a notched laminate under a cyclic tensile stress σ_{max}, the stress state near the notch will primarily be axial tension

and axial shear. The axial tension is due to the applied σ_{max} plus stress concentration effects, and the axial shear is due to the tendency of the notch core region to pull out. The tensile stress will exist only outside the core region of the notch, while the shear stress will exist inside as well. A close estimate of the tensile stress σ^n can be made by calculating the maximum overstress in the material adjacent to the notch, σ_{SCFM}, using the static failure model. Similarly, the shear stress τ^n can be closely approxmiated by the maximum shear stress in the notch region computed from the static failure model. Appendix D gives other, more approximate, methods for estimating σ^n and τ^n.

Appendix D also presents an approximate analysis of the fatigue failure characteristics in the core region (τ^n only) versus the adjacent overstressed material (τ^n plus σ^n). It is shown there that final fatigue failure predictions should not be significantly affected by ignoring the tensile stress σ^n in the notch region. Although stress states in some laminae can be different when one considers σ^n, the final laminate failure mode and failure stresses are essentially the same. Use is made of this result in examples given in Appendix G.

Combined stress effects on lamina fatigue.- Interaction effects of stress components on static failure have been known and studied for some time (see, for example, References 7 and 8). Experimental and analytical results indicate that the main in-plane stress interactions appear to be between transverse normal stress, σ_{22}, and axial shear stress, σ_{12}. It is reasonable to assume that static interaction results will be qualitatively true for fatigue loading. Under a laminate stress state of shear and/or tension, layer stresses will generally be combined axial normal stress, transverse normal stress, and axial shear stress. In the present formulation, the common assumption of uncoupled fatigue behavior between axial normal stress and the other in-plane stress components (such as assumed in Reference 9) will be maintained. Due, however, to the complexity of the experimental information

which is necessary to fully utilize the Reference 9 theory, a less complicated interaction between σ_{22} and σ_{12} is proposed. Fatigue tests of [90] and [±45] laminates are relatively easy to perform. The [90] tests will give transverse tension fatigue data directly. With some approximations or additional analysis work, [±45] tests can predict the axial shear behavior of a [0] laminate. It is desirable to be able to predict lamina fatigue behavior under combined transverse tension and in-plane shear knowing fatigue behavior either in axial shear only ([±45] laminate in tension), or in transverse tension only.

Appendix F describes the development of such a theory. A quadratic interaction is assumed to occur between transverse tension σ_{22} and axial shear σ_{12}. The physical basis for the interactions is described in the Appendix. If lamina fatigue data is known for either σ_{22} or σ_{12}, the effects of combined stresses can be computed from the theory. If fatigue data exists for both stress states, then σ_{12} - σ_{22} interaction is computed from σ_{22} data when σ_{12} is relatively low, and from σ_{12} data when σ_{22} is relatively low.

In the present work, therefore, axial tensile fatigue stress is assumed to cause changes in only axial Young's modulus and axial tensile strength. Combined effects of transverse tension or axial shear will be felt (through one or both of two quadratic interaction formulae) on axial shear modulus and axial shear strength, and on transverse Young's modulus and transverse tensile strength.

Fatigue Analysis Procedure

This subsection presents the methodological framework which has been developed to analyze the fatigue behavior of notched composite laminates. The analysis procedure utilizes: the static failure model; lamina fatigue properties in axial tension, axial shear, and/or transverse tension; and constant strain laminate

analysis techniques.

A notched laminate with known fiber orientation properties and constituent layer elastic, static failure, and fatigue properties is under cyclic fatigue loading at a maximum applied stress of σ_{max} and a stress ratio R. Initial static laminate properties are known either from experiment or from a laminate analysis prediction based on layer behavior.

The fatigue analysis is begun by first predicting the initial static strength in the axial, transverse, and off-axis propagation modes. The lowest of the three failure stresses will be the static failure strength of the notched laminate. From the static analysis, the average axial tensile and shear stresses σ^n and τ^n at the notch root are computed. The laminate is analyzed with σ^n and τ^n as an applied stress state, and the stresses in each layer are computed. A small increment of cycles is chosen (say, a decade). The maximum cyclic stress under axial tension, σ_{11}, is then used with axial tensile layer fatigue behavior to compute the degraded axial tensile properties of each layer. Next, the combined stress effects of σ_{22} and σ_{12} are determined on the lamina axial shear and transverse tensile properties from lamina fatigue behavior. The resulting degraded properties, which will generally be different for each layer, are then used in the laminate analysis to compute the new laminate elastic and failure properties near the notch. From these revised laminate properties, one can determine the residual strength of the notched laminate following the first increment in cyclic loading.

The laminate analysis is again performed using the new layer properties to determine the stresses in each layer under laminate stresses σ^n and τ^n. Again, the resulting layer stresses are used to determine the degraded properties of each layer after the second cyclic increment. The properties so determined are again used in the laminate analysis to predict laminate elastic and failure properties, and the new laminate properties are in turn used in

the static failure analysis to determine the residual strength. This procedure is repeated until either the residual strength is obtained at a given desired cycle, or until the notched laminate residual strength drops to σ_{max}.

This procedure is followed for the axial and transverse crack propagation modes, and also for the off-axis crack propagation mode. For a given N, the residual strength will be the lowest of σ_A, σ_T, and σ_θ. The fatigue lifetime, N_f, is the number of cycles at which the residual strength of the laminate drops to the maximum cyclic stress, σ_{max}.

A flow chart of this procedure is presented in Figure 14.

Nonuniform Fatigue Loading

The preceding discussions of fatigue analysis have centered upon constant values of maximum stress σ_{max} and stress ratio. The analysis can, however, be utilized to treat fatigue loading spectra which are not constant. It has been shown for metals that loading sequence can affect fatigue results, and it is anticipated that this effect may be even more pronounced for composites. Hence, the usual block loading approximation to a random spectra may not be a good one. However, if the loading spectrum exhibits the proper behavior, it can be broken into a series of small nonuniform block loading sequences as an approximation to the actual spectrum. Provided that a nonuniform fatigue loading spectrum can be approximated by nonuniform block loading, fatigue of a notched composite can be treated using the analysis presented herein by the following methodology:

The block loading spectrum is separated into loading blocks by constant σ_{max} and R. Each loading block of constant fatigue loading parameters is then broken down into subintervals whose sizes are dependent only upon calculation convenience. Fatigue laminate analysis begins on the first loading block exactly as presented in the preceding subsection. At the end of the number of

cycles which correspond to the end of the first loading block, all of the current laminate and layer properties will have been computed. Upon beginning for analysis for the second loading block, the laminate now has the "degraded" properties which resulted from the first loading block. Provided that layer fatigue data is available for the new R, the fatigue analysis can be continued using the new σ_{max}. The analysis can be continued from block to block until the desired residual strength properties have been obtained or until the notched laminate fails by fatigue "wearout". The key to such an analysis is obviously the availability of layer fatigue data for many different values of R and σ_{max} and an analysis technique to estimate the effects of sequential loading on a unidirectional layer.

CONCLUDING REMARKS

This report presents a semi-empirical analysis of fatigue of notched composites. The analysis incorporates heterogeneous material behavior and experimentally observed failure modes for fiber composite laminated materials. The analysis utilizes an approximate "materials engineering" approach along with experimental data.

The overall model is composed of essentially two parts: the overall conceptual framework, and the details of the mathematical description of each physical fatigue phenomenon. Hence, the model is flexible since assumptions that have been made to facilitate analysis can be altered or replaced if desirable or necessary without disturbing the overall framework. The philosophy by which the model has been constructed is "wearout", i.e., repeated loading causes changes in material properties near the notch. These property changes result in altered notched composite residual strengths and eventually cause fatigue failure.

Applications of the analysis presented in Appendix G show the following:

(1) Fatigue cycling can cause an initial increase in residual tensile strength of notched composites. Subsequent cycling may either cause a reversal of this trend and eventual fatigue failure, or it may result in a continued increase in strength and runout. Such behavior varies with notch size and laminate stacking geometry.

(2) Static failure modes may differ from fatigue failure modes in the same notched laminate. Therefore, a material exhibiting higher initial static strength may have a shorter fatigue lifetime, and vice-versa.

The fact that notched composites can have different static and fatigue failure modes is a result of high significance. A common assumption in structural reliability analysis is to assume a one-to-one correlation between static strength distribution and fatigue

strength distribution. A laminate with low static strength is also assumed to have a relatively short fatigue lifetime. The results of the present analysis indicate that in certain cases such an assumption may not be valid. In particular, when the mode of static failure differs from the mode of fatigue failure, a one-to-one correlation will probably not exist. The concept of static proof testing to ensure fatigue lifetime should therefore be critically re-examined.

The static failure model has been substantiated by experiment and analysis performed in References 2 and 6. However, fatigue data does not currently exist which is of the form necessary to corroborate the current fatigue analysis. Therefore, a comprehensive program should be undertaken to verify the applicability of the mathematical model and to correlate it with data from specific notched composite laminates. A large part of this program would be to critically evaluate mathematical and physical assumptions in light of new experimental data. Since examples have been performed for boron/epoxy, it is logical that experimental correlation be attempted first with these materials. Testing of other fiber composites (and hybrids thereof) should follow provided that a first-phase testing proves the applicability of the model.

The current model has distinct advantages in that only simple tests on simple laminates are required as inputs to the analysis. These tests are: residual strength and fatigue lifetime tensile tests of unnotched [0] laminates, [90] laminates, and/or [±45] laminates in tension. These tests, in order to apply to different loading situations and different laminates, should be conducted at several values of σ_{max} and R. Although the tests required are in depth, they are uncomplicated and relatively easy to perform. Once the results from these tests have been obtained for a given material, any laminate configuration and any notch geometry can be analyzed.

There are certain aspects to fatigue loading which have not been treated in the current model. The model is insensitive to stacking sequence, i.e., gross laminate properties are assumed to change with number of cycles and stress level, and order of layup does not enter the predictions. It has been observed (Reference 2, for example) that stacking sequence can have an effect upon the strength and also the mode of failure during static and fatigue loading. In addition, it is observed for certain laminates that areas of debonding occur between layers as well as growth of cracks parallel to fiber directions. At present, it is felt that both of these phenomena (stacking sequence dependence and interlaminar failure) are caused by the same phenomenon: interlaminar shear behavior near the pre-existing notch or the propagating crack. it is therefore recommended that a program be undertaken to quantitatively and qualitatively evaluate the effects of delaminations on fatigue behavior and provide a method for incorporating the effects of stacking sequence.

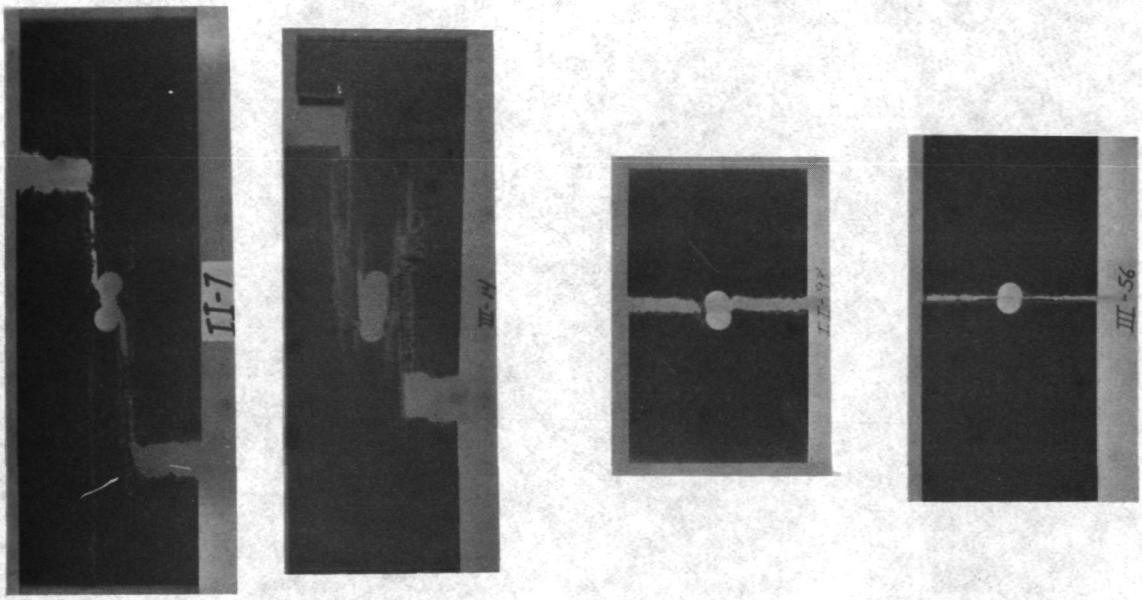

$[\pm 45/0_2]$ $[0_4/90_2/\pm 45]$ $[\ 45/0/\pm 45/0]$ $[0/\pm 45/90]$

(A) AXIAL (B) TRANSVERSE

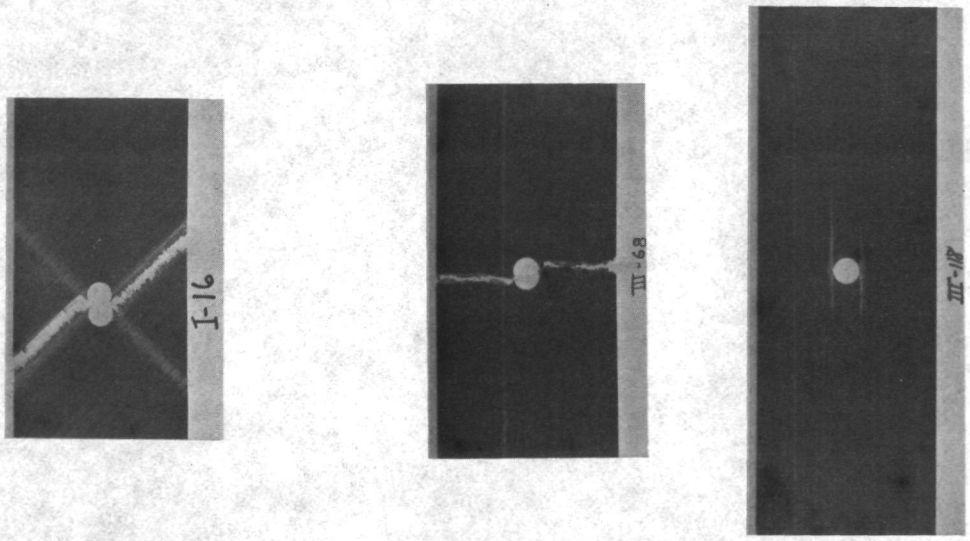

$[\pm 45]$ $[0_3/90/(\pm 45)_2]$

(C) OFF-AXIS (D) MIXED (A), (B)

FIGURE 1. Fatigue Failure Modes in Notched B/Ep Laminates (Ref. 2). Courtesy of Boeing-Vertol

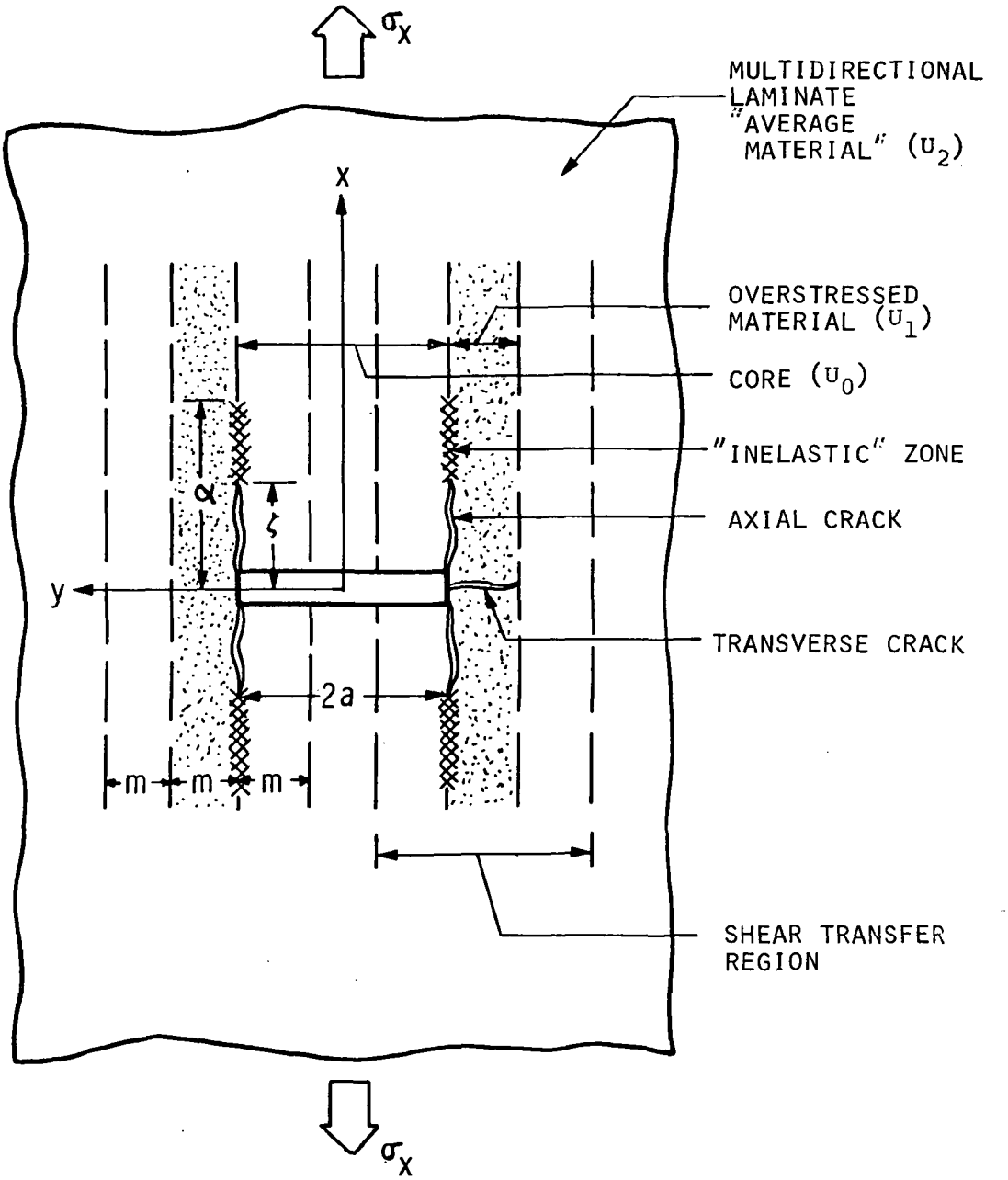

FIGURE 2. "MATERIALS ENGINEERING" MODEL FOR A NOTCHED LAMINATE

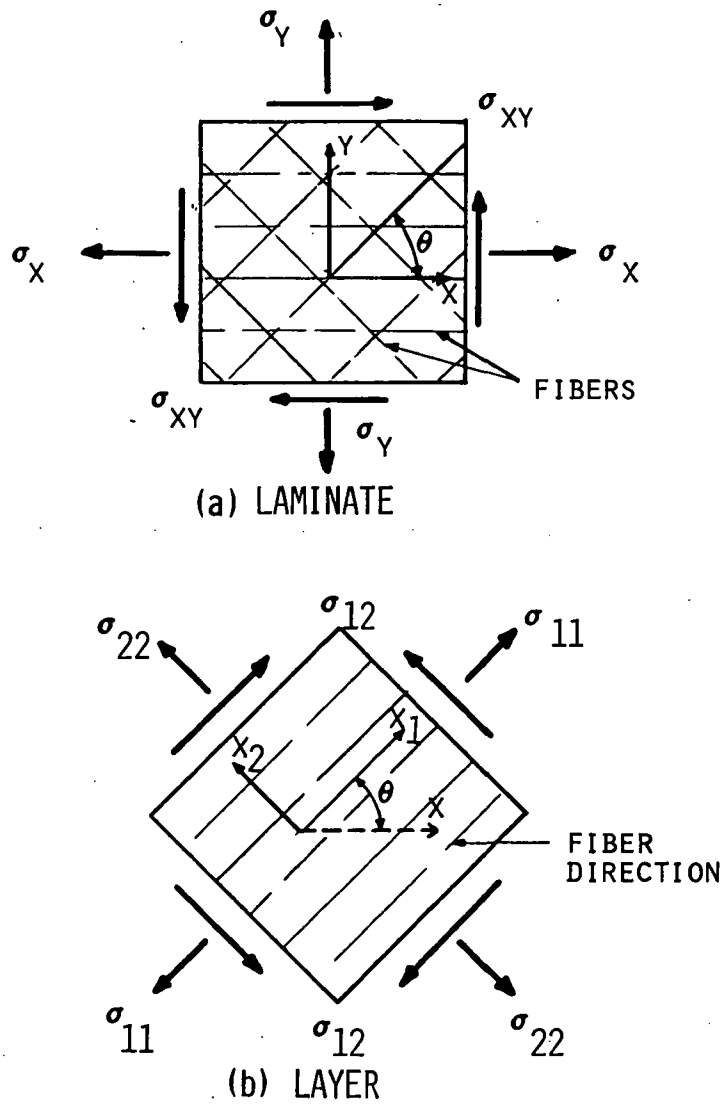

FIGURE 3. FIBER COMPOSITE STRESS AND COORDINATE SYSTEM CONVENTION

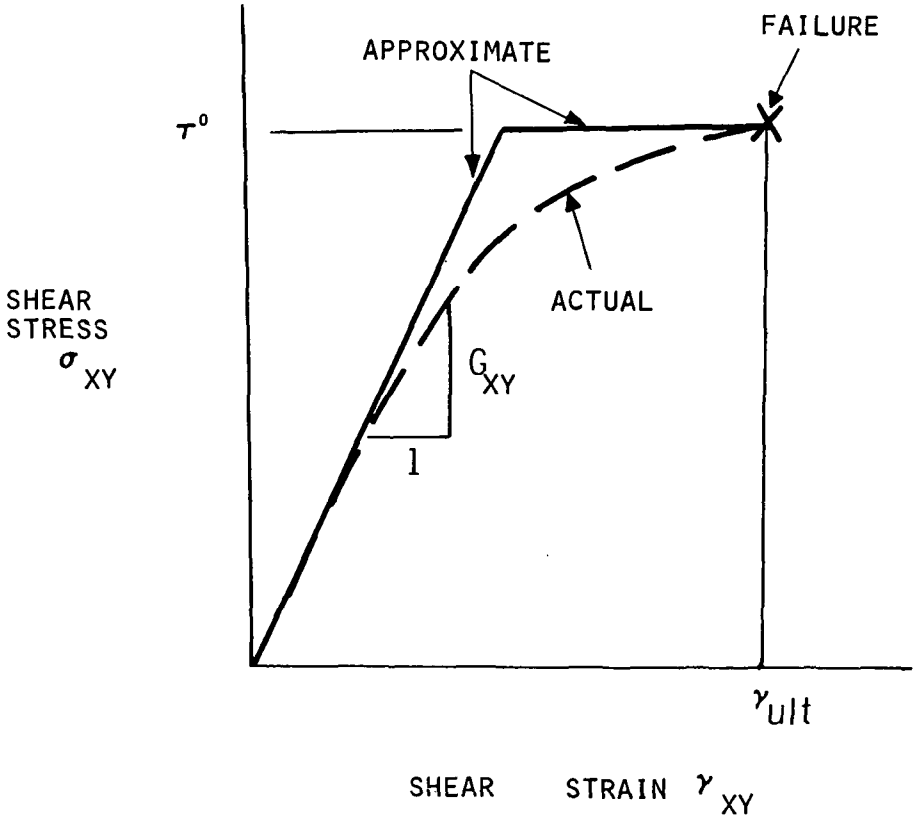

FIGURE 4. APPROXIMATION TO LAMINATE
AXIAL SHEAR STRESS-STRAIN BEHAVIOR

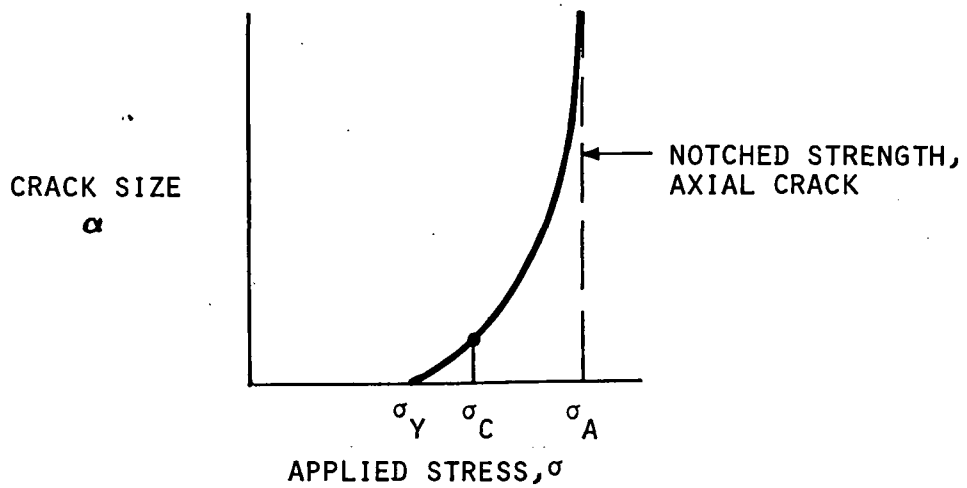

(a) AXIAL CRACK PROPAGATION

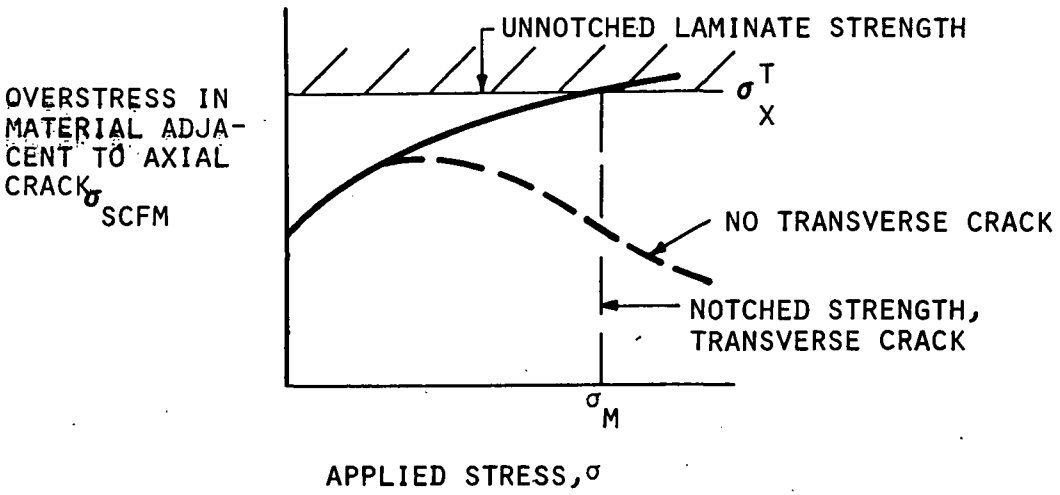

(b) TRANSVERSE CRACK PROPAGATION

FIGURE 5. TYPICAL STATIC FAILURE BEHAVIOR PREDICTED FROM MODEL.

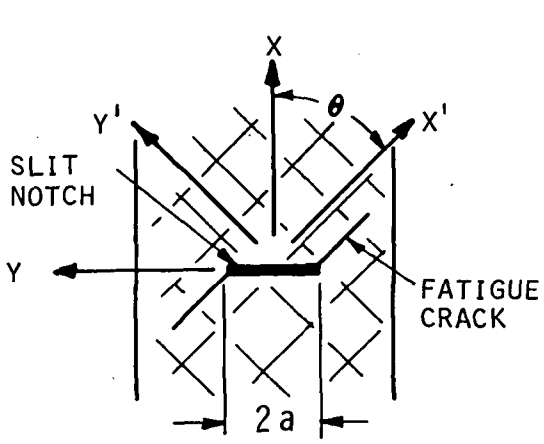

(a) LAMINATE GEOMETRY

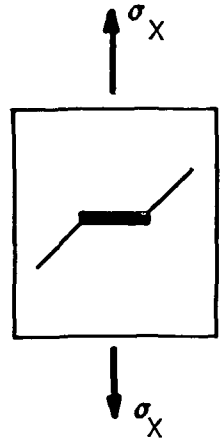

(b) XY STRESS STATE

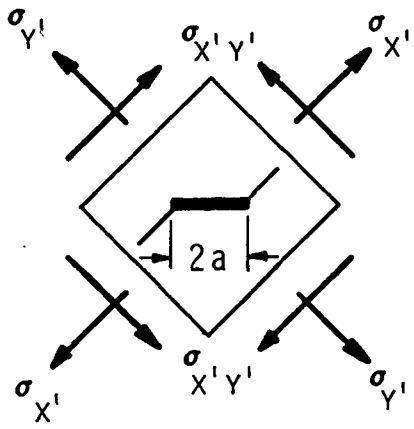

(c) X'Y' STRESS STATE

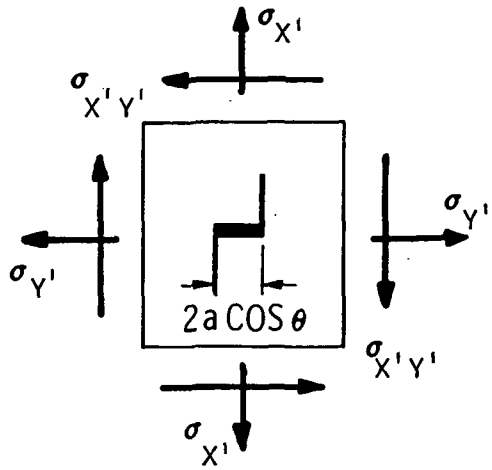

(d) EQUIVALENT AXIAL NOTCH

FIGURE 6. EQUIVALENT AXIAL CRACK PROBLEM FOR OFF-AXIS FAILURE

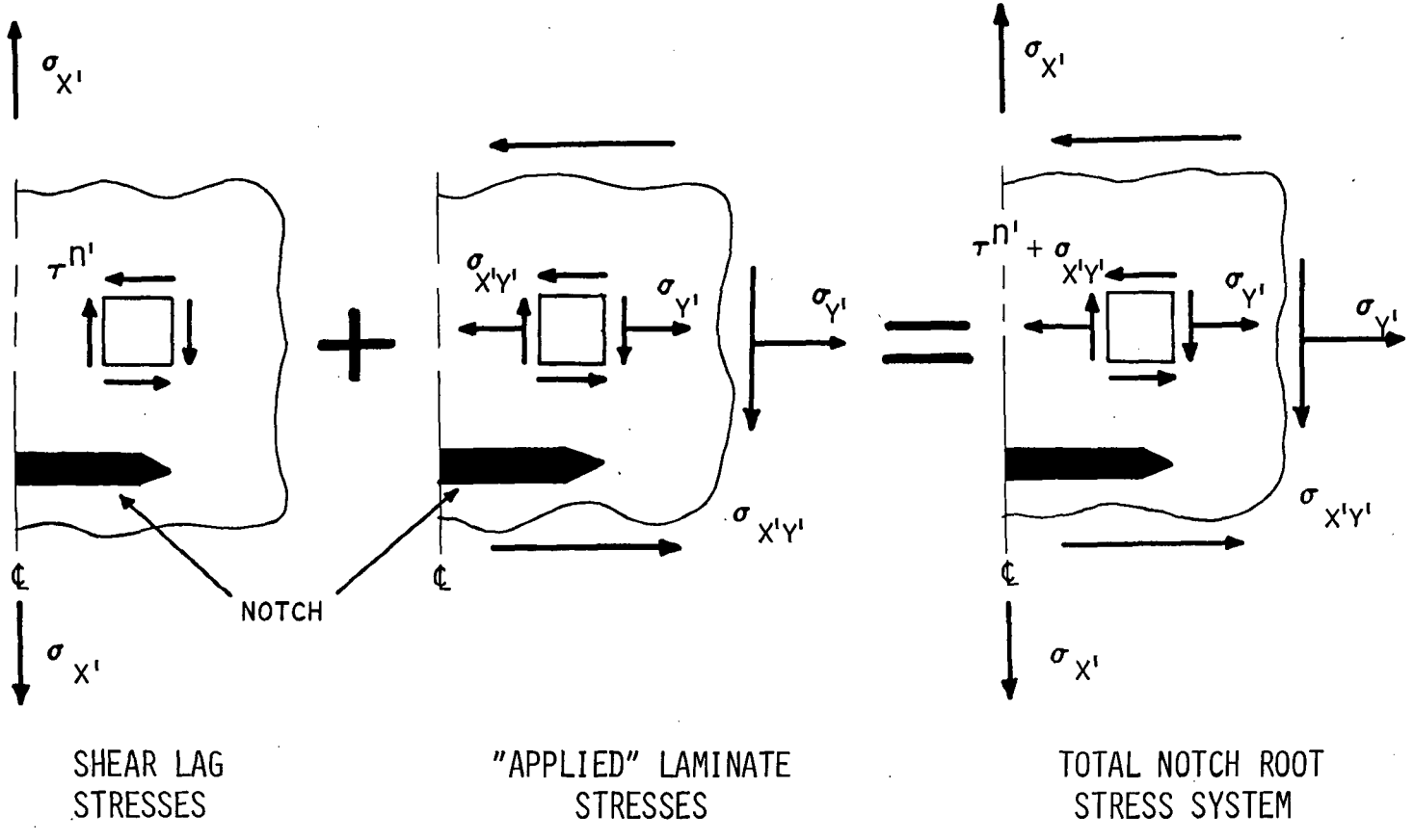

FIGURE 7. NOTCH ROOT LAMINATE STRESS IN OFF-AXIS COORDINATE SYSTEM

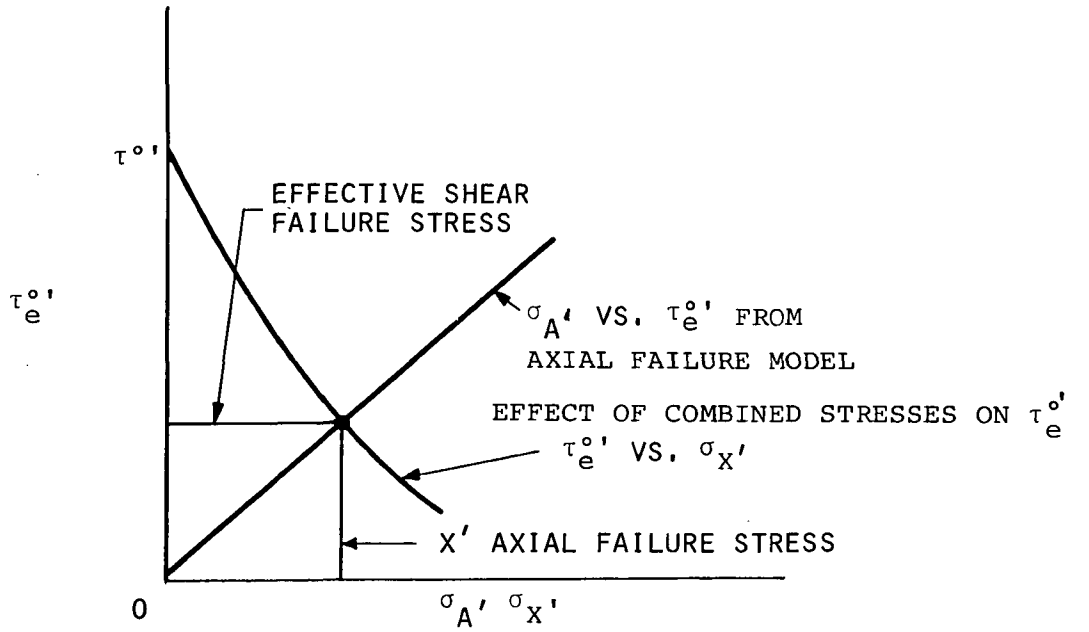

FIGURE 8. GRAPHICAL PROCEDURE FOR DETERMINING OFF-AXIS RESIDUAL STRENGTH OF NOTCHED LAMINATE

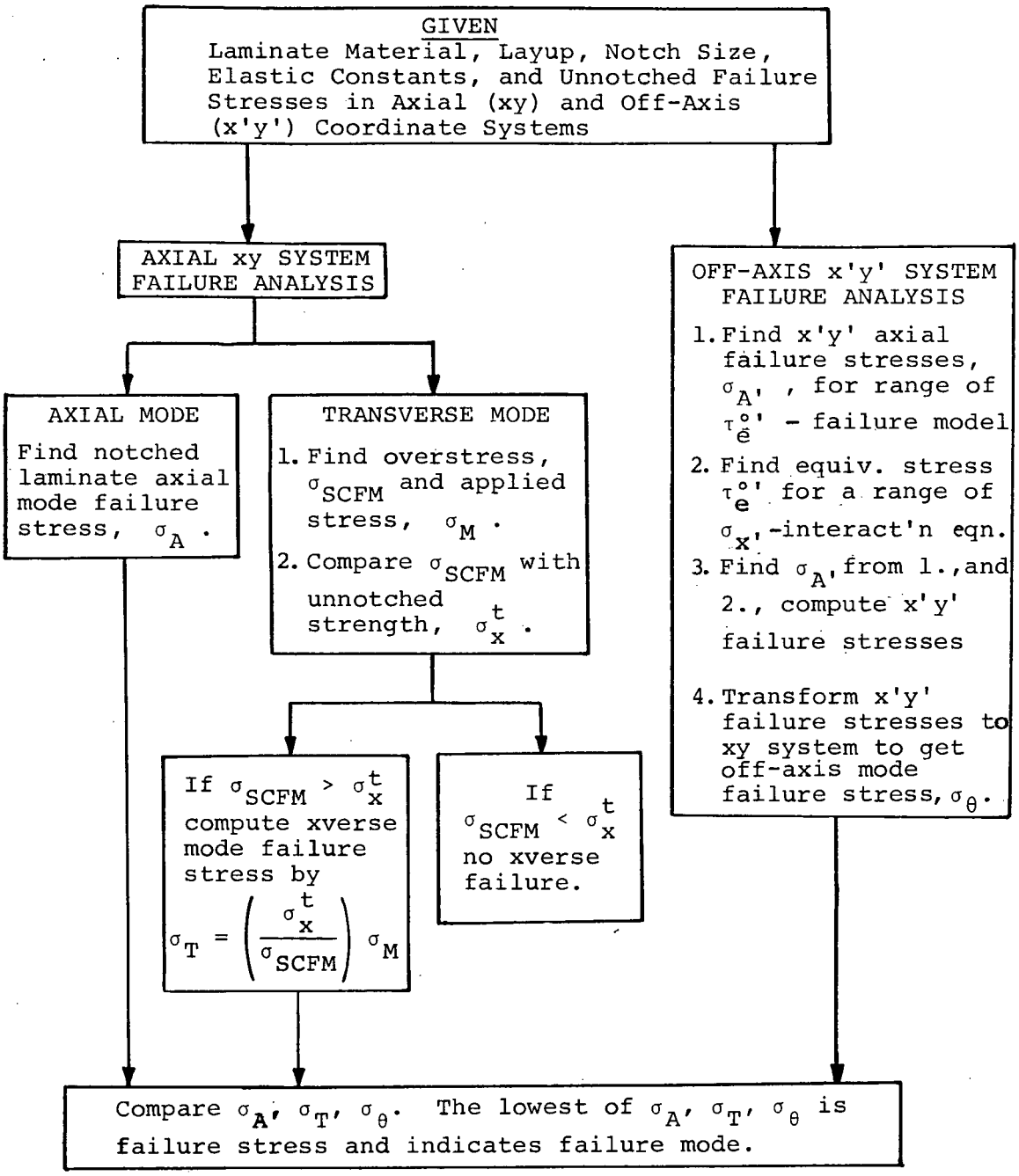

Figure 9. Static Failure Stress and Mode Determination Procedure for Notched Composites.

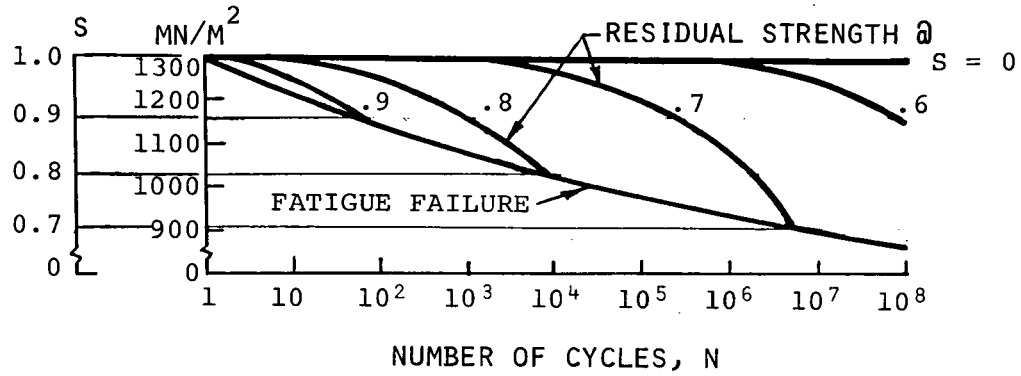

(a) AXIAL TENSILE STRENGTH, σ_{11}

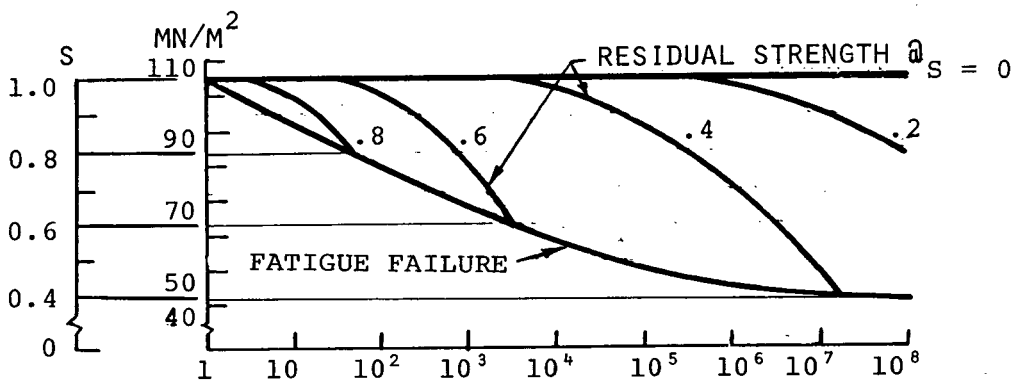

(b) AXIAL SHEAR STRENGTH, σ_{12}

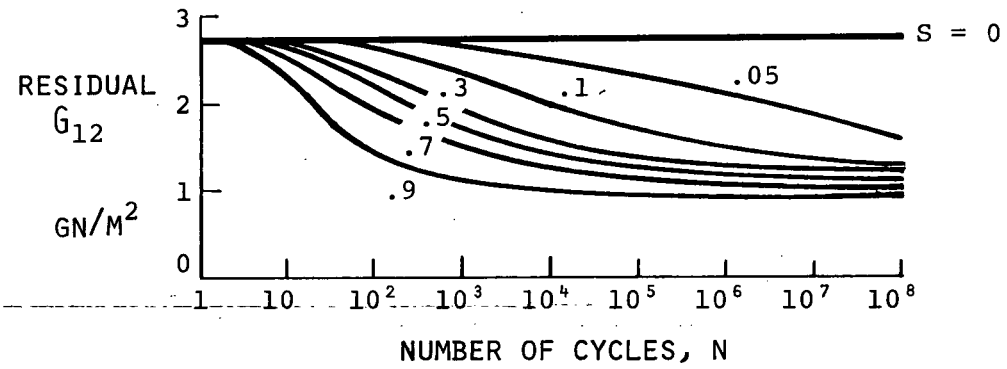

(c) AXIAL SECANT SHEAR MODULUS, G_{12}

FIGURE 10. TYPICAL FATIGUE BEHAVIOR AND LIFETIME OF [0] LAMINA REQUIRED TO GENERATE LAMINATE FATIGUE BEHAVIOR

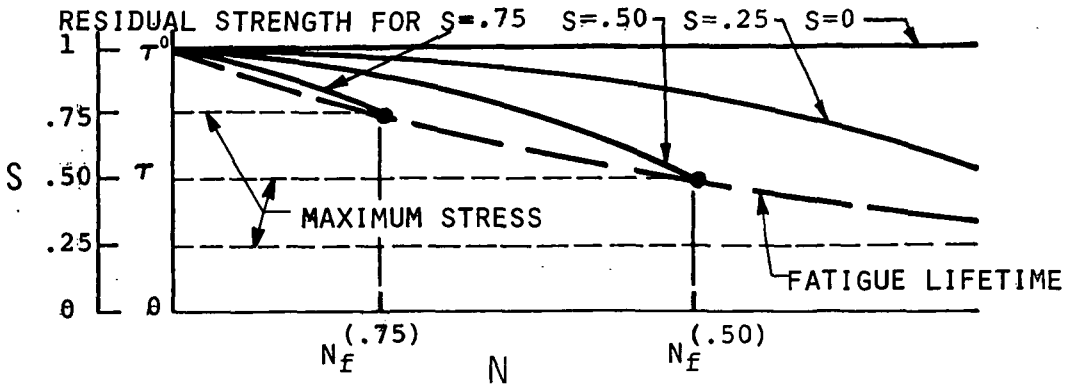

(a)LAMINATE AXIAL SHEAR RESIDUAL STRENGTH AND LIFETIME

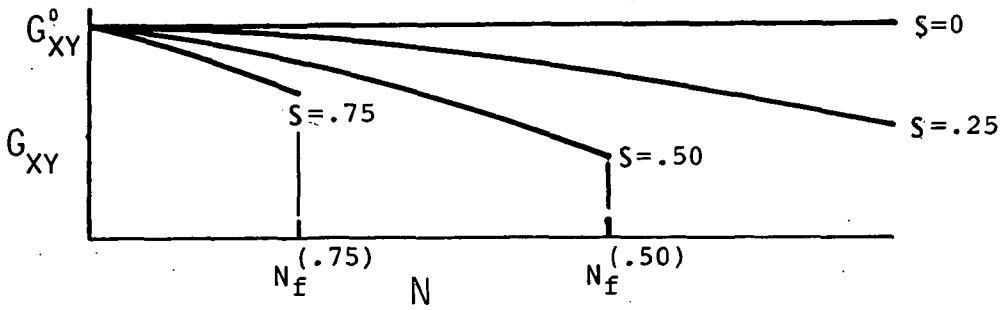

(b)LAMINATE AXIAL SHEAR RESIDUAL MODULUS

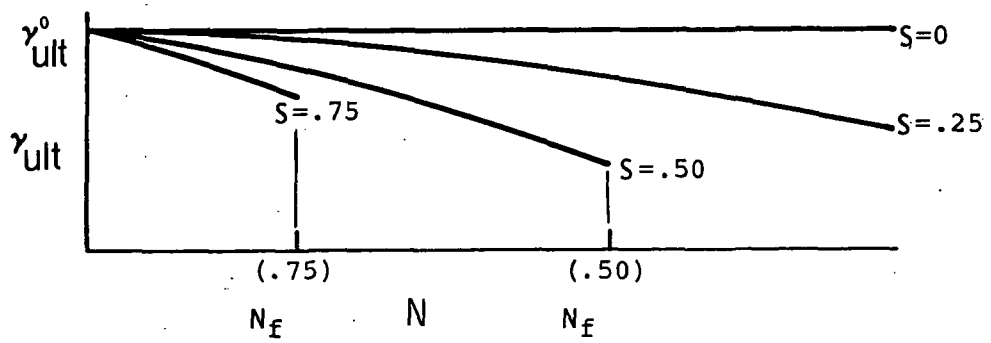

(c)LAMINATE AXIAL SHEAR RESIDUAL FAILURE STRAIN

FIGURE 11. TYPICAL LAMINATE FATIGUE LIFETIME AND RESIDUAL PROPERTY INFORMATION - AXIAL SHEAR AT NOTCH ROOT

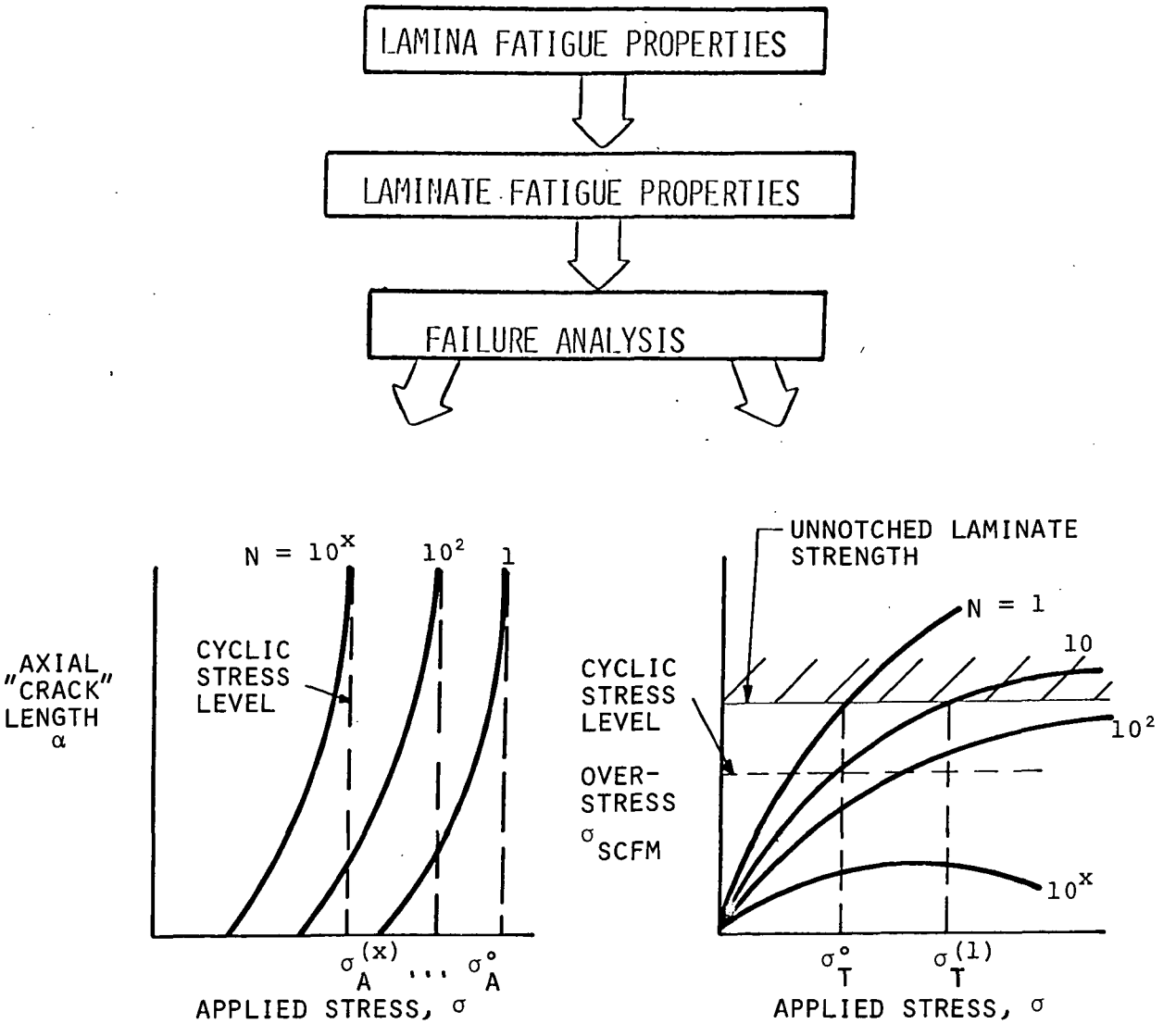

FIGURE 12. SCHEMATIC DIAGRAM OF METHOD FOR DETERMINING FATIGUE LIFETIME, RESIDUAL STRENGTH, AND AXIAL "CRACK" GROWTH OF NOTCHED LAMINATE.

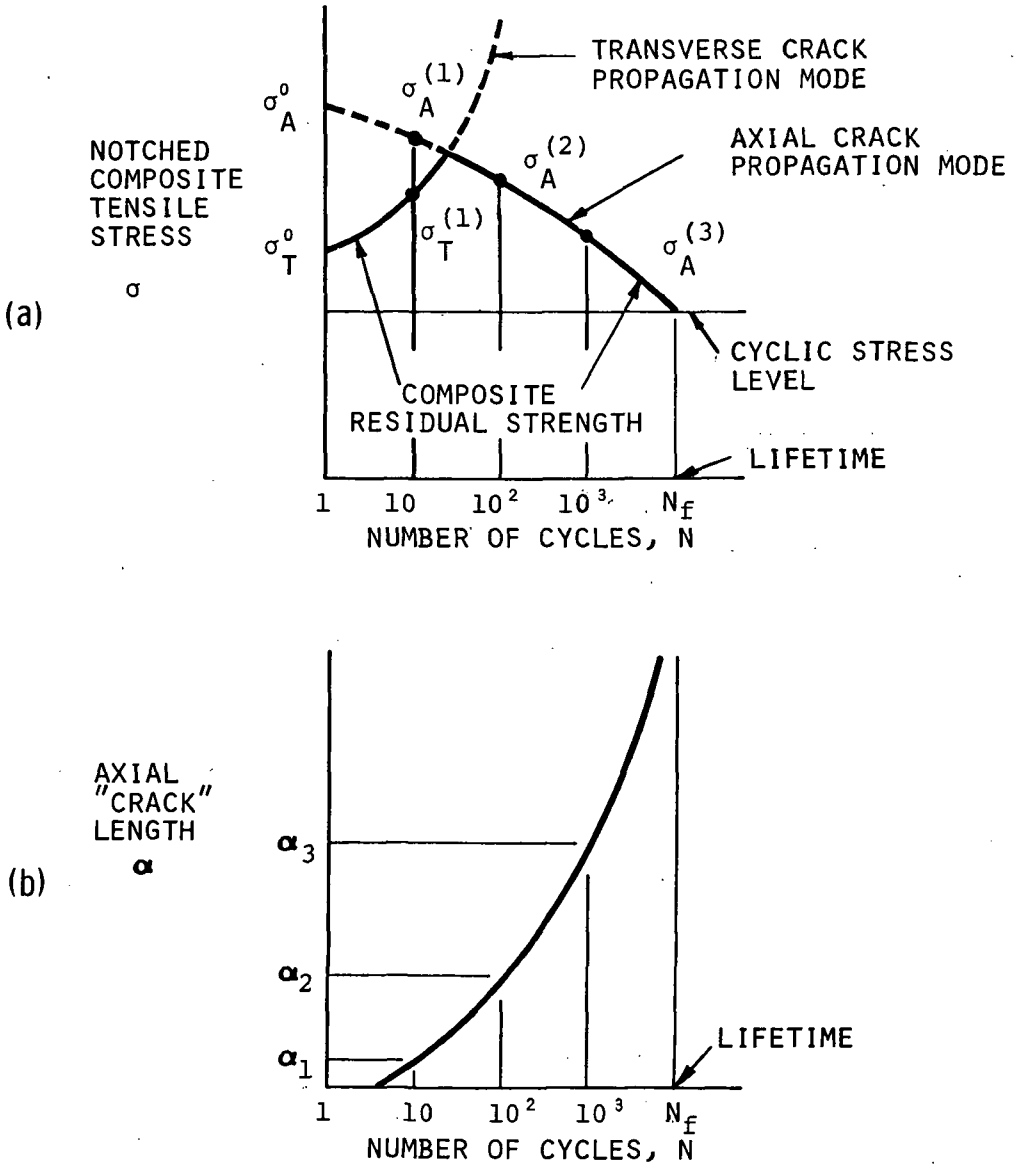

FIGURE 13. TYPICAL PREDICTED RESIDUAL STRENGTH, FATIGUE LIFETIME, AND AXIAL "CRACK" GROWTH OF NOTCHED LAMINATE.

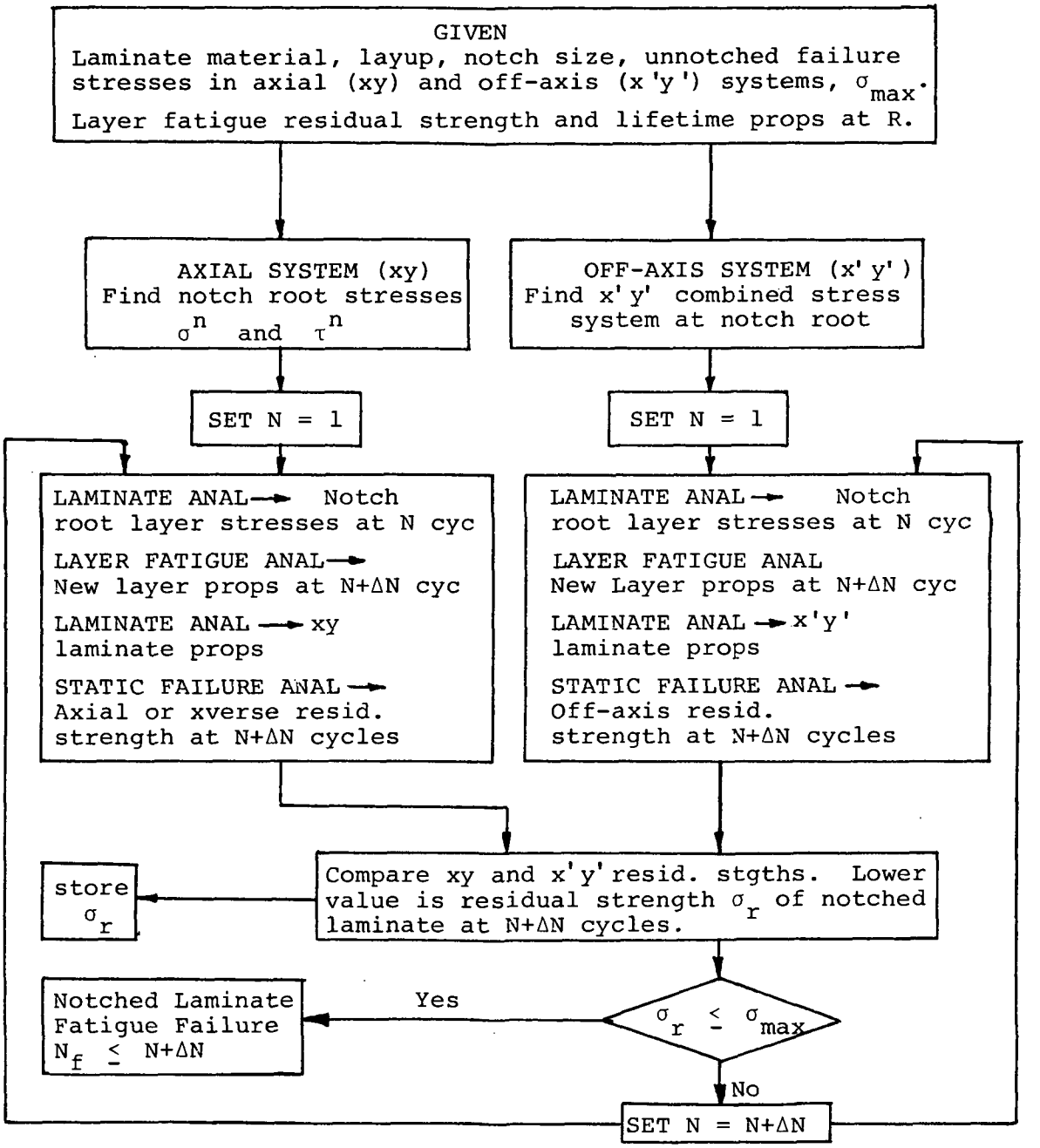

Figure 14. Fatigue Residual Strength and Lifetime Determination Procedure for Notched Composites.

APPENDIX A

GOVERNING EQUATIONS FOR FAILURE MODEL

Referring to Figure 2, main text , the equations of equilibrium in the various regions of shear stress transfer are as follows:

Region of In-plane Shear Damage (Axial Crack)

Equilibrium of the center core and adjacent overstressed regions in the x-direction gives:

$$n\ k\ h\ E_x \frac{d^2 U_0}{dx^2} = 0 \qquad \text{(A2)}$$

$$m\ j\ h\ E_L \frac{d^2 U_1}{dx^2} - \left(\frac{G_{xy} j\ h}{m} + \frac{G'_{90}\ j_{90} h}{m} \right) (U_1 - U_2) = 0 \qquad \text{(A2)}$$

where

j = number of layers in the laminate

j_{90} = number of 90 degree layers in the laminate

h = thickness of lamina

E_x = laminate longitudinal modulus

G_{xy} = axial shear modulus of the laminate

$U_2 = \sigma_g \frac{x}{E_L}$

σ_g = gross laminate stress

G'_{90} = contribution of the fiber bending stiffness to the modified shear modulus G_{90} of the 90 degree layer

$n = 2a$ = notch width.

It is obvious that only gross properties are used and no consideration is given to the fact that the axial and shear stiffness actually vary along the thickness coordinate. The last term in equation (A2) represents the modified shear stiffness of the 90

degree layers in the laminate and is derived herein by assuming that the fibers are clamped at two points separated by a length m which is the assumed region of shear transfer. The modified shear modulus G_{90} is the sum of the shear modulus of the 90 degree lamina and the contribution of the fiber bending stiffness in the 90 degree layers over a length m . As m increases, the fiber bending stiffness decreases and G_{90} approaches the conventional value of G_{xy} for the 90 degree laminate. In [0/±θ/90] laminates with $0° \leq \theta \leq 45°$, the bending stiffness of the fibers in ±θ layers is negligible.

Equations (A1) and (A2) are rewritten as:

$$n^* \, j \, A_f \, E_{Lf} \frac{d^2 U_0}{dx^2} = 0 \tag{A3}$$

$$m^* \, j \, A_f \, E_{Lf} \frac{d^2 U_1}{dx^2} - \left(\frac{G_{xy} \, j \, A_f}{m^* d^2 \, V_f} + \frac{G'_{90} \, j_{90} A_f}{m^* d^2 \, V_f} \right) (U_1 - U_2) = 0 \tag{A4}$$

where $E_{Lf} = E_x / V_f$,

V_f = fiber volume fraction,

d = 0° layer fiber spacing,

$A_f = V_f \, hd$;

$m^* = m/d$ = number of fibers in overstressed intact region in a 0° layer

$n^* = m/d$ = number of fibers in notch region in a 0° layer.

The above differential equations are nondimensionalized by assuming

$$U_{0,1} = \sigma_{gf} \left(\frac{V_f \, m^*}{E_{Lf} \, G_{xy}} \right)^{\frac{1}{2}} u_{0,1} \, d \tag{A5}$$

and

$$x = \left(\frac{E_{Lf} \, V_f \, m^*}{G_{xy}} \right)^{\frac{1}{2}} \xi \, d \tag{A6}$$

where $\sigma_{gf} = \sigma_g / V_f$.

Thus, we have

$$n^* \frac{d^2 u_0}{d\xi^2} = 0 \tag{A7}$$

$$\frac{m^* d^2 u_1}{d\xi^2} - (1 + r)(u_1 - \xi) = 0 \tag{A8}$$

where $r = \frac{j_{90}}{k} \frac{G'_{90}}{G_{xy}}$

The solution of equations (A7) and (A8) are,

$$u_0 = C_1$$

$$u_1 = \xi + C_2 (e^{\Delta\xi} - e^{-\Delta\xi}) \quad 0 \leq \xi \leq \zeta \tag{A9}$$

where $\Delta = (\frac{1 + r}{m^*})^{\frac{1}{2}}$ and C_1 and C_2 are constants.

The boundary conditions $\frac{du_0}{d\xi}(\xi = 0) = 0$ and $u_1 (\xi = 0) = 0$ have already been considered.

Inelastic Region

The following governing equations are derived for x-direction equilibrium in the inelastic zone (shear stress in shear region $= \tau^\circ$, shear strain $< \gamma_{ult}$)

$$n^* j A_f E_{Lf} \frac{d^2 U_0}{dx^2} - 2j h \tau^\circ - 2 \frac{G'_{90} j_{90} A_f}{m^* d^2 V_f} (U_0 - U_1) = 0 \tag{A10}$$

$$m^* j A_f E_{Lf} \frac{d^2 U_1}{dx^2} + j h \tau^\circ - \frac{G'_{90} j_{90} A_f}{m^* d^2 V_f} (U_1 - U_0)$$

$$- \frac{G_{xy} j A_f}{m^* d^2 V_f} + \frac{G'_{90} j_{90} A_f}{m^* d^2 V_f} (U_1 - U_2) = 0 \tag{A11}$$

where τ° = yield (failure) stress of the laminate.

In addition to the preceeding nondimensionalization of the displacements and the coordinates $U_{O,1}$, the yield shear stress τ° is nondimensionalized in the following manner:

$$\tau^\circ = \sigma_{gf} \left(\frac{G_{xy} V_f}{E_{Lf} m^*} \right)^{\frac{1}{2}} \bar{\tau}_y \cdot \qquad \text{(A12)}$$

where $\bar{\tau}_y$ is the nondimensional shear stress.

Equations (A10) and (A11) appear in nondimensionalized form as:

$$n^* \frac{d^2 u_0}{d\xi^2} - 2\bar{\tau}_y - 2r\,(u_0 - u_1) = 0 \qquad \text{(A13)}$$

$$m^* \frac{d\,u_1}{d\xi^2} + \bar{\tau}_y - r(u_1 - u_0) - (1 + r)\,(u_1 - \xi) = 0 \qquad \text{(A14)}$$

The solutions for equations (A13) and (A14) are:

$$\left.\begin{aligned} u_0 &= \xi - \frac{\bar{\tau}_y}{r} + C_3 e^{\gamma_1 \xi} + C_4 e^{-\gamma_1 \xi} + C_5 e^{\gamma_2 \xi} + C_6 e^{-\gamma_2 \xi} \\ u_1 &= \xi + B_1 (C_3 e^{\gamma_1 \xi} + C_4 e^{-\gamma_1 \xi}) + B_2 (C_5 e^{\gamma_2 \xi} + C_6 e^{-\gamma_2 \xi}) \end{aligned}\right\} \zeta \le \xi \le \alpha \qquad \text{(A15)}$$

where

$$\gamma_{1,2} = \left\{ \frac{2r\,(m^*+n^*)+n^*}{2m^*n^*} \pm \frac{1}{2m^*n^*} \left[\left(2r(m^*+n^*)+n^* \right)^2 - 8r\,m^*n^*(1+r) \right]^{\frac{1}{2}} \right\}^{\frac{1}{2}}$$

and $B_{1,2} = 1 - \frac{n}{2r} \gamma_{1,2}^2$.

It is evident that the above solutions are not valid for $r = 0$, as in the case of a laminate with no 90 degree layers. If $r = 0$, the solutions assume the form:

$$\left.\begin{aligned} u_0 &= \frac{\bar{\tau}_y}{n^*} \xi^2 + C_3 \xi + C_4 \\ u_1 &= \xi + \bar{\tau}_y + C_5 e^{\Delta \xi} + C_6 e^{\Delta \xi} \end{aligned}\right\} \zeta \le \xi \le \alpha \qquad \text{(A16)}$$

C_3, C_4, C_5 and C_6 are constants of integration.

Elastic Region

In the elastic region, the equations of equilibrium are:

$$n^* \frac{d^2 u_0}{d\xi^2} + 2(1 + r)\ (u_1 - u_0) = 0 \qquad \text{(A17)}$$

$$m^* \frac{d^2 u_1}{d\xi^2} - (1 + r)\ (u_1 - u_0) + (1 + r)\ (\xi - u_1) = 0 \qquad \text{(A18)}$$

The solutions of equations A17 and A18 are:

$$\left.\begin{aligned} u_0 &= \xi + C_7\, e^{-\beta_1 \xi} + C_8\, e^{-\beta_2 \xi} \\ u_1 &= \xi + B_3\, C_7\, e^{-\beta_1 \xi} + B_4\, C_8\, e^{-\beta_2 \xi} \end{aligned}\right\} \alpha \le \xi \qquad \text{(A19)}$$

where

$$\beta_{1,2} = \left[\frac{(m^* + n^*)}{m^* n^*}\frac{(1 + r)}{} \pm \frac{1 + r}{m^* n^*}\{m^{*2} + n^{*2}\}\right]^{\frac{1}{2}}$$

and

$$B_{3,4} = 1 - n^* \beta_{1,2}^2/2(1 + r)$$

and C_7 and C_8 are constants of integration. In order to ensure finite stresses at ∞, terms involving positive exponentials have been eliminated from the displacements in equation A19. This boundary conditions of the problem are (ζ is nondimensional distance from notch to axial crack tip; and α is nondimensional distance from notch to beginning of elastic zone - the "inelastic length"):

$$\left.\begin{aligned} u_1\ (\xi = 0) &= 0 \\ \frac{d\, u_0}{d\xi}\ (\xi = 0) &= 0 \end{aligned}\right\} \qquad \text{(A20)}$$

$$\left.\begin{aligned} u_0\ (\xi = \zeta^-) &= u_0\ (\xi = \zeta^+) \\ \frac{d\,u_0}{d\xi}\ (\xi = \zeta^-) &= \frac{d\,u_0}{d\xi}\ (\xi = \zeta^+) \\ u_1\ (\xi = \zeta^-) &= u_1\ (\xi = \zeta^+) \\ \frac{d\,u_1}{d\xi}\ (\xi = \zeta^-) &= \frac{d\,u_1}{d\xi}\ (\xi = \zeta^+) \end{aligned}\right\} \qquad \text{(A21)}$$

$$\left.\begin{aligned} u_0\ (\xi = \alpha^-) &= u_0\ (\xi = \alpha^+) \\ \frac{d\,u_0}{d\xi}\ (\xi = \alpha^-) &= \frac{d\,u_0}{d\xi}\ (\xi = \alpha^+) \\ u_1\ (\xi = \alpha^-) &= u_1\ (\xi = \alpha^+) \\ \frac{d\,u_1}{d\xi}\ (\xi = \alpha^-) &= \frac{d\,u_1}{d\xi}\ (\xi = \alpha^+) \end{aligned}\right\} \qquad \text{(A22)}$$

$$\frac{d\,u_0}{d\xi}\ (\xi \to \infty) = \frac{d\,u_1}{d\xi}\ (\xi \to \infty) = 1 \qquad \text{(A23)}$$

and

$$u_0\ (\xi = \alpha^+) - u_1\ (\xi = \alpha^-) = \bar{\tau}_y \quad . \qquad \text{(A24)}$$

The boundary conditions of Equations A20 and A23 have already been used. Hence, there remain a total of nine boundary conditions and nine unknowns which consist of the eight constants C_1, C_2, C_3, C_4, C_5, C_6, C_7, C_8 and the nondimensional yield shear stress $\bar{\tau}_y$.

Derivation of the Modified Shear Modulus for a 90 Degree Laminate

It is argued that the shear modulus of a 90 degree laminate is not correctly represented by the conventional value of G_{xy} when the shear transfer zone defined by the length m in Figure 2 is of the order 10^{-1} because of material heterogeneity. To show that this is indeed true, the actual shear modulus of a 90 degree laminate is derived below by considering the fiber and matrix phases separately.

Consider a 90 degree lamina of width 2ℓ and of infinite length which is clamped at the two edges as illustrated in Figure A-1. Suppose that the lamina is subjected to a differential displacement. As a result of the deformation, the strain component ε_y in the matrix and fiber will consist of the bending strain contribution, the shear strain as a result of this bending strain and the shear strain arising out of the displacement compatibility at the fiber matrix interface. Referring to Figure A-2 compatibility of displacements at the fiber-matrix interface require that

$$\frac{h^*}{2}\left(U_{y,x} + \gamma_f - \frac{\tau_{xy_f}}{G_f}\right) = c\left(\frac{\tau_{xy_m}}{G_m} - \gamma_m - U_{y,x}\right) \qquad \text{(A25)}$$

where U_y = displacement in the y direction

$U_{y,x} = \frac{dU_y}{dx}$

γ = bending shear strain

G = shear modulus

The subscript f refers to the fiber and m to the matrix. It is assumed that U_y is independent of the y direction. Also, from stress equilibrium $\tau_{xy_f} = \tau_{xy_m} = \tau_{xy}$.

The solution for τ_{xy} from Equation (A25) is,

$$\tau_{xy} = \frac{G_f}{(1+g_2)}\left(U_{y,x}\, g_1 + \gamma_f\, g_2 + \frac{\gamma_m\, G_m}{G_f}\right) \qquad \text{(A26)}$$

where

$$g_1 = \frac{G_m}{G_f}\frac{1}{(1-V_f)},\ g_2 = V_f g_1 \text{ and } V_f = \text{fiber volume fraction.}$$

The total strain energy (S.E.) of the fiber and matrix consists of the bending strain energy, bending shear strain energy, and shear strain energy arising from the shear stress τ_{xy}. Therefore,

$$S.E. = \left(\frac{E_f I_f}{2} + \frac{E_m I_m}{2}\right)\int_0^{\ell} (U_{y,xx})^2 \, dx$$

$$+ \left(\frac{\kappa E_f^2 I_f^2}{2a_f G_f} + \frac{\kappa E_m^2 I_m^2}{2a_m G_m}\right)\int_0^{\ell} (U_{y,xxx})^2 \, dx$$

$$+ \frac{G_f}{(1+g_2)^2}\left(\frac{h^*}{2} + \frac{c G_f}{G_m}\right) \int_0^{\ell} \left(g_1 U_{y,x} + g_2 \frac{\kappa V}{a_f G_f}\right)^2 dx \qquad \text{(A27)}$$

where E = Young's modulus

I = moment of inertia

a = cross sectional area

κ = shear coefficient and

V = shear force.

The form of displacement assumed is,

$$U_y = Bx^3 \qquad \text{(A28)}$$

where B is a constant. The differential displacement will give rise to a shear force S across the cross section at $x = \ell$. Equating the internal strain energy to the external work done by S,

$$6E_f I_f B^2 \ell^3 + 18 \kappa \frac{E_f^2 I_f^2}{a_f G_f} B^2 \ell$$

$$+ \frac{g_1^2 G_f}{g_2(1+g_2)} \frac{h^*}{2} 9B^2 \left(\frac{\ell^5}{5} + g_3^2 \ell + \frac{2}{3} g_3 \ell^3\right) = S B\ell^3 \qquad \text{(A29)}$$

where $g_3 = \frac{2V_f \kappa E_f I_f}{a_f G_f}$. The bending and bending shear strain energies in the matrix are neglected.

Further manipulation of Equation (A29) yields,

$$G_{90} = \frac{S}{(h+2c)} \frac{1}{A\ell^2} = \frac{V_f E_f}{2} \left(\frac{h^*}{\ell}\right)^2 \left\{1 + \kappa \frac{E_f}{4G_f} \left(\frac{h^*}{\ell}\right)^2\right\} + 4.5\left(\frac{1}{5} + \frac{g_3^2}{\ell^4} + \frac{2}{3}\frac{g_3}{\ell^2}\right) \frac{G_m}{(1-V_f)\left(1 + \frac{G_m}{G_f}\frac{V_f}{1-V_f}\right)} \quad \text{(A30)}$$

It is obvious that G_{90} represents the modified shear modulus of the 90-degree lamina. For $(h^*/\ell) << 1$, Equation (A30) can be written as,

$$G_{90} = \frac{0.9\ G_m}{(1-V_f)\left(1 + \frac{G_m}{G_f}\frac{V_f}{1-V_f}\right)} \quad \text{(A31)}$$

which is conventional shear modulus G_{xy} of the 90-degree lamina as obtained from the stiffness in series model. Note that the factor 0.9 results from the approximate nature of the displacement in Equation (A28). In Equation(A30)the first term on the right hand side may be designated as the contribution to the shear modulus from the bending stiffness of the fibers and will be termed as G'_{90}. Hence,

$$G'_{90} = \frac{V_f E_f}{2}\left(\frac{h^*}{\ell}\right)^2 \left\{1 + \kappa \frac{E_f}{4G_f}\left(\frac{h^*}{\ell}\right)^2\right\} \quad \text{(A32)}$$

If the shear strain τ_{xy}/G_m reaches the yield value, it is apparent that $G_{90} = G'_{90}$. Thus if the shear strain attains its ultimate value when fiber matrix debonding results, the 90 degree lamina will still have a residual stiffness G'_{90} to resist differential displacement. For a through-the-thickness axial crack to propagate either in a $[0/90]_s$ or $[0/\pm45/90]_s$ laminate, the fibers in the 90 degree lamina should break. This will be the case when

the maximum strain ε_y exceeds its ultimate value. Maximum ε_y occurs at $x = \ell$ at a distance farthest from the neutral axis in the fiber and its magnitude is,

$$\varepsilon_{y_{max}} = \frac{h^*}{2\ell} \left\{ U_{y,x} \left(1 - \frac{g_1}{1+g_2} \right) + \gamma_f \left(1 - \frac{g_2}{1+g_2} \right) \right\}_{x=\ell} \tag{A33}$$

Hence the maximum fiber stress is,

$$\sigma_{y_{max}} = \frac{E_f}{\ell} U_d \left\{ \frac{3}{2} \frac{h^*}{\ell} \left(1 - \frac{g_1}{1+g_2} \right) + \frac{\kappa}{4} \frac{E_f}{G_f} \left(\frac{h^*}{\ell} \right)^3 \frac{1}{1+g_2} \right\} \tag{A34}$$

where $U_d = A\ell^3$ = differential displacement over the length ℓ .

Figure A-3 illustrates the variation of G_{90} with m*, the number of intact fibers in the 0° layer. It is clear that for m* < 5, the shear modulus G_{xy} underestimates the stiffness of the 90 degree laminate. However, for m* > 9, G_{90} approaches the value G_{xy}.

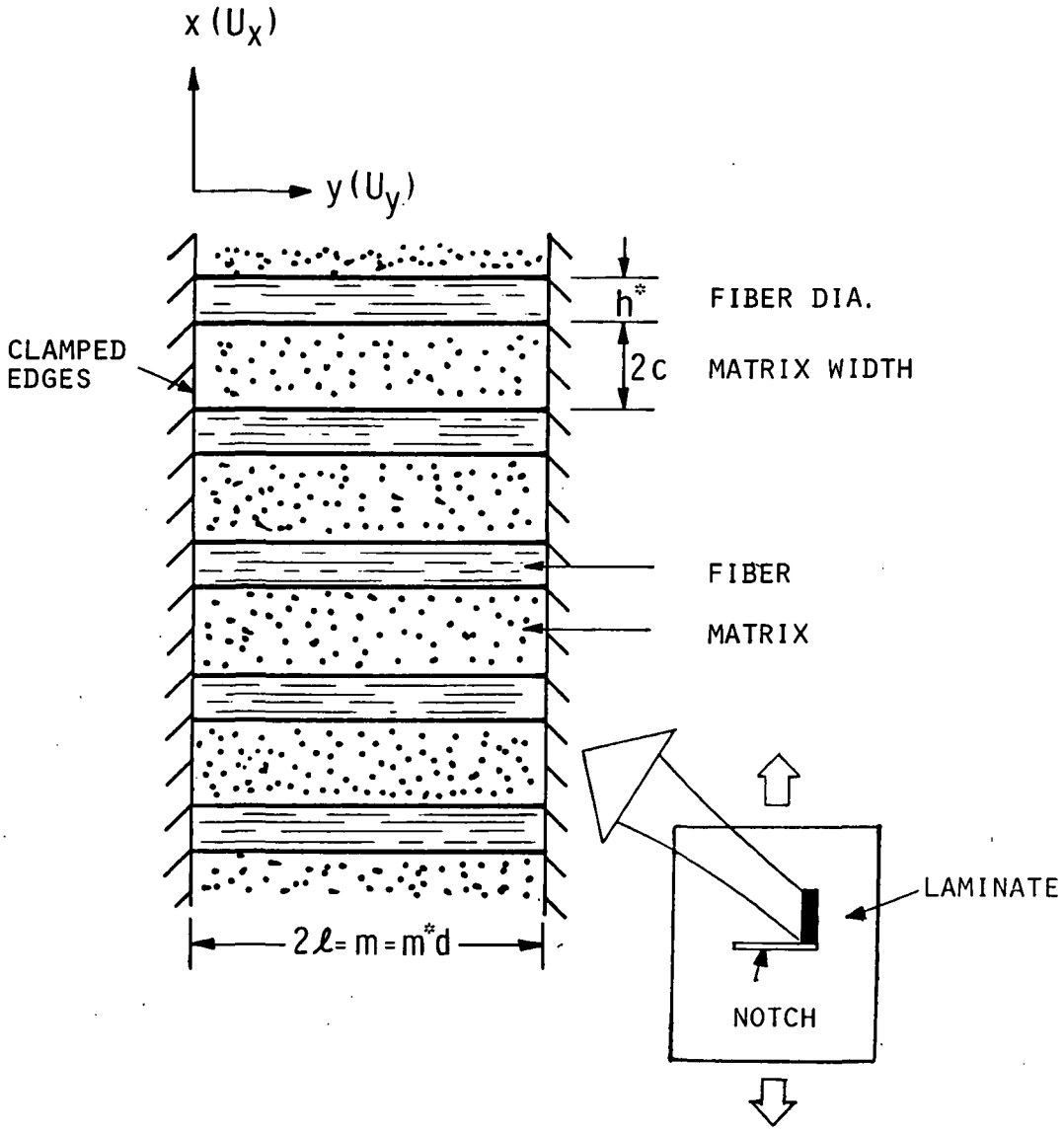

FIGURE A-1, [90] LAMINATE WITH CLAMPED EDGES.

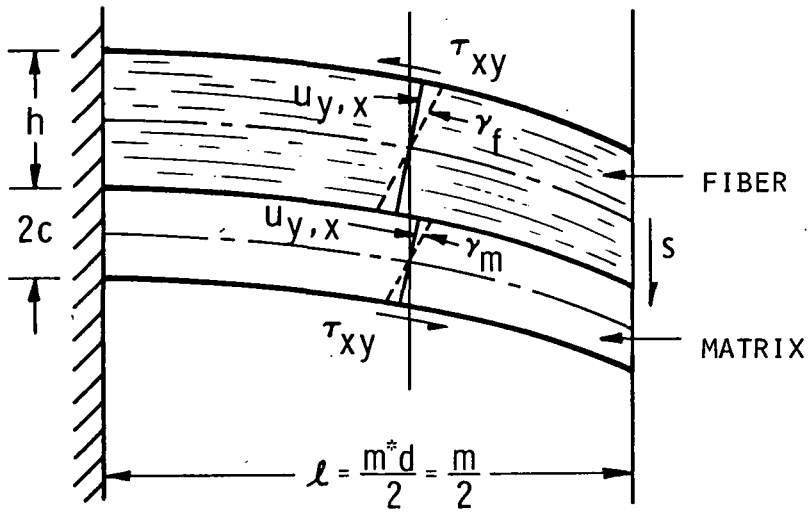

FIGURE A-2, DEFORMATION OF A [90] LAMINATE SUBJECTED TO AN IN-PLANE SHEAR LOAD.

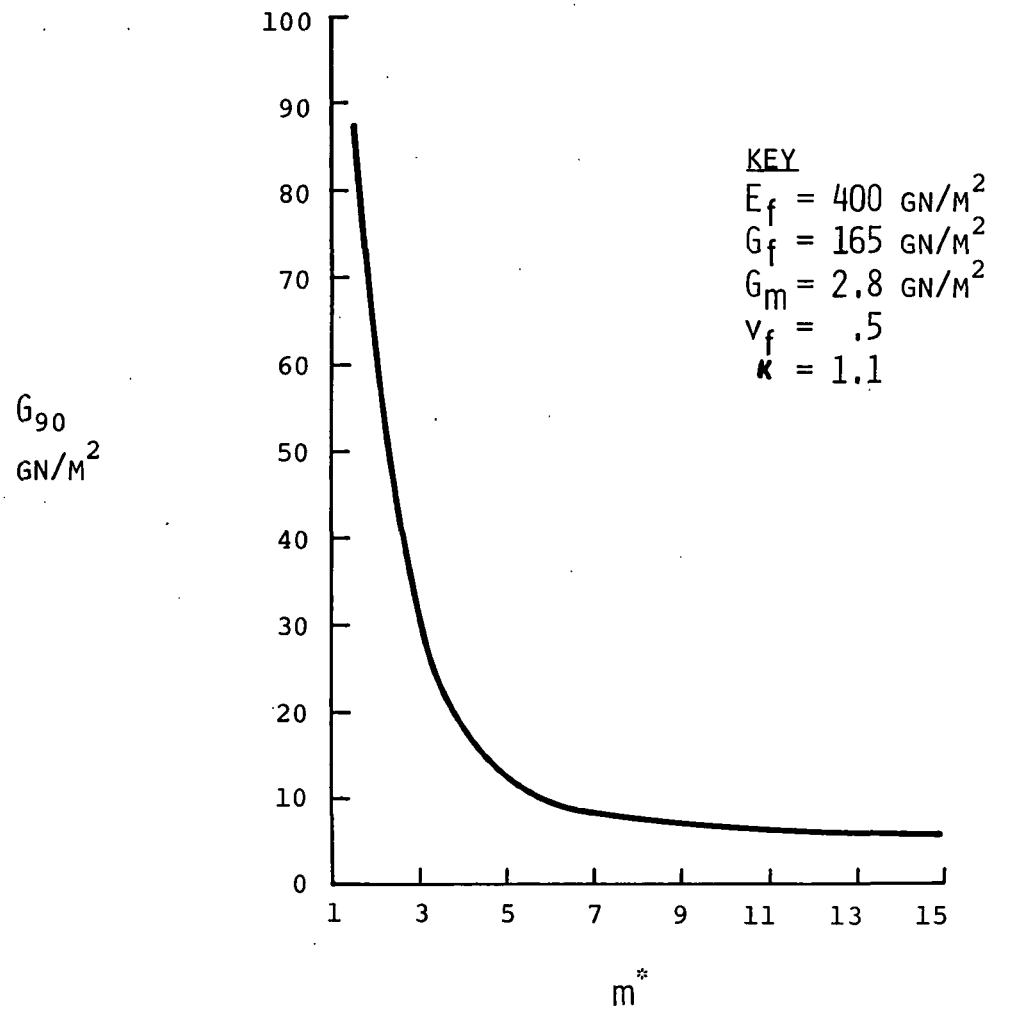

FIGURE A-3; VARIATION OF 90° LAYER SHEAR MODULUS, G_{90}, WITH THE NUMBER OF INTACT FIBERS IN 0° LAYER, m*.

APPENDIX B

COMBINED STRESS EFFECTS ON LAMINATE STATIC AXIAL CRACKING

Performing an exact analysis of axial cracking including transverse tension $\sigma_{y'}$ and applied axial shear $\sigma_{x'y'}$ in addition to axial tension $\sigma_{x'}$ is difficult. Therefore, the effect of shear and transverse normal stresses is taken into account in an approximate fashion. The presence of laminate gross transverse tension $\sigma_{y'}$ and axial shear $\sigma_{x'y'}$ is treated by superimposing these stresses on the axial shear stress at the notch root which would exist due to only $\sigma_{x'}$ (see Figure 7, maintained). The main effect of this superposition upon the shear lag analysis will be to increase the likelihood of x'y' axial shear failure.

Throughout the loading process, the presence of applied axial shear stress $\sigma_{x'y'}$ will reduce the amount of axial shear stress required from the shear-lag analysis to cause axial cracking. The effect of applied shear is therefore taken into account reducing the x'y' laminate shear strength $\tau^{\circ}{}'$ directly by $\sigma_{x'y'}$. The effect of the transverse normal stress $\sigma_{y'}$ is assumed to further reduce the shear strength according to an empirical quadratic interaction formula.

The resulting effect of axial shear and transverse stresses is, therefore, to change the laminate axial shear strength inputted into the standard tensile strength analysis. This changed, or effective, shear strength $\tau^{\circ}_{e}{}'$ is found from the equation

$$\left(\frac{\sigma_{y'} + \sigma^{d}_{y'}}{\sigma^{p}_{y'}}\right)^2 + \left(\frac{\tau^{\circ}_{e}{}'}{\tau'^{d}}\right)^2 = 1 \qquad \text{(B1)}$$

where

$\tau^{\circ}_{e'}$ = the effective shear strength for given $\sigma_{y'}$ and $\sigma_{x'y'}$

$$\sigma^{p}_{y'} = \frac{\sigma^{c}_{y'} + \sigma^{t}_{y'}}{2}$$

$$\sigma^{d}_{y'} = \frac{\sigma^{c}_{y'} - \sigma^{t}_{y'}}{2}$$

$\sigma^{t}_{y'}$ = tensile strength of the unnotched laminate in the y' direction

$\sigma^{c}_{y'}$ = compression strength of the unnotched laminate in the y' direction

$$\tau'^{d} = \frac{\tau^{\circ'} - \sigma_{x'y'}}{\left[1-(\sigma^{d}_{y'}/\sigma^{p}_{y'})^{2}\right]^{\frac{1}{2}}}$$

$\tau^{\circ'}$ = shear strength of the unnotched laminate in the x'y' coordinate system.

For a given laminate and fiber orientation, increased applied stress σ will cause proportional increases in the stresses $\sigma_{y'}$ and $\sigma_{x'y'}$. This means that the effective reduced shear strength, $\tau^{\circ}_{e'}$ will change (and generally decrease) with increased tensile loading.

APPENDIX C

STATIC FAILURE ANLAYSIS EXAMPLES

This appendix gives examples of the notched laminate static failure analysis procedure. Unidirectional and multidirectional laminates are given separate consideration to bring out details of the analysis and to illustrate the major differences between the two systems. Laminates chosen for example computations are [0] and $[0_2/\pm 45]$ boron/epoxy.

Unidirectional Systems

Unidirectional composites are special from the failure sense in that the only crack propagation modes are along the zero degree fiber in the load direction or transversely across the composite normal to the loading direction. As such, only the axial and transverse crack propagation modes need to be considered, and off-axis cracking is not a possibility. Input data to the failure analysis are the unnotched laminate unidirectional tensile strength σ_x^t, the unnotched laminate shear strength $\tau°$, the laminate shear modulus G_{xy}, the laminate extensional modulus E_x, the laminate ultimate strain in axial shear γ_{ult}, notch size 2a, and over-stressed zone size m.

As an example of the procedure for determining static failure of unidirectional composites, a boron/epoxy [0] laminate is analyzed. As mentioned previously, the analysis predicts the stress σ_A at which an axial crack grows to infinity under an applied tensile stress, σ. The analysis also determines the maximum stress, σ_{SCFM}, which exists in the material adjacent to the notch and the corresponding applied laminate stress, σ_M, at which it occurs. In all cases, $0<\sigma_M<\sigma_A$.

It is to be expected that failure strengths of a notched composite will vary with the constituent material properties of the

laminate and the notch size. Figure C-1 illustrates, for a typical [0] boron/epoxy composite laminate with a 2.54cm notch, how the axial failure stress and the adjacent material overstress with corresponding laminate tensile stress can vary with properties. In this example, laminate shear failure stress, τ°, and the shear failure strain, γ_{ult}, are varied and the shear modulus G_{xy} is held constant. Generally speaking, lower values of τ° and γ_{ult} will give notched laminates with lower axial crack propagation failure strengths. Also, this same trend of lower τ° and γ_{ult} will reduce the laminate stress concentration and therefore lower the tendency for a transverse crack to develop. For increasing values of τ° and γ_{ult}, the reverse situation is true. Axial crack propagation in the axial direction is impeded with increasing τ° and γ_{ult}, and stress concentrations in material adjacent to the notch are increasing. Therefore, tendency of the notched laminate to fail by a transverse crack propagation mode is enhanced by increasing τ° and γ_{ult}.

Material properties for a typical [0] unnotched B/Ep laminate are given in Table C-1. To obtain predictions of the failure model for static notched laminate strength, the typical failure shear stress and shear failure strain from Table C-1 of 105 MN/m^2 and .038 m/m, respectively, are entered into Figure C-1a. The resulting prediction for axial crack propagation failure stress is about 380 MN/m^2. In Figure C-1b, the predicted value of maximum composite overstress is σ_{SCFM}=930 MN/m^2, which is considerably less than the unnotched tensile strength of 1300 MN/m^2 for the laminate. The transverse tensile failure mode will, therefore, not occur. Static failure predictions for this laminate and notch size are that the notched composite will fail due to axial crack propagation at a stress level of 380 MN/m^2.

Figure C-2 illustrates the variation of axial crack propagation mode failure stress and maximum composite overstress for a 0.635 cm notched boron/epoxy material. The model predicts σ_A = 580 MN/m^2 and σ_{SCFM} = 1030 MN/m^2. Since the composite overstress is still

less than 1300 MN/m^2 (the failure stress for the unnotched laminate), transverse crack propagation will still not occur for this laminate. However, the 0.635cm notch axial crack propagation mode strength is considerably higher than for the 2.54cm notch. This trend generally follows observed experimental behavior for the effect of notch size on strength of notched composite laminates (Reference 2).

Multidirectional Systems

Failure predictions for multidirectional composite laminates differ significantly from [0] composite laminates in two major ways. First, as discussed previously, there are three possible failure modes rather than two. These are: axial crack propagation along a zero degree fiber, transverse crack propagation across the specimen normal to the direction of loading, and off-axis crack propagation along one of the off-axis fiber directions. The second main difference is in the stress-strain behavior in axial shear. For [0] laminates, the stress-strain behavior in axial shear is nonlinear, and can be approximated by a bilinear elastic/plastic stress strain curve. For multidirectional laminates, the constraining effect of the fibers will tend to eliminate matrix nonlinear effects. As a result, stress-strain behavior for almost any loading condition on a multidirectional laminate will be nearly linearly elastic to failure. Therefore, to a good degree of approximation, $\gamma_{ult} = \tau^\circ/G_{xy}$. For multidirectional laminates, therefore, shear stress-strain behavior can be completely described knowing only τ° and G_{xy}. For [0] laminates, however, γ_{ult}, τ°, and G_{xy} can all be independent variables.

As an example of the method used to predict the failure mode and failure stress of a notched multidirectional laminate, a boron/epoxy $[0_2/\pm45]$ laminate with a 2.54cm slit center notch is selected. It is assumed that this laminate has the overall properties shown in Table C-2 which are predicted from unidirectional proper-

ties given in Table C-1. The laminate predictions were made using a standard constant-strain laminate analysis technique and utilized a maximum stress failure criterion. While agreement with experimental data is not exact, the predicted values to be used are reasonably close to experimental values.

Axial/transverse crack propagation.- Laminate properties shown in Table C-2 were utilized in the analysis described in Appendix A and the main text. The variation of σ_A and σ_{SCFM} with the laminate shear properties $\tau°$ and G_{xy} were calculated from the analysis. Figure C-3 shows the results in graph form. The failure stresses in the axial and transverse crack propagation modes can be determined from Figure C-3 if laminate shear properties are known. It is seen that the predicted value of axial crack propagation stress for the specific laminate properties in Table C-2 is $\sigma_A = 250$ MN/m^2. From Figure 11b, the maximum overstress in material adjacent to the notch is $\sigma_{SCFM} = 545$ MN/m^2. When this number is compared to the 710 MN/m^2 tensile failure stress of the unnotched laminate, it is concluded that transverse crack propagation will not take place. This notched laminate is therefore predicted to fail by axial crack propagation at $\sigma_A = 250$ MN/m^2.

Off-axis crack failure.- Once the failure stress has been determined for the axial/transverse modes, it is necessary to determine the stress which would cause off-axis cracking. In this case, off-axis cracking could occur along fibers in the ±45 degree directions. For the off-axis analysis, the laminate is considered in an x'y' coordinate system where x' lies along the -45° fibers in the direction of the crack. The resulting laminate is a $[0/+45_2/90]$ laminate in the x'y' coordinate system as shown in Figure C-4a. The laminate stress state in this coordinate system is $\sigma_{x'} = \sigma/2$, $\sigma_{y'} = \sigma/2$, and $\sigma_{x'y'} = \sigma/2$.

For computational purposes, it is assumed that a $[0/+45_2/90]$ laminate exhibits the same notched composite failure characteris-

tics as does a [0/±45/90] laminate. Elastic and unnotched failure properties were predicted from a constant strain laminate analysis using a maximum stress failure criterion. Results for these are shown in Table C-3 for $[0_2/\pm45]$, $[0/+45_2/90]$, and [0/±45/90] boron/epoxy laminates. For comparison, experimental results for the $[0_2/\pm45]$ laminate from Reference 10 are also shown in Table C-2. Note that only the axial shear modulus, G_{xy}, and the shear failure stress, $\tau°$, differ to any great extent between the $[0/+45_2/90]$ and [0/±45/90] laminates. Therefore, results of the failure model for a [0/±45/90] laminate are used with the shear modulus and failure shear stress for the $[0/+45_2/90]$ laminate to predict the x' axial failure stress, $\sigma_{A'}$. It is noted that since we are dealing with a slit notch, the effective notch width in the x'y' coordinate system is now 2.54cm x cos 45°, or 1.80cm. (Figure C-4a).

The off-axis propagation mode strength for the $[0_2/\pm45]$ laminate is given as a function of $G_{x'y'}$ and $\tau°'$ in Figure C-4b. Using the shear modulus and axial shear strength for the $[0/+45_2/90]$ laminate gives a value of 445 MN/m^2 for $\sigma_{A'}$ (not shown in the figure). This value, however, is not the failure stress of the notched laminate in the x' coordinate system, because it includes the effects of only $\sigma_{x'} = \sigma/2$. The effects of $\sigma_{y'}$ and $\sigma_{x'y'}$ have yet to be determined. As evidenced by equation (B1), Appendix B the failure stress in x'y' shear to be used in the analysis is dependent upon the values of $\sigma_{y'}$ and $\sigma_{x'y'}$. For this laminate, $\sigma_{x'} = \sigma_{y'} = \sigma_{x'y'} = \sigma_{A'}$. Equation (B1) may therefore be rewritten for this particular system to read:

$$\left(\frac{\tau_e^{\circ\prime}}{\tau^{\circ\prime} - \sigma_{A'}}\right)^2 + \frac{\sigma_{A'}^2 + 2\sigma_{A'}\sigma_{y'}^d}{\sigma_{y'}^{p2}[1-(\sigma_{y'}^d/\sigma_{y'}^p)^2]} = 1 \qquad (C1)$$

This equation may be solved for $\tau^{\circ\prime}$ if $\sigma_{A'}$ is known. However, the particular value of $\tau^{\circ\prime}$ desired is the one which corresponds to the failure stress σ which is at present unknown. Therefore, following the procedure outlined in the main text, several values are chosen for $\sigma_{A'}$ between 0 and 445 MN/m^2, and the corresponding values of $\tau_e^{\circ\prime}$ are calculated from equation (C-1). The curve of Figure C-4b is then entered with each of these $\tau_e^{\circ\prime}$ values and a corresponding $\sigma_{A'}$ is computed. The calculated $\sigma_{A'}$ which coincides with the value of the assumed $\sigma_{A'}$ is the desired failure stress. In this case, the failure stress is found to be 176 MN/m^2. The corresponding $\sigma_e^{\circ\prime}$ is shown in Figure C-4b. Since for $\theta = 45°$ $\sigma_{A'} = \sigma_{x'} = \sigma/2$, the axial tensile stress in the x-direction which causes 45° off-axis cracking is $\sigma = 352$ MN/m^2.

Predicted failure mode and failure stress.- The stress at which off-axis cracking occurs is higher than the failure stress of 250 MN/m^2 predicted for the 0° axial crack propagation mode. Therefore, the static failure mode predicted for the 2.54cm notched B/Ep $[0_2/\pm45]$ laminate is axial crack propagation in the x-direction at an applied tensile stress of 250 MN/m^2.

TABLE C-1

TYPICAL [0] BORON/EPOXY ELASTIC
AND FAILURE PROPERTIES

MODULI (GN/m^2)	INITIAL TANGENT	SECANT TO FAILURE
Young's E_{11}	207	207
Young's E_{22}	22.8	17.4
Shear Modulus G_{12}	6.4	2.8
Axial Poisson's Ratio, ν_{12}	0.21	0.21

FAILURE STRESSES (MN/m^2)	
Axial Tension σ_{11}^t	1296
Axial Compression σ_{11}^c	2496
Transverse Tension σ_{22}^t	69
Transverse Compression σ_{22}^c	310
Axial Shear τ_{12}^o	105

FAILURE STRAINS (m/m)	
Axial Tension	6.27×10^{-3}
Axial Compression	12.07×10^{-3}
Transverse Tension	3.95×10^{-3}
Transverse Compression	17.80×10^{-3}
Axial Shear (Engineering) γ_{ult}	38.25×10^{-3}

TABLE C-2

BORON/EPOXY LAMINATE ELASTIC AND FAILURE PROPERTIES

LAMINATE	$[0_2/\pm45]$ EXPERIMENT, REF. 10	LAMINATE ANALYSIS RESULTS*		
		$[0_2/\pm45]$	$[0/45_2/90]$	$[0/\pm45/90]$
Axial tens. failure stress σ_x^t (MN/m^2)	717	710	266	325
Axial tens. failure strain 10^{-3} m/m	6.6	6.3	4.06	4.24
Axial shear failure stress $\tau°$ (MN/m^2)	-	285	416	285
Axial shear failure strain γ_{ult} 10^{-3} m/m	-	9.96	-	-
Axial Young's modulus E_x (GN/m^2)	116	112	65.6	76.5
Trans. Young's modulus E_y (GN/m^2)	33	32.6	65.6	76.5
Axial shear modulus G_{xy} (GN/m^2)	-	28.6	18.9	28.6
Axial Poisson's ratio ν_{xy}	0.70	0.75	-	-

*Constant strain analysis, max. stress failure criterion

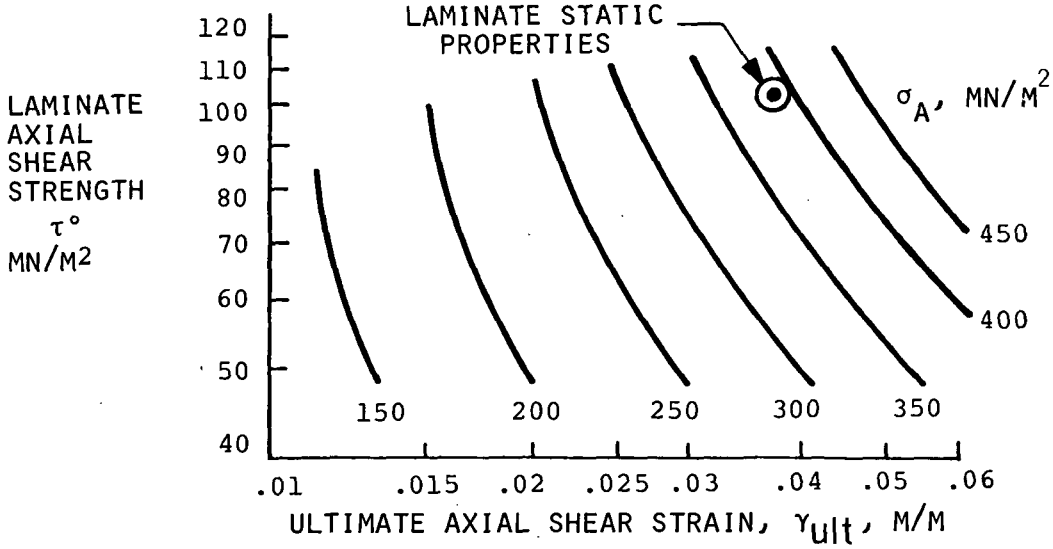

(a) NOTCHED LAMINATE TENSILE STRENGTH, σ_A, AXIAL CRACK FAILURE MODE.

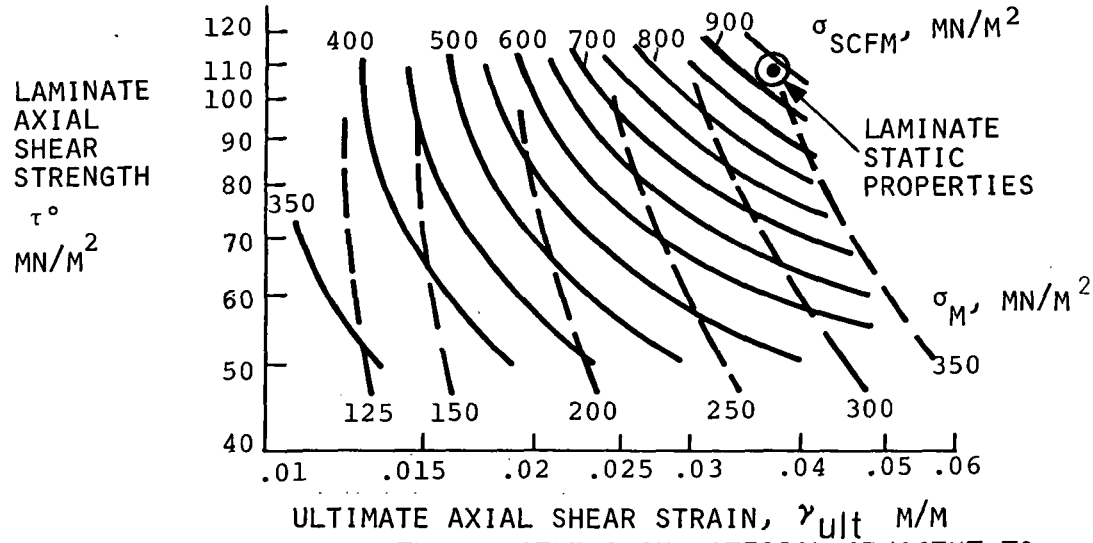

(b) COMPOSITE OVERSTRESS IN MATERIAL ADJACENT TO NOTCH, σ_{SCFM}, AND CORRESPONDING FAR FIELD APPLIED GROSS STRESS, σ_M.

FIGURE C-1. STATIC FAILURE BEHAVIOR OF [0] BORON/EPOXY NOTCHED LAMINATE. NOTCH SIZE = 2.54 cm.

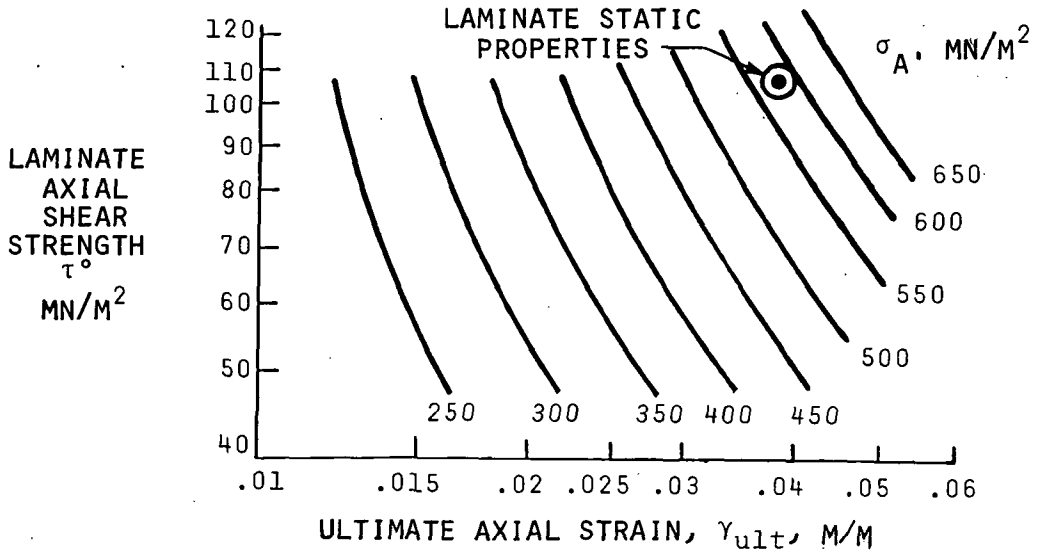

(a) NOTCHED LAMINATE TENSILE STRENGTH, σ_A, AXIAL CRACK FAILURE MODE

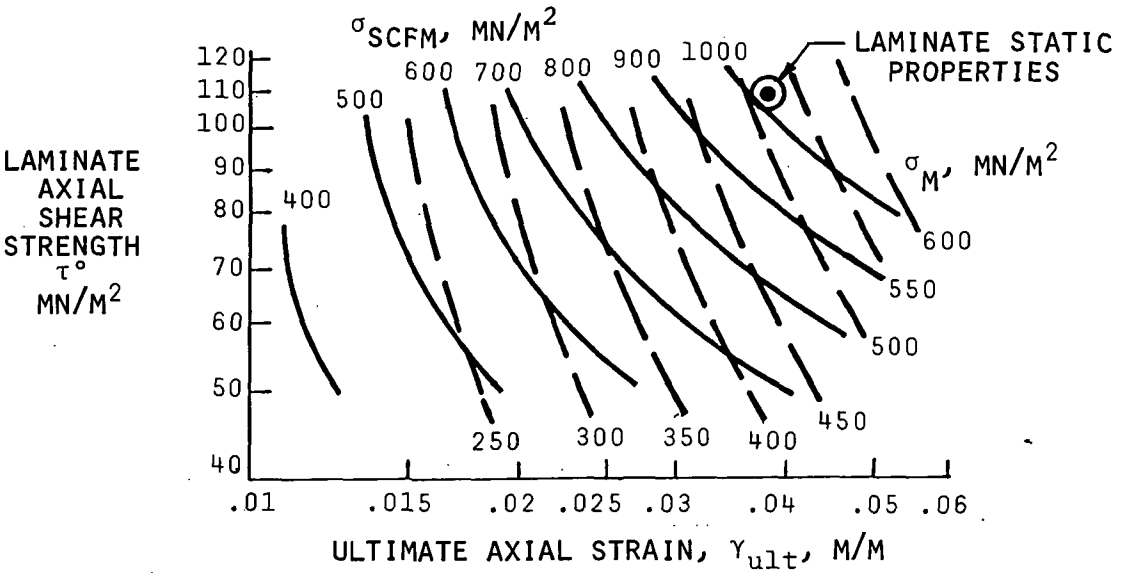

(b) COMPOSITE OVERSTRESS NEAR NOTCH σ_{SCFM}, AND CORRESPONDING FAR FIELD APPLIED GROSS STRESS, σ_M.

FIGURE C-2. STATIC FAILURE BEHAVIOR OF [0] BORON/EPOXY NOTCHED LAMINATE. NOTCH SIZE = 0.635 CM.

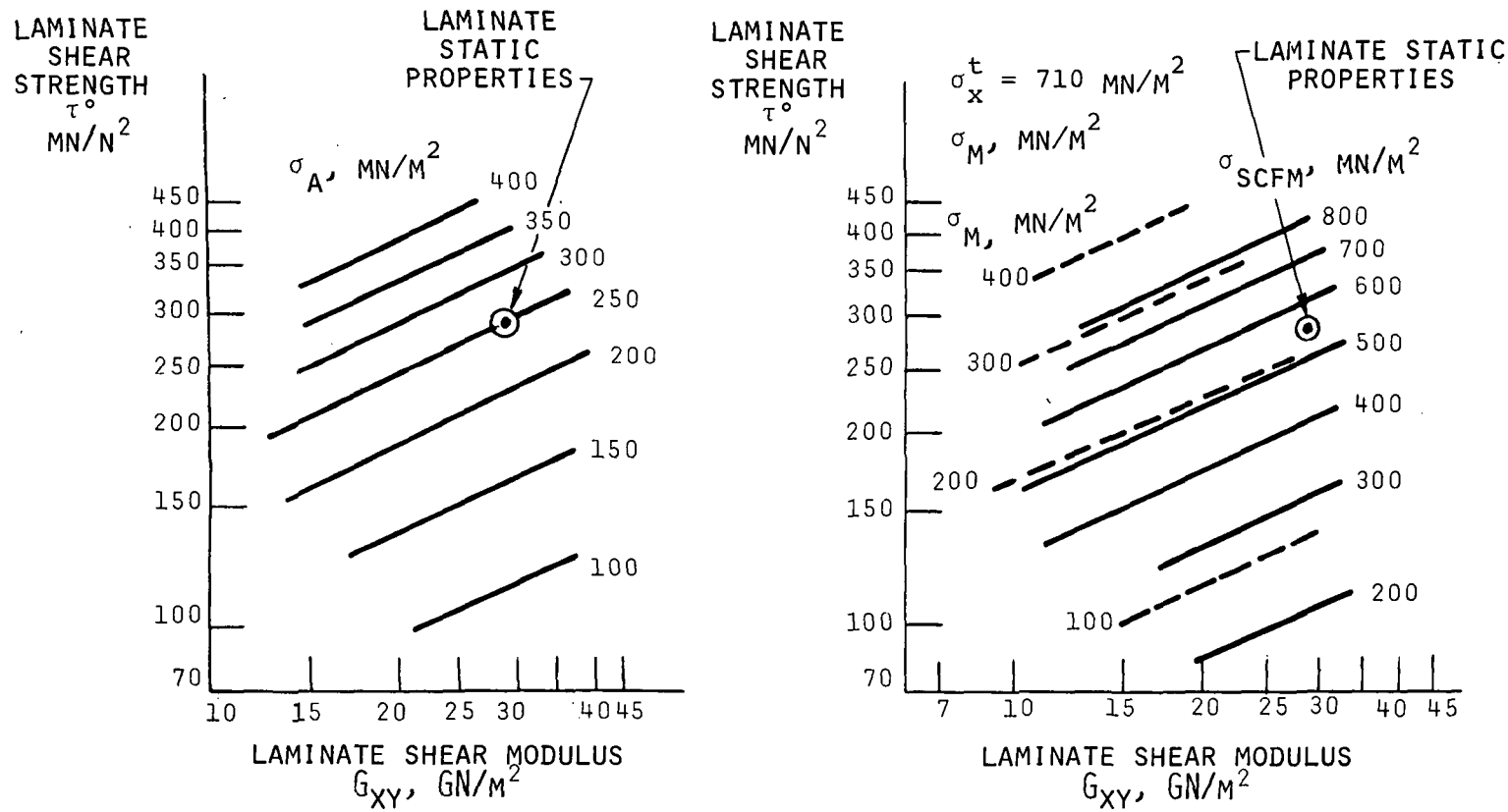

(a) NOTCHED LAMINATE TENSILE STRENGTH, σ_A, AXIAL CRACK FAILURE MODE

(b) COMPOSITE OVERSTRESS NEAR NOTCH, σ_{SCFM}, AND CORRESPONDING FAR FIELD APPLIED GROSS STRESS, σ_M

FIGURE C-3. STATIC FAILURE BEHAVIOR OF BORON/EPOXY [0_2/±45] NOTCHED LAMINATE. NOTCH SIZE = 2.54 CM.

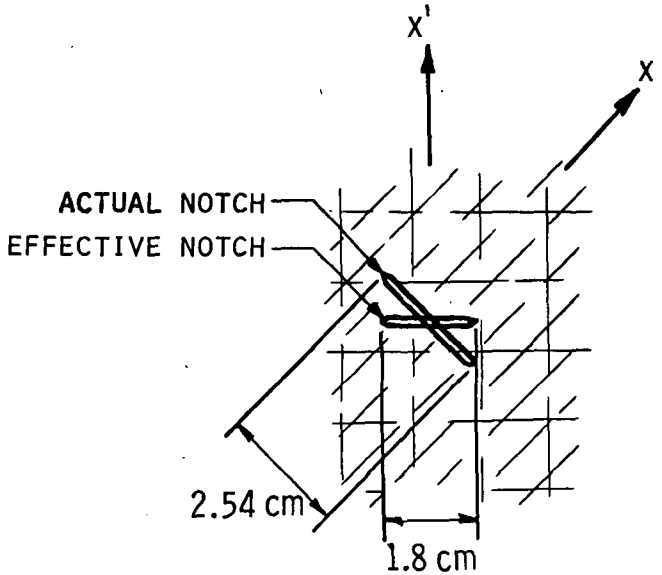

(a) EQUIVALENT AXIAL PROBLEM FOR OFF-AXIS FAILURE

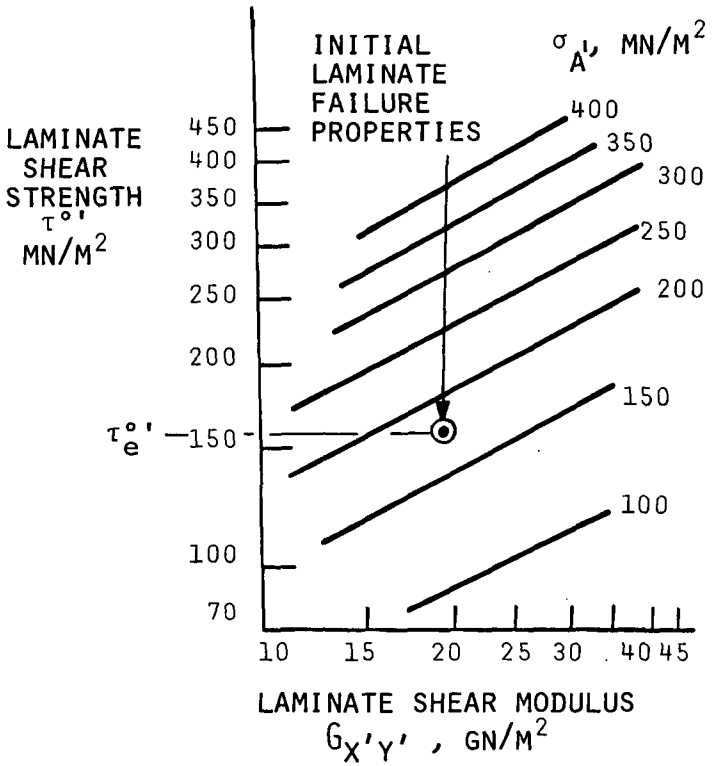

(b) NOTCHED LAMINATE TENSILE STRENGTH, $\sigma_{A'}$, AXIAL CRACK FAILURE MODE IN X'Y' SYSTEM

FIGURE C-4. OFF-AXIS FAILURE BEHAVIOR OF BORON/EPOXY [$0_2/\pm45$] SLIT NOTCHED LAMINATE. NOTCH SIZE = 2.54 cm.

APPENDIX D

NOTCH ROOT STRESS STATE CONSIDERATIONS

Knowing the notch room stress state during cyclic loading is critical to determination of material property degradation in the notch region. This appendix discusses methods for obtaining these stresses, evaluates the relative importance of laminate axial shear and axial tension, and discusses the relative effects of lamina stresses on laminate property degradation.

Laminate Stress State Near Notch

Inside the core region near the notch, laminate material will be under a stress state which is primarily axial shear. Outside the core region in the overstressed material adjacent to the notch, axial tension will be present in addition to axial shear. In general, the stress levels will decrease with increasing distance from the notch. The static failure model is capable of predicting the variation of shear stress, τ, and the composite overstress in adjacent material, σ_{SCF}, as functions of distance x from the notch. (τ is assumed constant with y in the shear transfer region, and σ_{SCF} is assumed constant with y in the overstressed zone). Theoretically, these stresses could be used to predict material property degradation as a function of x and number of cycles N. A static failure analysis could be developed which allowed material properties to vary with x, and a fatigue analysis could be performed taking into account the spacial variation in fatigue-degraded properties.

Such a procedure is beyond the scope of the present effort. Instead, it is assumed that enough accuracy can be obtained by selecting an average stress state in the notch region, and allowing all material to degrade uniformly. This average stress state will be one of axial shear, τ^n, and/or axial tension, σ^n.

The most accurate method of predicting τ^n and σ^n under an applied cyclic stress σ_{max} is to utilize the static failure analysis under the laminate stress σ_{max}. The maximum shear stress, τ_M, and maximum overstress in adjacent material, σ_{SCFM}, can be computed from this analysis. It can therefore be assumed that the notch root stresses causing the major material property changes are:

$$\tau^n = k_1 \tau_M \qquad \text{(D1)}$$
$$\sigma^n = k_2 \sigma_{SCFM}$$

Where the k's are empirical constants which can be chosen either analytically to represent "average" stresses or experimentally to fit test data.

Stress concentrations predicted by the static failure analysis are typically 1.2 - 1.5. A second less accurate method of selecting notch root tensile stress would be to set:

$$\sigma^n = k_3 \sigma_{max} \quad , \quad k_3 = 1.2 - 1.5 \qquad \text{(D2a)}$$

A companion assumption for estimating average notch root shear stress is to assume that the maximum shear stress at the notch bears the same relationship to laminate axial shear failure strength $\tau°$ as the laminate cyclic maximum stress, σ_{max}, bears to the initial static axial mode failure strength of the notched laminate, $\sigma_A°$. Since this is approximate, it is anticipated that an empirical factor might be necessary to achieve the necessary correlation with experimental data. This results in the following equation:

$$\tau^n = k_4 \frac{\sigma_{max}}{\sigma_A^\circ} \tau° \qquad \text{(D2b)}$$

An alternate estimate of τ^n to go with (D2a) is the reduced laminate axial shear strength, $\tau°_{\sigma max}$, which would cause static failure of the notched laminate to occur at σ_{max}:

$$\tau^n = k_5 \tau°_{\sigma max} \qquad \text{(D2c)}$$

In all cases, the k_i are empirical constants of order unity.

Effects of Stress Components in Laminate Fatigue

It is desirable to determine the relative importance of laminate axial shear stress, τ^n and axial normal stress, σ^n, to the fatigue degradation of material around the notch. If σ^n does not contribute significantly to degradation, then the core and overstressed regions will degrade to approximately the same degree. Fatigue analysis can be performed using a simple shear stress state, which is easier to handle analytically than combined tension and shear. Also, the lamina fatigue data base generally required for analysis includes fatigue behavior under axial normal stress, transverse normal stress, and axial shear stress. If it could be demonstrated that one of the stress components (σ_{11} for example) caused negligible damage compared with the others, the required data base for fatigue analysis could be reduced.

To investigate the above topics, selected boron/epoxy laminates from the family $[0_i/\pm45_j/90_k]$ are analyzed. Standard constant strain laminate analysis techniques are used to determine layer stresses under laminate stress states which approximate the states of stress near the notch. Two stress states are considered: (1) unit xy shear stressing and (2) equal unit tensile stressing in the x direction coupled with unit xy shear stressing (see Figure 3 main text).

Laminates analyzed are [0], [0/90], [±45], [0/±45], $[0_2/\pm45]$ and [0/±45/90]. The results are shown in Tables D-1 and D-2. The stresses σ_{11}, σ_{22} and σ_{12}, shown in column 4, Table D-2, are the layer stresses due to the unit laminate gross state stress shown in the far left hand column. (σ_{11} is normal stress in the fiber direction, σ_{22} is normal stress transverse to the fiber direction, and σ_{12} is axial shear stress, Figure 3b). The relative sizes of these stresses are important to deciding whether or not a particular stress component causes damage. Accordingly, their ratios are shown in columns 5 through 7. A lower case t indicates normal tensile stress and a lower case c indicates normal compres-

sive stress. Since the sign of the shear stress is irrelevant to failure, it is always positive. The symbols t/c, etc. in column 6 indicate that σ_{11} is tensile and σ_{22} is compressive, etc.

As a rough gauge of the importance of a particular stress component to the fatigue degradation occurring in a particular layer, the relative stress ratios for each layer are compared to ratios of the static failure stresses for a unidirectional layer. The static failure stresses for boron/epoxy are shown in Table C-1, Appendix C, and their ratios are shown in Table D-1. The computed stress ratios for each layer and loading condition are shown in columns 5 - 7, Table D-2. In column 8, Table D-2, is given an estimate of the fatigue failure mode for each layer which was obtained by comparing each layer stress ratio with the corresponding failure stress ratios. As an example of the procedure followed, consider the [±45] laminate under the pure shear stress state $\sigma_{xy} = 1$. Laminate analysis shows that axial tensile and transverse tensile stresses were both enormously higher than axial shear stresses. Therefore, axial shear is not a likely fatigue failure mechanism with the [±45] laminate. In the +45° layer, the ratio of σ_{11} to σ_{22} is 14.6, with σ_{11} tensile and σ_{22} compressive. The ratio of equivalent static failure loads, shown under t/c as 4, is obviously much lower than the relative stress ratio in the laminate. This would indicate that axial tensile stress is the most likely candidate for causing fatigue failure in the +45° layer. On the other hand, the -45° layer experiences axial compression and transverse tension. The stress ratio of 14.6 c/t, when compared with a static failure ratio of 36 c/t, indicates that the tensile stress is probably not high enough to cause significant fatigue damage, and the main fatigue damage most likely results from a matrix damage mode in transverse tension.

Based upon the individual layer results, an estimate is made of the layers in each laminate which are most likely to fail under xy fatigue loading. A prediction is then made of the mode of fail-

ure. Results are shown in column 9 of Table D-2.

A camparison of results for all laminates analyzed under the pure shear and combined tension shear stress state shows the following:

(a) Significant differences in lamina stress states exist between pure shear and combined tension/shear cracking, but

(b) These differences do not appear to significantly affect the outcome of fatigue failure predictions except possibly for the [±45] laminate.

It is concluded that inclusion of axial laminate tension σ^n in the notch root stress state for fatigue analysis may not be necessary. A final judgement, however, should await more complete analysis and experimental data.

It is seen from column 9, Table D-2, that all lamina stress components play an important role in fatigue behavior in the notch region. Lamina fatigue data base tests should therefore be performed under axial tension, transverse tension, and axial shear. It is noted that axial shear is important only to unidirectional [0] and bidirectional [0/90], [±45] laminates. For typical aerostructure layups such as [0/±45], [0/±45/90], and $[0_2/\pm 45]$, shear is not an important source of lamina degration. This indicates that, for these laminates, lamina fatigue data base tests need only be performed on tensile specimens with [0] and [90] configurations to develop σ_{11} and σ_{22} data.

TABLE D-1. UNIDIRECTIONAL BORON/EPOXY COMPOSITE STATIC FAILURE STRESSES AND FAILURE STRESS RATIOS

STRESS COMPONENT	STATIC TENSILE STRENGTH σ^t, MN/m^2	STATIC COMPRESSIVE STRENGTH σ^c, MN/m^2
σ_{11}	1296	2496
σ_{22}	69	310
σ_{12}	105.5	

RATIOS OF STATIC FAILURE STRESSES		
$\frac{\sigma_{11}}{\sigma_{12}}$	t*	12
	c**	24
$\left\lvert\frac{\sigma_{11}}{\sigma_{22}}\right\rvert$	t/t***	19
	t/c	4
	c/t	36
	c/c	8
$\frac{\sigma_{22}}{\sigma_{12}}$	t	0.7
	c	3

* Indicates tensile normal stress
** Indicates compressive normal stress
*** Gives sign of σ_{11} and σ_{22} stresses, respectively

TABLE D-2. PREDICTED IMPORTANCE OF STRESS COMPONENTS TO FATIGUE OF NOTCHED LAMINATES

(1) LAMINATE STRESS STATE (σ_x, σ_y, σ_{xy}) (See Fig. 3a)	(2) LAMINATE	(3) LAYER θ DEG.	(4) Layer Stresses (See Fig. 3b.) σ_{11}	σ_{22}	σ_{12}	(5) $\frac{\sigma_{11}}{\sigma_{12}}$	(6) $\frac{\sigma_{11}}{\sigma_{22}}$	(7) $\frac{\sigma_{22}}{\sigma_{12}}$	(8) PROBABLE LAYER FAILURE MODE**	(9) IMPORTANT LAYERS & MODES IN FATIGUE**
(0,0,1)	[0]	0°	0	0	1	0	-	0	S	S, 0
	[0/90]	0° 90°	0 0	0 0	1 1	0 0	- -	0 0	S S	S, 0 S, 90
	[±45]	+45° -45°	1.872 -1.872	-0.128 0.128	0 0	∞t* ∞c	14.6 t/c* 14.6 c/t	∞c ∞t	AT, TT } 15 t/t	AT, +45 TT, -45
	[0/±45]	0° +45° -45°	0 2.738 -2.738	0 -0.187 0.187	0.074 0 0	0 ∞t ∞c	- 14.6 t/c 14.6 c/t	0 ∞c ∞t	S AT, TT } 15 t/t	- AT, +45 TT, -45
	[0/±45/90]	0° +45°	0 3.564 -3.564 0	0 -0.244 0.244 0	0.096 0 0 0.096	0 ∞t ∞c 0	- 14.6 t/c 14.6 c/t -	0 ∞c ∞t 0	S AT, TT } 15 t/t S	- AT, +45 TT, -45 -
	[0_2/±45]	0° +45° -45°	0 3.564 -3.564	0 -0.244 0.244	0.096 0 0	0 ∞t ∞c	- 14.6 t/c 14.6 c/t	0 ∞c ∞t	S AT, TT } 15 t/t	- AT, +45 TT, -45
(1,0,1)	0	0°	1	0	1	1t	t/t	0	S	S, 0
	[0/90]	0° 90°	1.844 -0.028	0.028 0.156	1 1	1.8t 0.03c	66 t/t 0.2 c/t	0.03t 0.16t	S S	S, 0 S, 90
	[±45]	+45° -45°	2.780 -0.964	-0.036 0.220	0.5 0.5	5.6t 1.9c	77 t/c 4.4 c/t	0.07c 0.4t	S S, TT	- S, TT, -45
	[0/±45]	0° +45° -45°	2.606 2.979 -2.497	-0.137 -0.163 0.212	0.074 0.064 0.064	35t 47c 39c	19 t/c 18.3 t/c 11.8 c/t	1.9c 2.4c 3.3t	AT AT, TT } 14 t/t	- AT, +45 TT, -45
	[0/±45/90]	0° +45° -45° 90°	2.690 4.472 -2.655 -0.874	-0.030 -0.152 0.335 0.214	0.096 0.048 0.048 0.096	28t 93t 55c 9.1c	90 t/c 29 t/c 7.9 c/t 4.1 c/t	0.31c 3.2c 7t 2.2t	AT AT, TT } 13 t/t TT	- AT, +45 TT, -45 -
	[0_2/±45]	0° +45° -45°	1.828 3.797 -3.33	-0.085 -0.22 0.267	0.096 0.043 0.043	19t 88t 77c	22 t/c 17 t/c 12.5 c/t	0.9c 5.1c 6.2t	AT AT, TT } 14 t/t	- AT, +45 TT, -45

* t = normal tensile stress, c = normal compressive stress
t/c = σ_{11} tensile and σ_{22} compressive etc.

** AT = axial tension, TT = transverse tension, S = axial shear.
Also shown are stress component ratios between modes most likely to fail.

APPENDIX E

OFF-AXIS LAMINATE COMBINED STRESS STATE IN FATIGUE

In an off-axis fatigue failure analysis, transverse laminate stress $\sigma_{y'}$ and axial shear stresses $\sigma_{x'y'}$ are present in addition to axial tension $\sigma_{x'}$. This appendix presents two methods for determining the combined stress effects on the notch root material fatigue behavior. One is a laminate analysis technique, and the other is an empirical method.

The laminate analysis technique of determining off-axis x'y' laminate shear property degradation utilizes the laminate stress state around the notch (Figure 7, main text) directly in a laminate analysis to obtain individual layer stresses. These stresses are used with individual layer fatigue data to predict changes in individual layer properties. Laminate analysis is then used to reconstruct laminate shear properties from the changed layer properties. It is expected that this first method will be the more accurate.

The empirical method is based on the assumption that laminate transverse tension and axial shear can be treated by adding to the shear stress which would exist due to only axial $\sigma_{x'}$ tension. First, it is assumed that the tensile stress $\sigma^{n'}$ and the shear stress which would be present at the notch root due to the tensile stress $\sigma_{x'}$ can be chosen by methods previously presented in Appendix D. The applied laminate shear stress, $\sigma_{x'y'}$, is assumed to add directly to $\tau^{n'}$. Transverse tension $\sigma_{y'}$ is assumed to cause an artificial increase in shear stress through an empirical quadratic interaction. The result is an off-axis effective notch root shear $\sigma_e^{n'}$ which empirically takes into account the combined stress state at the notch. This effective shear can be found from the equation:

$$\left(\frac{\sigma_{y'} + \sigma^{d}_{y'}}{\sigma^{p}_{y'}}\right)^{2} + \left(\frac{\tau^{n'}_{e}}{\tau'^{p}}\right)^{2} = 1 \qquad \text{(E1)}$$

Where $\tau^{n'}_{e}$ = effective laminate notch shear stress, and

$$\tau'^{p} = \frac{\tau^{n'} + \sigma_{x'y'}}{[1 - (\sigma^{d}_{y'}/\sigma^{p}_{y'})^{2}]^{\frac{1}{2}}}$$

$$\sigma^{d}_{y'} = \frac{\sigma^{c}_{y'} - \sigma^{t}_{y'}}{2}$$

$$\sigma^{p}_{y'} = \frac{\sigma^{c}_{y'} + \sigma^{t}_{y'}}{2}$$

$\sigma^{t}_{y'}$ is the laminate tensile strength in the y' direction, $\sigma^{c}_{y'}$ is the compressive strength of the laminate in the y' direction. Once $\tau^{n'}$ has been determined, an x' axial fatigue analysis is performed using methods previously outlined.

APPENDIX F

INTERACTION EFFECTS OF LAYER STRESS COMPONENTS IN FATIUGE

Interaction effects of stress components on static failure have been known and studied for some time (see, for example, References 7 and 8). Results of research in this area have been along two lines. One is empirical wherein forms for failure interaction equations under combined stresses are assumed and fit to test data (Reference 7, for example). The second consists of micromechanical anlaysis approaches which take account of known heterogeneities and failure modes to analytically arrive at failure interaction behavior (Reference 8). Experimental and analytical results indicate that the main in-plane stress interactions appear to be between transverse normal stress, σ_{22}, and axial shear stress, σ_{12}.

It is reasonable to assume that static interaction results will be qualitatively true for fatigue loading. Hashin and Rotem (Reference 9) have developed a quadratic interaction theory which empirically treats the fatigue of a unidirectional layer under combined axial shear and transverse normal stresses. In their theory, axial stress is assumed to be uncoupled from the other two stress components in fatigue. In the present formulation, the assumption of uncoupled fatigue behavior between axial normal stress and the other in-plane stress components will be maintained. Due, however, to the complexity of the experimental information which is necessary to fully utilize the Hashin-Rotem theory, a less complicated interaction between σ_{22} and σ_{12} will be proposed here. Fatigue tests of [90] and [±45] laminates are relatively easy to perform, and, with some approximations or additional analysis work, will reasonably predict the transverse tensile and axial shear behavior of a [0] laminate. It is, therefore, desirable to be able to predict lamina fatigue behavior under combined transverse tension and in-plane shear knowing fatigue behavior either in axial shear only ([±45] laminate in tension), or in transverse tension only.

The physical basis for the proposed empirical interaction is as follows. Failure under axial shear and transverse normal stresses are both related to matrix or fiber-matrix interface failure. If one makes the further assumption that failure under both stress components is phenomenologically similar on an atomistic level, then one could in principle predict fatigue failure properties in axial shear from those in transverse normal stress and vice versa.

In the succeeding development, it will be assumed that axial shear σ_{12} is the stress component for which experimental results are available, and the effects of σ_{22} upon this information is desired. The development for the effects of σ_{12} in known σ_{22} behavior is identical, and is not presented here.

Suppose that the complete fatigue lifetime and residual strength behavior of a unidirectional lamina in axial shear is known from experiment. From this information, it must be possible to determine the fatigue lifetime, residual shear strength, residual shear failure strains at a given N for a given maximum cyclic shear stress level. The effect of the additional transverse normal stress component will be assumed to accelerate fatigue degradation. This will be done through an increased "effective" shear stress level and a resulting "effective" $S_{12} = \sigma_{12}/\tau^{\circ}_{12}$ (here, τ°_{12} is lamina static axial shear strength). It is necessary that S^{e}_{12}, the effective S_{12} be equal to the actual S_{12} when σ_{22} is zero. Also, as σ_{22} approaches its failure value in either tension or compression, it is reasonable to assume that its effect is similar to cycling at an effective shear stress close to the static failure shear stress, τ°.

Two possible forms of interaction between S^{e}_{12} and σ_{22} are shown in Figure F-1. One form of interaction is linear and the other is quadratic. The quadratic curve generally gives more weight to higher levels of transverse stress and less weight to the lower levels of transverse stress. In addition, it lowers S^{e}_{12} when small to moderate amounts of transverse compression are ap-

plied. These are physically logical possibilities because moderate compressive stresses can retard crack propagation in either Mode 1 or Mode 2. The difficulty with this quadratic relationship is that for simple forms of a quadratic curve, it can predict a negative value. This situation is illustrated in the figure.

The approach taken here is to utilize a quadratic interaction formula with a zero minimum for S_{12}. The equation to be used is as follows:

$$\left(\frac{\sigma_{22} + \sigma_{22}^{d}}{\sigma_{22}^{p}}\right)^2 + \left(\frac{1 - S_{12}^{e}}{S^{p}}\right)^2 = 1 , \quad S_{12}^{e} \geq 0 \tag{F1}$$

(If $S_{12}^{e} < 0$ from above, set $S_{12}^{e} = 0$)

where

$$\sigma_{22}^{p} = \frac{\sigma_{22}^{c} + \sigma_{22}^{t}}{2} , \quad \sigma_{22}^{d} = \frac{\sigma_{22}^{c} - \sigma_{22}^{t}}{2} ,$$

$$S^{p} = \frac{S_{12} - 1}{[1 - (\sigma_{22}^{d}/\sigma_{22}^{p})^2]^{\frac{1}{2}}}$$

and the ^{c} and ^{t} refer to static failure stresses in compression and tension, respectively. The calculated value of S_{12}^{e} is used in place of S_{12} to predict layer axial shear property degradation from experimentally determined layer fatigue behavior. It is expected that the combined stress state will also cause degradation in transverse tensile properties. Specifically, transverse normal strength and transverse Young's modulus are anticipated to exhibit the greatest changes. It will be assumed that the degradations which occur in transverse normal strengths and transverse Young's modulus occur to the same degree as axial shear strength and axial shear modulus. Specifically, the same fractional reduction will be assumed in E_{22} as G_{12}, and in σ_{22}^{t} as τ_{12}°.

The procedure for determining the effect of transverse normal property degradations in a unidirectional layer is, therefore, to (a) determine, from laminate analysis techniques, the values of σ_{12} and σ_{22} in a given layer, (b) compute the effective non-dimensional maximum stress S^e_{12} from equations (F1), (c) utilize an experimentally determined axial shear fatigue wearout curve to determine the change in axial shear failure strength and axial shear modulus with number of cycles N, and (d) calculate the degradation of transverse Young's modulus and transverse normal strength by assuming that the reductions in these values are fractionally the same as have occurred in their shear mode counterparts.

If the situation is reversed, ie, transverse normal stress fatigue results are available and it is desired to determine the effect of σ_{12}, an exactly analogous procedure and equations are used.

It is expected that the predicted effect of σ_{22} on σ_{12} will be most accurate when σ_{22} is relatively small, and that the effect of σ_{12} on σ_{22} will be most accurate when σ_{12} is relatively small. In either situation, it is expected that prediction of pure transverse tension fatigue behavior from pure shear test results and vice versa may not give accurate results. It is therefore recommended that both transverse normal stress and axial shear data be obtained if it is known that both stress components will be important to fatigue degradations. Equation (F1) can then be used for situations where σ_{12} is dominant, and its counterpart for σ_{22} (not developed here) can be used when σ_{22} is dominant. It is noted that results of Appendix D indicate that σ_{22} is dominant for common $[0_i/\pm45_j/90_k]$ boron/epoxy laminates.

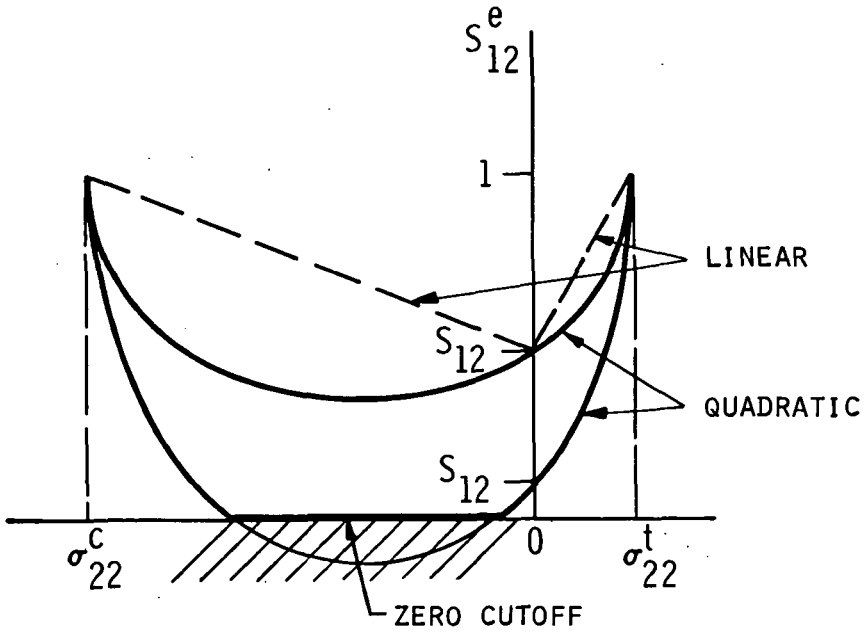

FIGURE F-1. "EFFECTIVE" SHEAR STRESS IN FATIGUE DUE TO TRANSVERSE TENSION.

APPENDIX G

FATIGUE FAILURE ANALYSIS EXAMPLES

Since fatigue analysis of unidirectional and multidirectional composite laminates differs in several respects, they will be treated separately through examples in more detail in this appendix.

Unidirectional Systems

As with static failure, the fatigue failure behavior of unidirectional laminates differs from multidirectional laminates. The fatigue failure modes for a unidirectional laminate can only be axial crack propagation or transverse crack propagation. Off-axis modes do not exist because of the lack of off-axis fibers along which the crack might propagate. In addition, there is currently no reason to postulate a relationship between $\tau°$, G_{xy}, and γ_{ult} as can be done for the nearly elastic multidirectional systems. Most importantly, the fatigue behavior of unidirectional systems will be dominated by matrix behavior since the laminate has no fiber systems running across an axial crack. Therefore, the fatigue analysis can be performed utilizing only fatigue behavior in axial shear of the unidirectional layer.

Example.- The procedure to be followed in analyzing unidirectional systems is exemplified by treating two hypothetical fatigue property variations of boron/epoxy laminate with a 0.64cm notch under cyclic loading. Figure G-1 illustrates these variations, termed Material A and B, respectively. Material A consists of a constant shear strength $\tau°$, a constant elastic shear modulus G_{xy}, and a decreasing ultimate shear strain γ_{ult} with number of cycles N. Material B, on the other hand, has constant G_{xy}, decreasing $\tau°$ and increasing γ_{ult} with number of cycles. Figure G-2 illustrates how the axial and transverse failure stresses vary with changes in laminate axial shear properties. Since G_{xy} is constant for both materials, the only variables are $\tau°$ and γ_{ult}.

Consider, first, the axial crack propagation mode, Figure G-2a. Material A and material B property variations with number of cycles are shown as straight lines with arrows indicating the direction of increasing N. Material A exhibits a decrease in the axial fatigue strength of the notched composite, while material B exhibits an increase in the axial crack propagation strength. Assume that in both cases the maximum cyclic stress for the laminate is 400 MN/m^2. From the figure it is seen that at somewhat less than 10^3 cycles, material A strength has been reduced to the maximum cyclic stress, and the material fails. Material B on the other hand, exhibits an always increasing axial fatigue propagation strength, so that run-out is predicted in this case.

It is necessary to also consider the transverse crack propagation mode. Figure C-2b shows variations of the overstress adjacent to the notch σ_{SCFM} and the corresponding laminate tensile stress σ_M with laminate material shear properties. For material A, it is seen that the overstress is initially near 1,000 MN/m^2 while the notched tensile strength is almost 1,300 MN/m^2. As cycling progresses, the maximum overstress in adjacent material decreases, removing any possibility that material A will fail in a transverse crack propagation mode.

For material B, the initial static strength prediction is, of course, identical to material A: transverse crack propagation does not occur initially because the overstress is less than the un-notched laminate strength. As cycling continues, σ_{SCFM} for material B decreases with N, although not quite as rapidly as for material A. For material B, therefore, the transverse crack propagation mode never occurs, and all fatigue and residual failures will be due to axial crack propagation. The resulting residual strength versus number of cycles for material B is seen to increase as shown in Figure C-3b.

The computation of axial "crack" length α, with number of cycles is illustrated in Figure G-4 for both materials A and B.

The curves of axial crack length versus applied stress are plotted for properties at 1, 10^2, and 10^3 fatigue cycles. As discussed in the main text, the axial crack length at any given number of cycles is obtained from the intersection of the α versus σ curve with the line representing the maximum cyclic stress. The resulting axial crack length growth with number of cycles is shown in Figure G-5. Material A exhibits very little crack growth until after 10^2 cycles. It then develops a fast running crack as the number of cycles approaches 10^3. At this point, the axial crack propagates to infinity, causing failure. For material B, stable crack growth is observed out past 10^3 cycles.

To facilitate comparison of effect of notch size in [0] B/Ep laminates, static failure analysis results were plotted for a 2.54 cm notch. The results are shown in Figure G-6. A direct comparison point by point for given sets of laminate shear properties show that larger notch size generally weakens the strength of the material in the axial crack propagation mode and makes failure by transverse crack propagation considerably less likely. These results are true both for static failure and fatigue failure.

Discussion.- It is emphasized that the preceding examples of unidirectional fatigue behavior are examples only, and the material behavior in axial shear which has been utilized in the examples is hypothetical. It must not be taken as even an estimate of the actual laminate behavior. The example does serve to illustrate that different fatigue behavior for notched composites is predictable from the mathematical models. It is also noted that the variations of σ_A, σ_{SCFM}, and σ_M with axial shear material properties (Figures G-2 and G-6) are valid predictions. They provide a method of comparison of notched composite behavior for different notch sizes, as discussed previously.

Multidirectional Systems

The primary region of material degradation in a notched composite laminate is the region immediately surrounding the notch.

In the example presented here, the axial shear stress is assumed to dominate the notched composite behavior, and the axial tensile stress is neglected (Appendix D). Following a short discussion of the differences between unidirectional and multidirectional laminate behavior, an example is then given for fatigue behavior of a notched boron/epoxy $[0_2/\pm45]$ laminate using assumed unidirectional layer material behavior.

Differences between unidirectional and multidirectional laminates.- In addition to failure mode differences between [0] and multidirectional laminates there are major differences between the two types of laminate which are important from a fatigue standpoint. These differences relate mainly to the kinds of layer fatigue and failure information necessary to predict laminate fatigue behavior.

A [0] laminate under axial tension has no fibers extending across the axial crack which is growing from the notch. The behavior of this laminate in axial shear, therefore, is primarily matrix controlled (although the fibers contribute by their presence through geometrical factors). Since unnotched 0° specimens generally exhibit excellent fatigue characteristics, degradation of a unidirectional notched laminate due to the tensile stresses present will be minimal, and axial shear fatigue behavior will dominate. Unidirectional laminate axial shear properties can be determined approximately from tensile tests of a [±45] unnotched laminate.

In a $[0_i/\pm45_j/90_k]$ laminate, on the other hand, the presence of many ±45° fibers will significantly increase the shear stiffness of the laminate. Considerable tensile stresses will now be felt in the fiber direction of the ±45° layers. Also, due to the constraining effect of the ±45° layers, shear stress levels in the 0 and 90° layers will be small and transverse normal stresses will dominate (see Appendix D). Although layer axial tensile properties are less affected by fatigue loading than layer transverse tensile properties, the axial stress levels in the ±45° layers are also

considerably higher than the shear stresses in the 0 and 90° layers. Therefore, consideration must be given to the axial tensile and transverse tensile fatigue characteristics of layers as well as the axial shear fatigue characteristics.

Example.- To illustrate the application of the foregoing fatigue model analysis to notched composite laminates, a boron/epoxy $[0_2/\pm45]$ laminate will be analyzed. The laminate is assumed to contain a 2.54cm slit notch. Since at this time incomplete experimental data are available, hypothetical variations of tensile and shear properties will be assumed. It will also be assumed in the present example that the axial Young's modulus of a layer, E_{11}, does not change significantly with cyclic loading. It will, however, be assumed that the axial tensile strength of a unidirectional layer does exhibit some degradation as shown in Figure G-7. The curve shown for fatigue lifetime has been taken from experimental data presented in Reference 2, but the residual strength curves associated with the S-N curve are hypothetical. In axial shear, σ_{12}, the behavior shown for residual strength and fatigue lifetime has been approxmiated from tests presented in Reference 2 and from an S-N curve for epoxy material alone in tension shown in Reference 10. While an attempt was made to fabricate as realistic a curve as possible, these numbers must be regarded as purely hypothetical. The curve shown for variation of axial shear modulus G_{12} with N has been estimated from scanty data presented in Reference 2. Again, this curve must be regarded as hypothetical.

The results of the failure analysis are shown in Figure G-8 for the axial and transverse crack propagation modes. Increments for fatigue property variations were chosen as shown in Table G-1. It was assumed for simplicity's sake that σ^n does not contribute to fatigue degradation. The results of the fatigue analysis for each layer are also shown in Table G-1. Predictions of laminate properties from layer properties are presented along with resulting failure stresses in the axial and transverse crack propagation

modes. The variations of laminate axial shear properties with number of cycles are shown plotted in Figure G-8.

For off-axis cracking, static failure analysis results for $\sigma_{A'}$ are shown in Figure G-9 for the laminate. Note that for off-axis analysis purposes, the laminate is now a $[0/\pm 45_2/90]$ laminate with a 1.9cm slit notch. To determine the degradation of x'y' shear properties during cyclic loading, the method of effective shear stress at the notch root was selected, equation (E1). The value of the average effective notch shear stress as computed from equation (E1) is shown in Table G-2 along with the results of the laminate and fatigue property degradation analyses for each increment in cyclic loading considered. Also shown in this table are the resulting laminate properties at each incremental cycle, and the resulting residual strength of the notched composite in the off-axis propagation mode. Laminate properties as a function of number of cycles are also plotted in Figure G-9 to illustrate their effect on off-axis strength. It is noted that $\tau^{\circ}_{e}{}'$, not $\tau^{\circ}{}'$, is plotted in this figure, since it is the effective reduced shear strength which controls notched laminate behavior.

As seen from the numbers tabulated in Tables G-1 and G-2, and the graphs in Figures G-8 and G-9, the off-axis propagation mode and the transverse crack propagation mode never occur for this laminate. The failure mode for initial static failure through the fatigue lifetime of the notched laminate is axial crack propagation. The resulting residual strength versus N curve is shown in Figure G-10. Note that, initially, the strength of the notched laminate increases with the number of cycles, due to a beneficial stress redistribution inside the laminate caused by decreasing shear modulus in 0° and 90° layers. Static residual failure in this region is due to a shear failure in the laminate which has been initiated by transverse tensile failure in the -45° layers. After approximately 10^2 cycles, the residual strength of the laminate begins to decrease until it reaches the cyclic maximum stress at approximately 5×10^6 cycles, which is the notched laminate fatigue lifetime, N_f. The decreasing

portion of the residual strength curve is due to laminate axial shear failure precipitated by axial tensile failure of the +45° layers.

Figure G-11 shows how key elastic and strength properties degrade for this particular laminate as a function of number of cycles. In this case, it is seen that the laminate axial modulus, E_x and the axial shear modulus, G_{xy}, do not vary significantly with fatigue loading. The maximum change is within a few percent. On the other hand, the axial shear strength has degraded considerably and is the main cause of laminate fatigue failure in this situation. Although this example is based upon hypothetical behavior for layer fatigue, it serves to illustrate that a comprehensive analysis can be performed provided that the proper input information is available. Also, the example shows that the assumption of a constant laminate axial Young's modulus remains valid as long as the axial Young's modulus of a layer does not significantly change with fatigue loading.

As a means of assessing the effect of notch size on the static and fatigue failure behavior of a $[0_2/\pm45]$ boron/epoxy laminate, the results of the static failure analysis for a 0.64cm notch with varying $\tau°$ and G_{xy} are presented in Figures G-12 and G-13. Although the fatigue example is not redone here, it is seen by comparing strength properties on a point by point laminate input property basis that the laminate with the smaller notch size is generally the stronger. A complete comparison for fatigue behavior must await valid input data and resulting re-analysis of both the 2.54 and 0.64cm notch laminates.

TABLE G-1

LAMINATE AND FATIGUE ANALYSIS RESULTS FOR
$[0_2/\pm 45]$ B/Ep, 2.54 cm. NOTCH
AXIAL/TRANSVERSE CRACK MODES
$S = 0.85$, $\tau^n = 243$ MN/m^2

	No. of Cycles N	1	10^2	10^3	10^4	10^6	N_f 5 x 10^6
Laminate Elastic Properties GN/m^2	E_x	112	111.5	110.4	109.9	109.3	109.2
	G_{xy}	28.6	28.4	27.97	27.80	27.60	27.50
Unnotched Laminate Failure Stresses MN/m^2	σ_x^t	710	705	697	694	689	688
	τ°	285	359	351	339	284	246
Notched Laminate Failure Stresses MN/m^2	σ_A	250	324	317	310	255	217
	σ_{SCFM}	545	690	676	648	538	469
	σ_T	Since $\sigma_{SCFM} < \sigma_x^t$, trans crack never occurs					

TABLE G-2

LAMINATE AND FATIGUE ANALYSIS RESULTS FOR
$[0_2/\pm 45]$ B/Ep, 2.54 cm. NOTCH OFF-AXIS CRACK MODE
$S = 0.85$, $\tau_e^{n'} = 161$ MN/m^2

	No. of Cycles	1	10^2	10^4	10^6	10^8
Laminate Elastic Properties	$E_{x'}$ (GN/m^2)	65.55	65.30	64.43	64.09	63.45
	$E_{y'}$ (GN/m^2)	65.55	65.30	64.43	64.09	63.45
	$\nu_{x'y'}$	0.146	0.144	0.139	0.137	0.133
	$G_{x'y'}$ (GN/m^2)	18.88	18.79	18.44	18.31	18.05
Unnotched Laminate Failure Stresses	$\sigma_{x'}^t$ (MN/m^2)	266	280	315	312	306
	$*\tau^{o'}$ (MN/m^2)	416	415	411	409	397
x' Axial Failure Stress	$\sigma_{A'}$ (MN/m^2)	175.8	179.3	184.8	183.4	179.3
Laminate Tensile Failure Stress Off-Axis Mode	σ_{45} (MN/m^2)	351.6	358.5	369.6	366.8	358.5

$*\tau_e^{o'}$ (not presented in this table) is used in failure computations, Figure G-9).

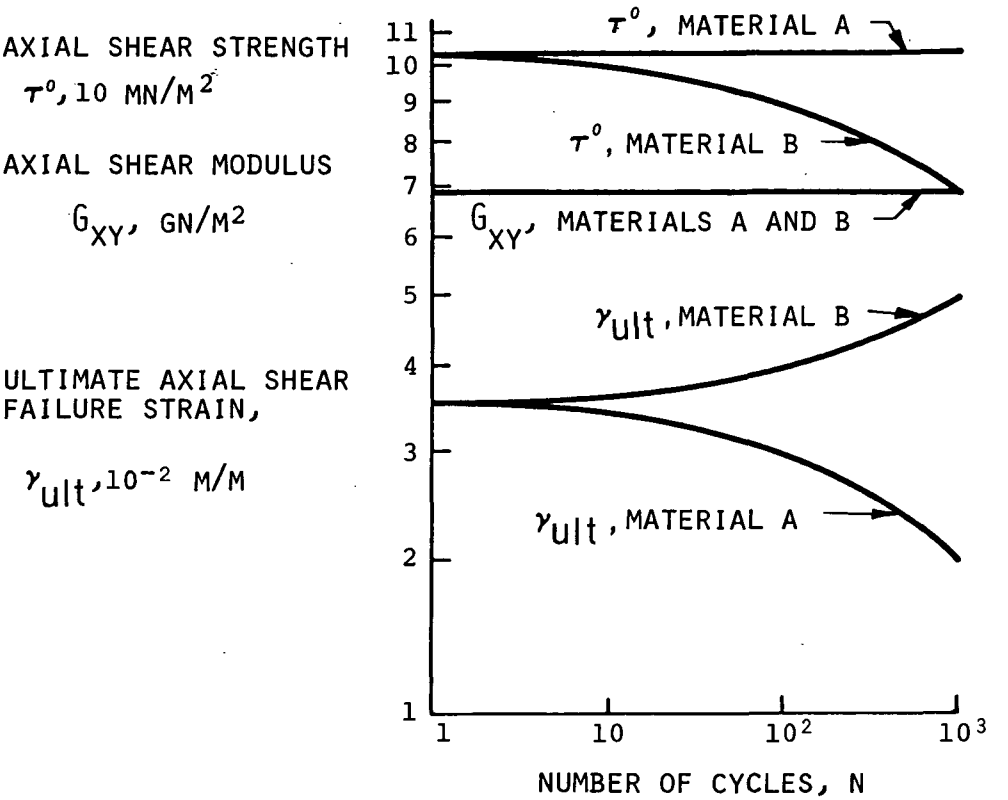

FIGURE G-1. SHEAR PROPERTY DEGRADATION FOR HYPOTHETICAL MATERIALS A AND B. CYCLIC LOADING AT σ_{XY} = 76 MN/M^2.

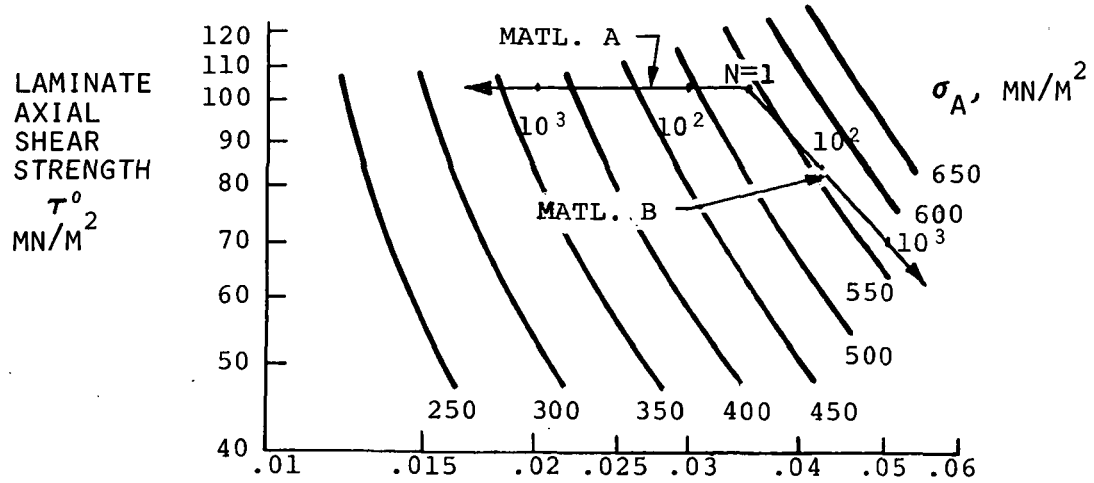

(a) NOTCHED LAMINATE TENSILE STRENGTH, σ_A, AXIAL CRACK FAILURE MODE.

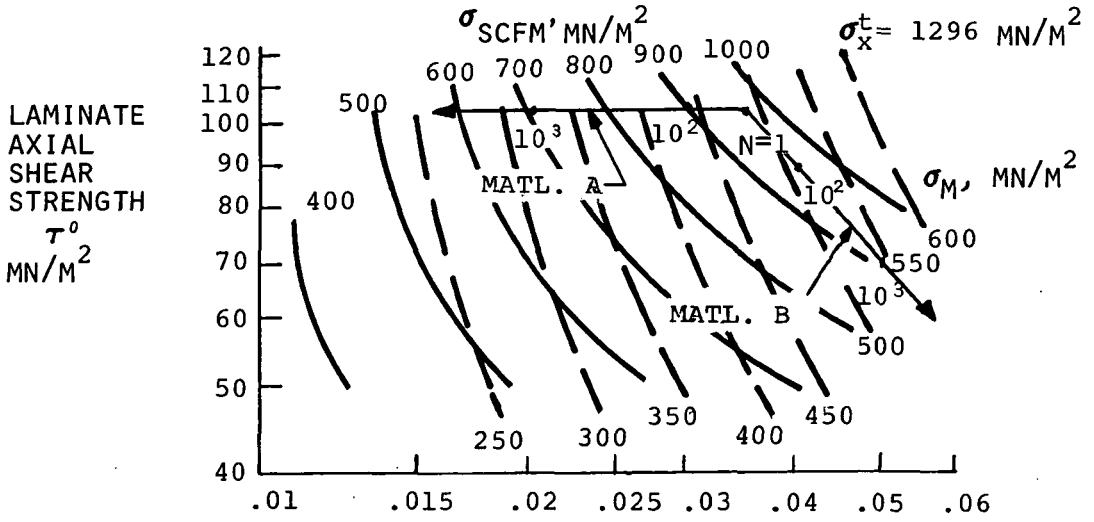

(b) COMPOSITE OVERSTRESS IN MATERIAL ADJACENT TO NOTCH, σ_{SCFM}, AND CORRESPONDING FAR FIELD APPLIED GROSS STRESS, σ_M.

FIGURE G-2. STATIC AND FATIGUE BEHAVIOR OF BORON/EPOXY [0] NOTCHED LAMINATE. NOTCH SIZE = 0.64 CM . σ_{MAX} = 400 MN/M^2.

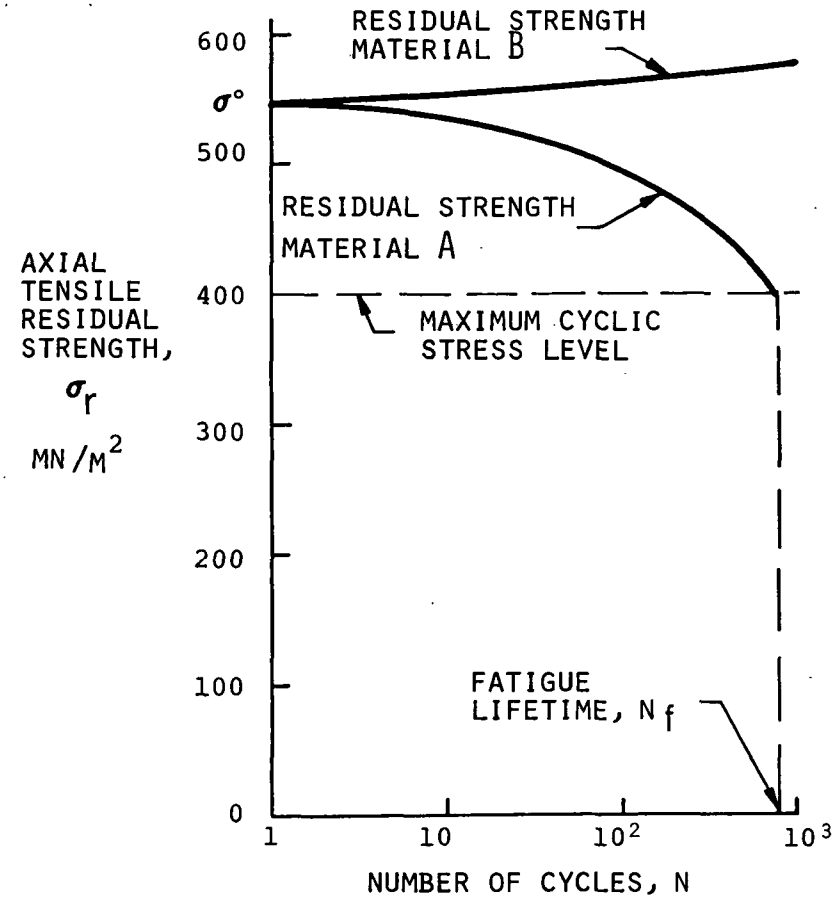

FIGURE G-3. RESIDUAL STRENGTH AND LIFETIME FOR 0.64 CM NOTCHED HYPOTHETICAL [0] B/Ep LAMINATE CYCLED AT S = 0.735.

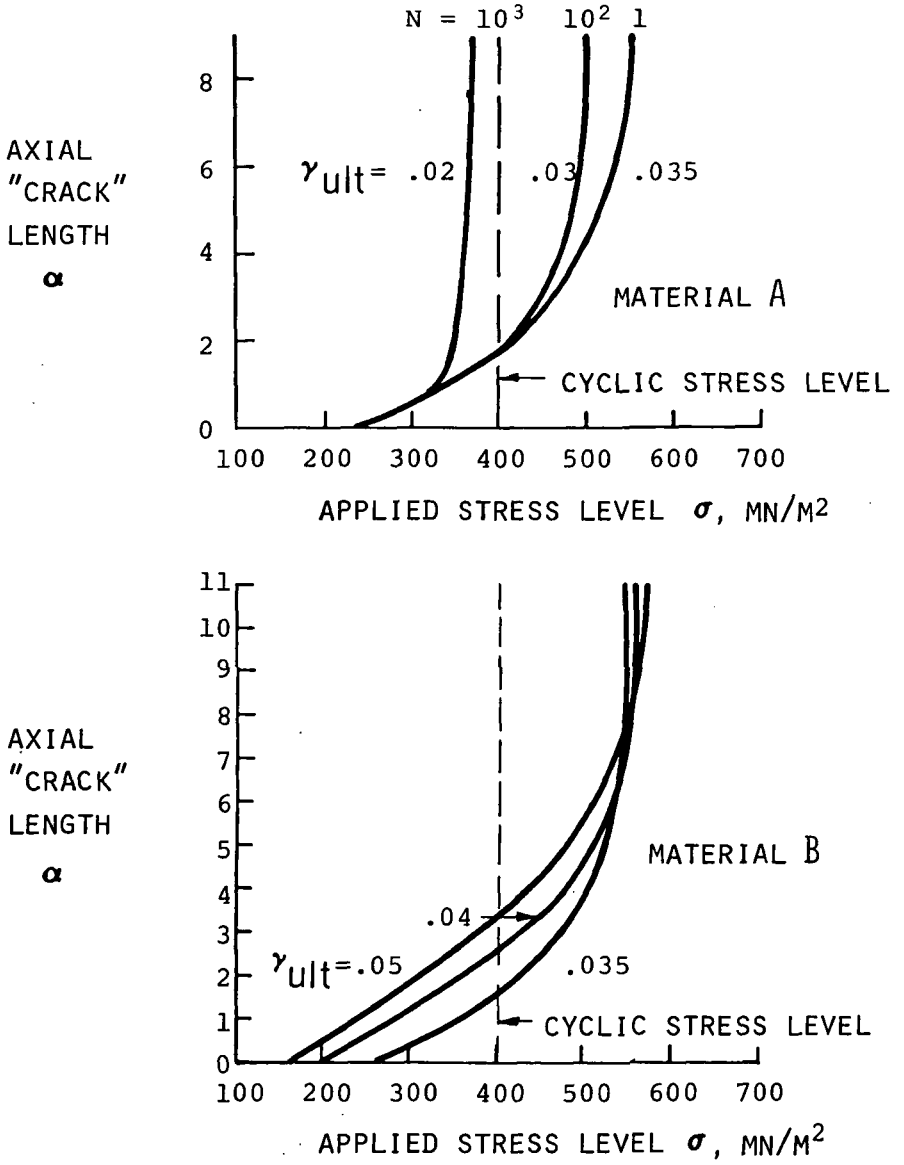

FIGURE G-4. STATIC AXIAL "CRACK" GROWTH FOR 0.64 CM NOTCHED [0] B/EP LAMINATES COMPOSED OF HYPOTHETICAL MATERIALS A AND B HAVING PROPERTIES WHICH EXIST AFTER CYCLING AT σ = 400 MN/M^2 FOR 1, 10^2, AND 10^3 CYCLES.

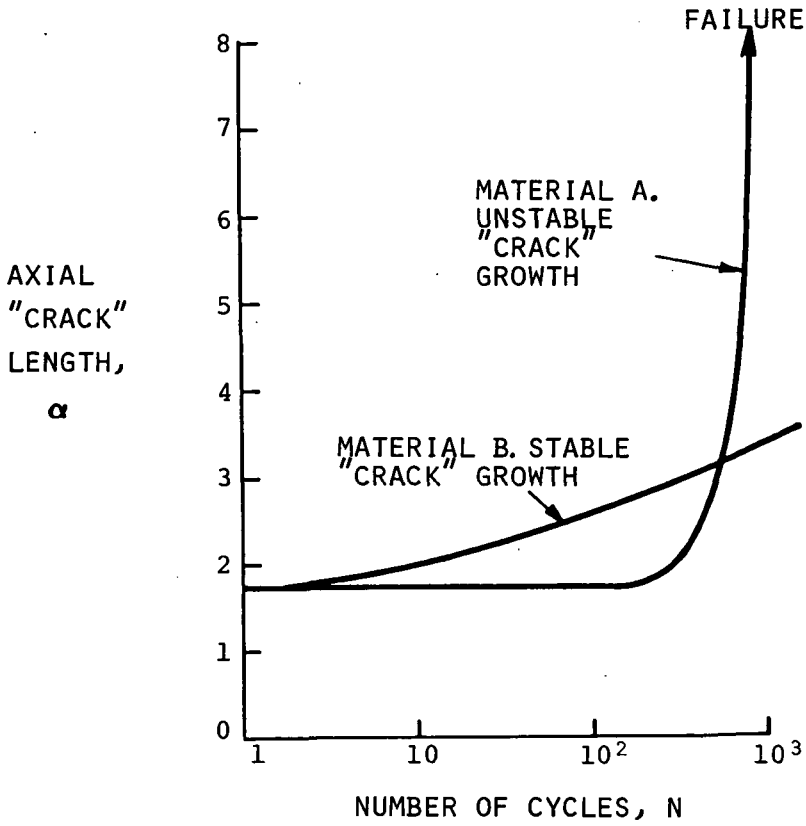

FIGURE G-5. PREDICTED FATIGUE AXIAL "CRACK" GROWTH FOR 0.64 CM NOTCHED [0] B/E_p LAMINATE COMPOSED OF HYPOTHETICAL MATERIALS A AND B HAVING PROPERTIES WHICH EXIST AFTER CYCLING AT σ_{MAX} = 400 MN/M².

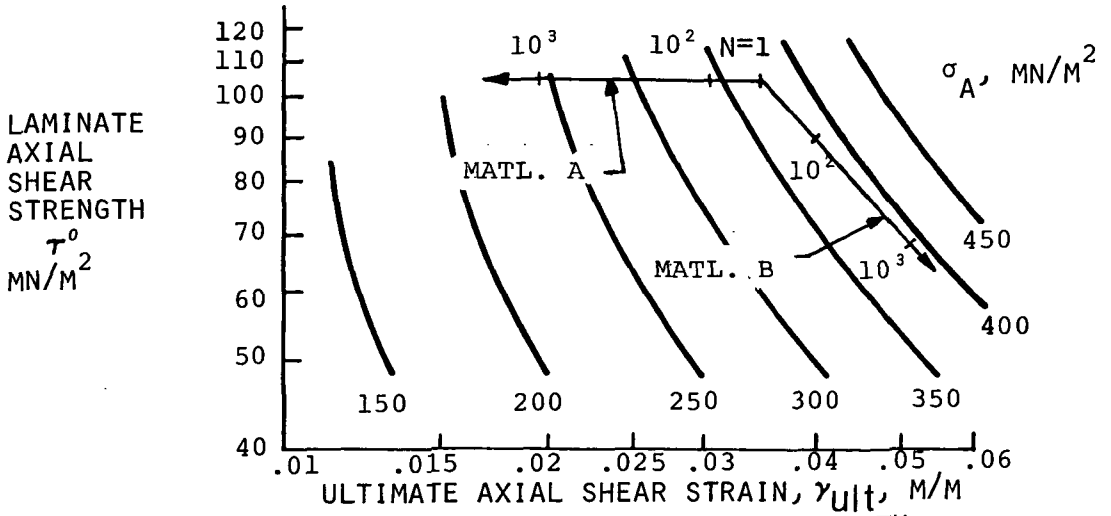

(a) NOTCHED LAMINATE TENSILE STRENGTH, σ_A, AXIAL CRACK FAILURE MODE.

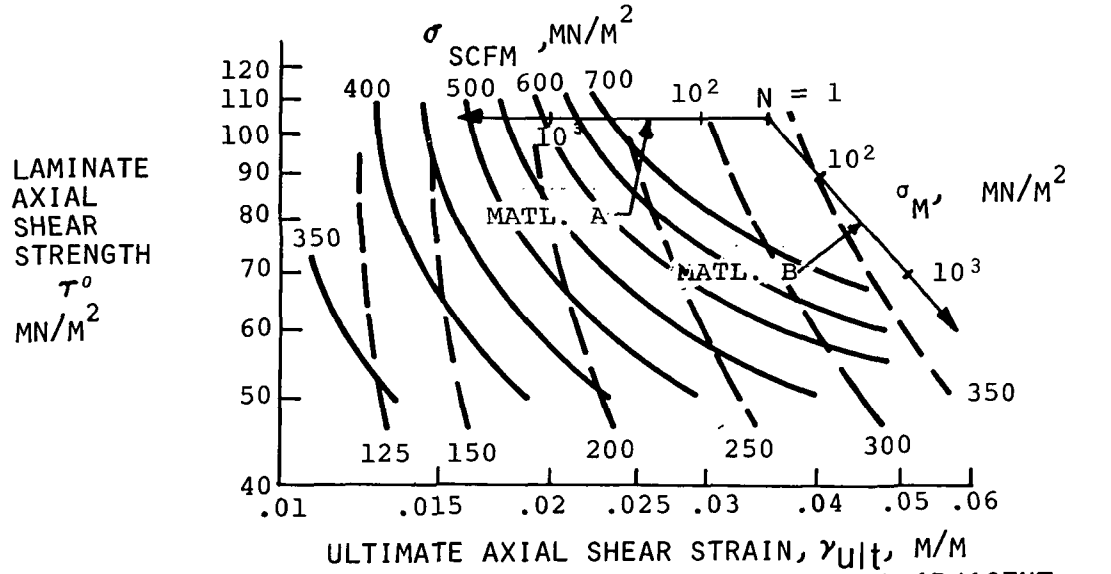

(b) COMPOSITE OVERSTRESS IN MATERIAL ADJACENT TO NOTCH, σ_{SCFM}, AND CORRESPONDING FAR FIELD APPLIED GROSS STRESS, σ_M.

FIGURE G-6. STATIC AND FATIGUE BEHAVIOR OF BORON/EPOXY [0] LAMINATE, NOTCH SIZE = 2.54 CM.

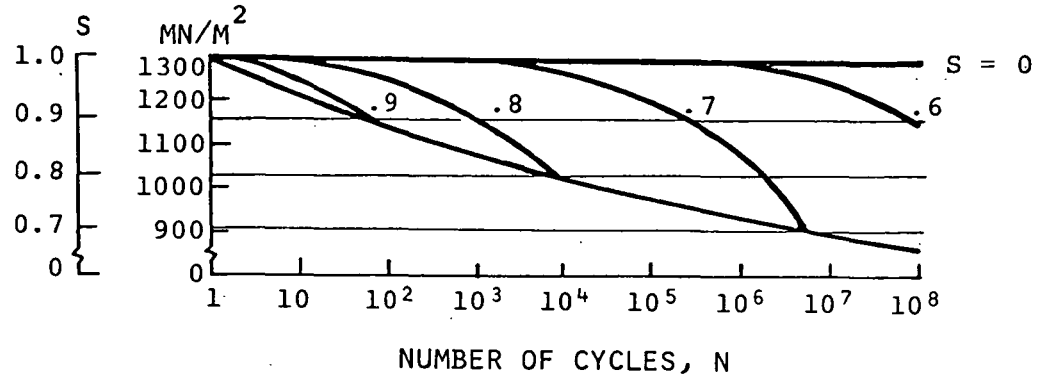

(a) AXIAL TENSILE STRENGTH, σ_{11}

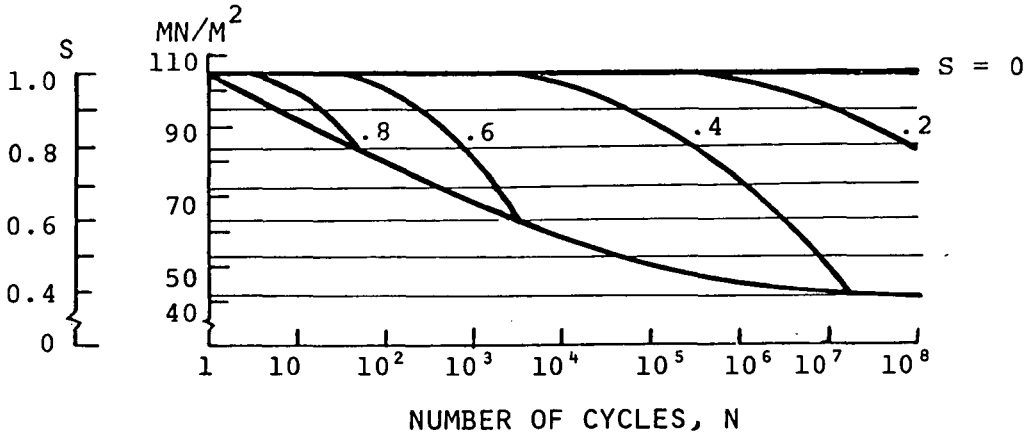

(b) AXIAL SHEAR STRENGTH, σ_{12}

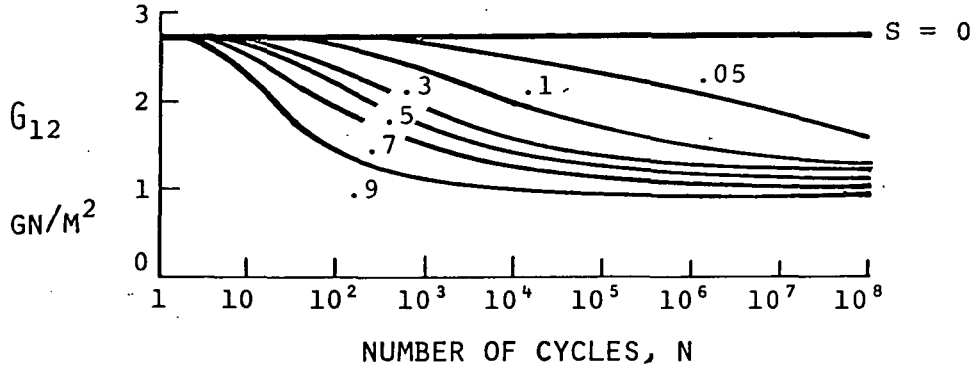

(c) AXIAL SECANT SHEAR MODULUS, G_{12}

FIGURE G-7. HYPOTHETICAL VARIATIONS OF FATIGUE BEHAVIOR AND LIFETIME OF [0] BORON/EPOXY

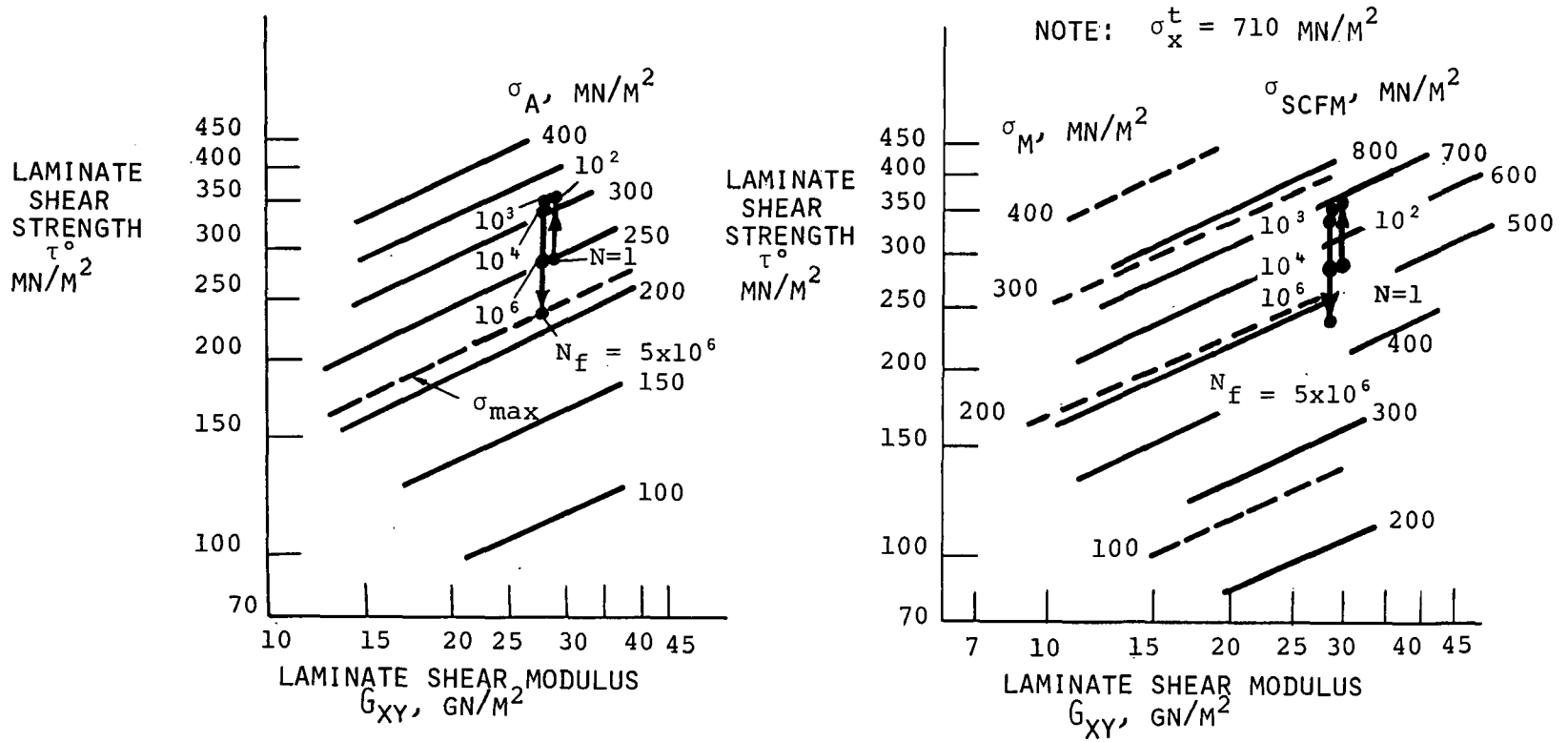

(a) NOTCHED LAMINATE TENSILE STRENGTH σ_A, AXIAL CRACK FAILURE MODE

(b) COMPOSITE OVERSTRESS NEAR NOTCH, σ_{SCFM}, AND CORRESPONDING FAR FIELD APPLIED GROSS STRESS, σ_M

FIGURE G-8. STATIC AND FATIGUE BEHAVIOR OF BORON/EPOXY [$0_2/\pm45$] NOTCHED LAMINATE. NOTCH SIZE = 2.54 CM

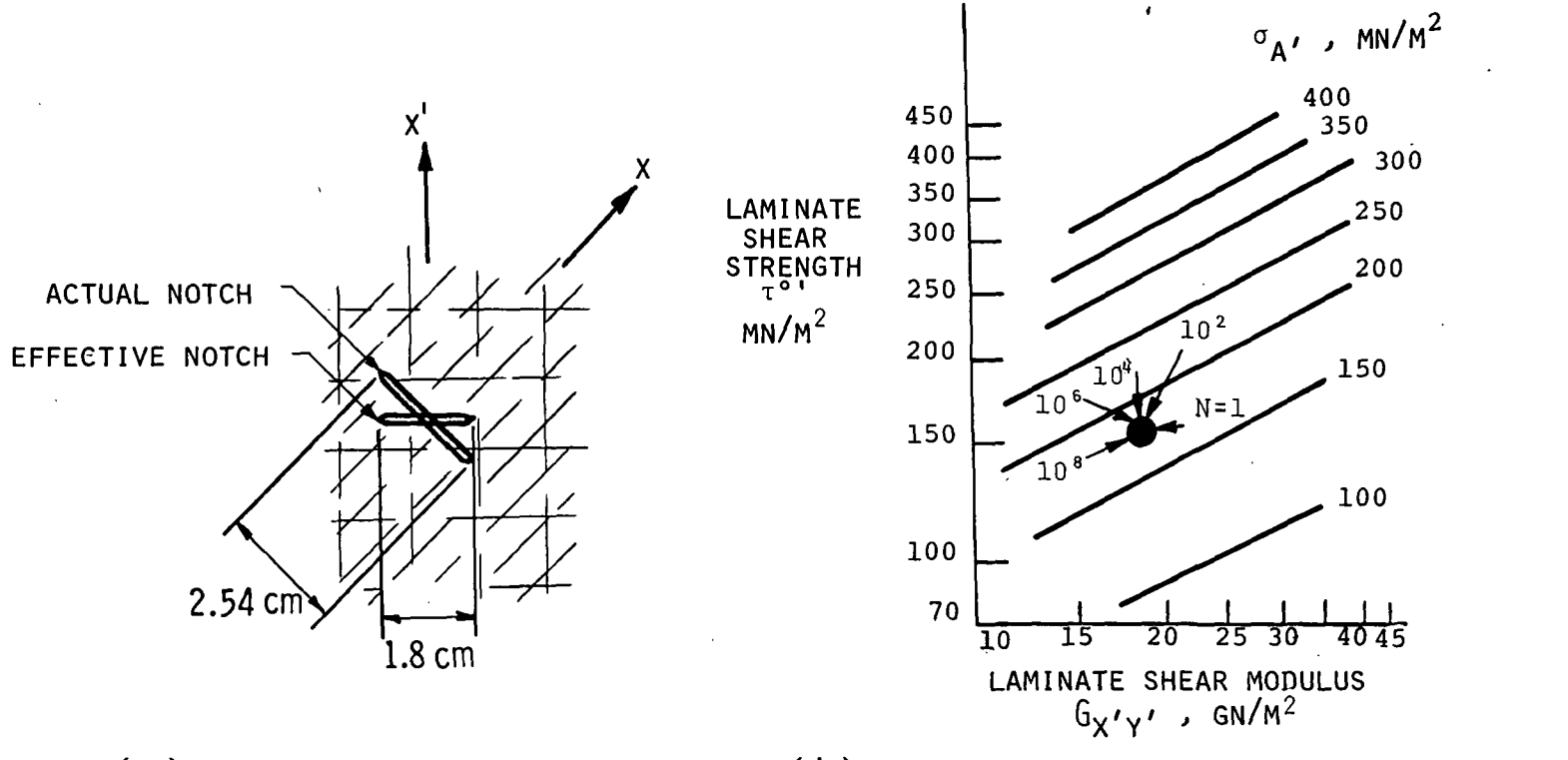

(a) EQUIVALENT AXIAL PROBLEM FOR OFF-AXIS FAILURE

(b) NOTCHED LAMINATE TENSILE STRENGTH, $\sigma_{A'}$, AXIAL CRACK FAILURE MODE IN X'Y' SYSTEM

FIGURE G-9. OFF-AXIS FATIGUE BEHAVIOR OF $[0_2/\pm45]$ SLIT NOTCHED LAMINATE. NOTCH SIZE = 2.54 CM

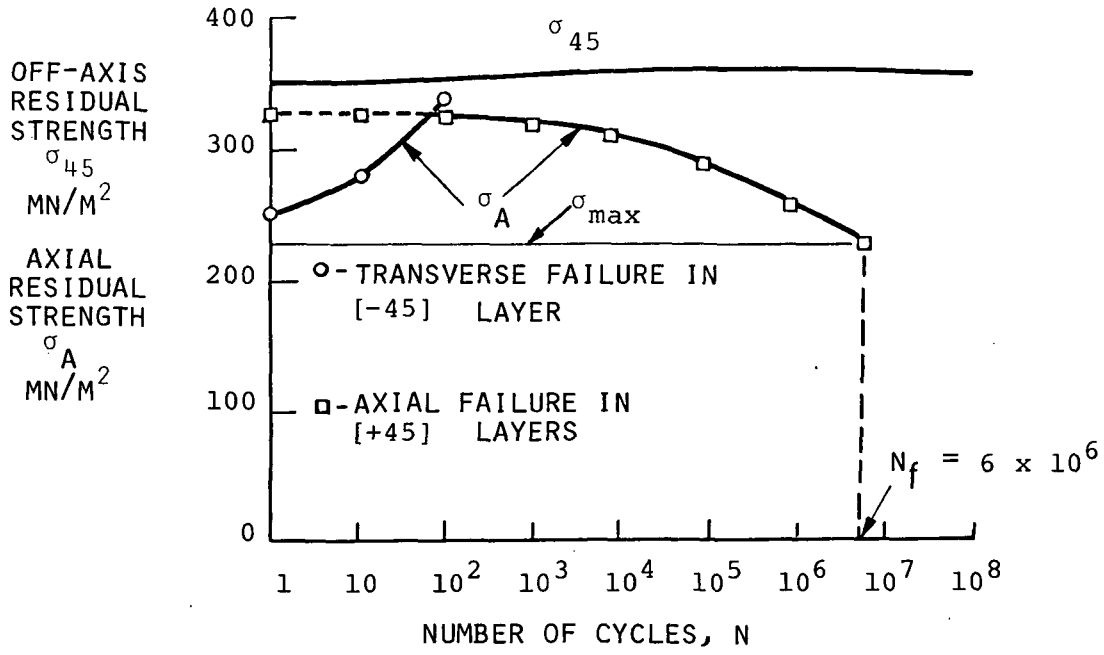

FIGURE G-10. RESIDUAL STRENGTH OF NOTCHED [0_2/±45] BORON/ EPOXY LAMINATE CYCLED AT S = 0.85 . NOTCH SIZE = 2.54 cm

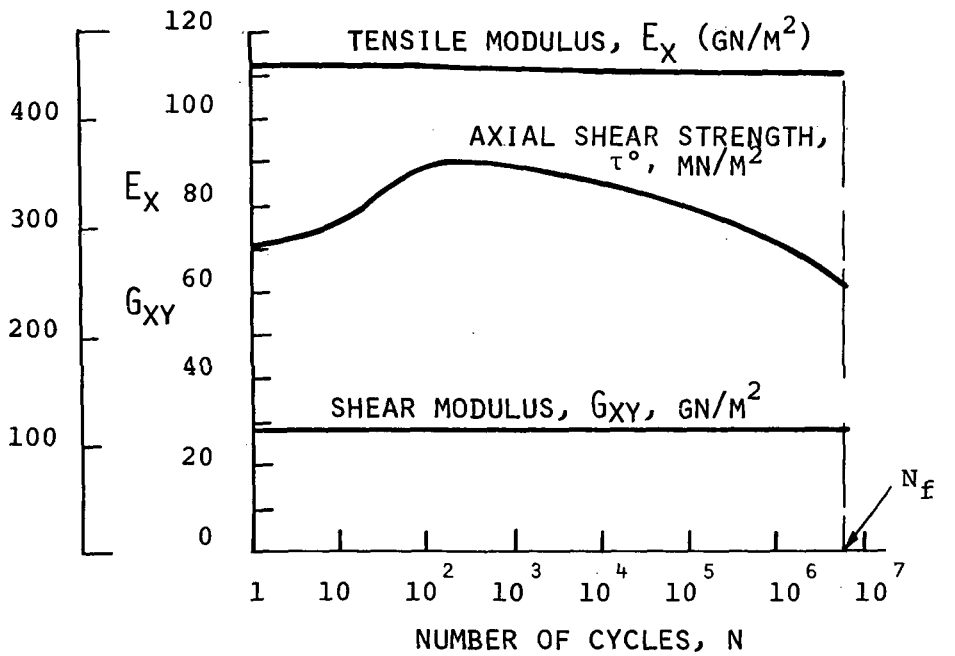

FIGURE G-11. PREDICTED LAMINATE AXIAL MODULI AND SHEAR STRENGTH OF NOTCHED [0_2/±45] BORON/EPOXY LAMINATE CYCLED AT S = 0.85. NOTCH SIZE = 2.54 CM

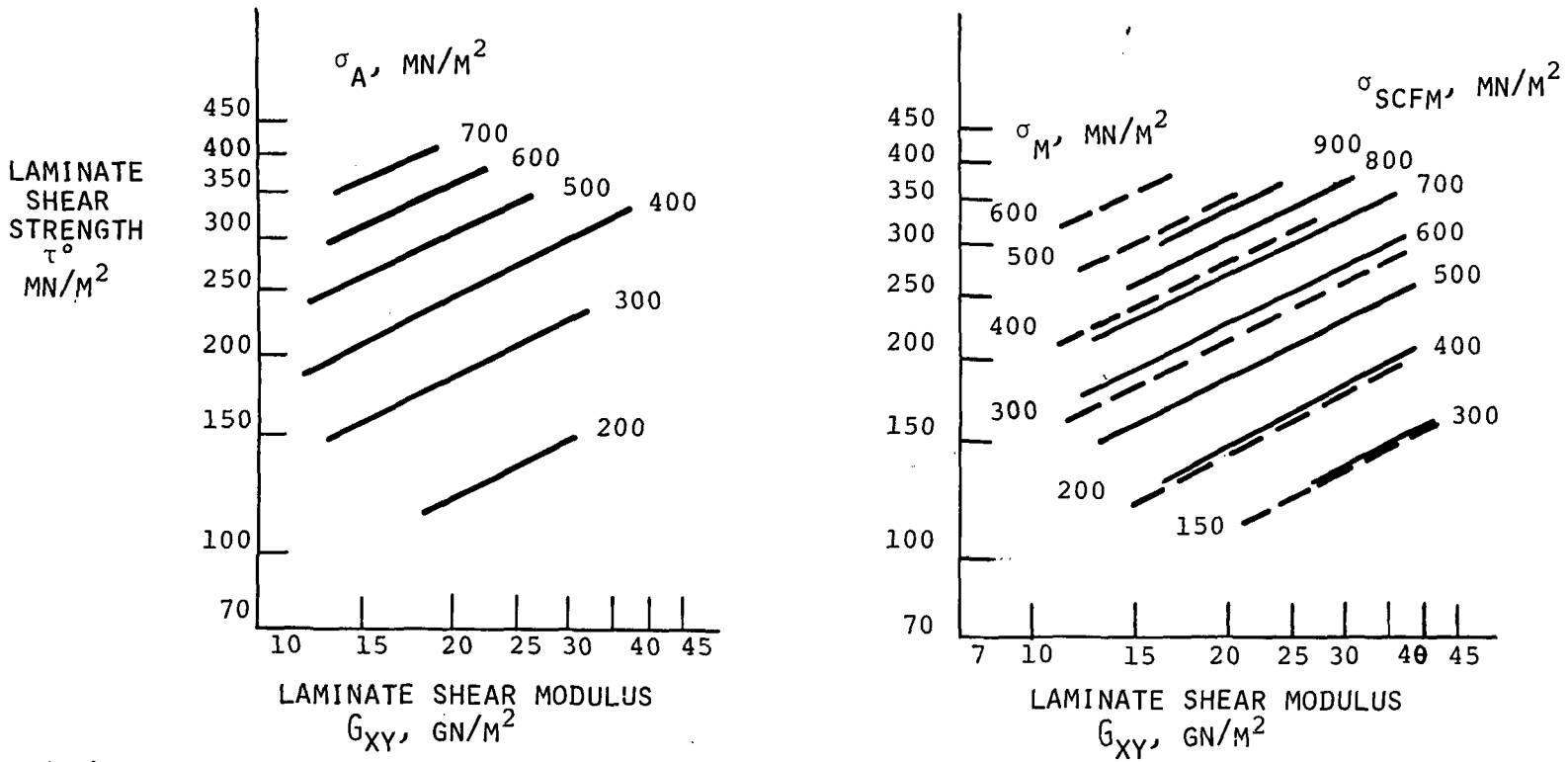

(a) NOTCHED LAMINATE TENSILE STRENGTH, σ_A, AXIAL CRACK FAILURE MODE

(b) COMPOSITE OVERSTRESS NEAR NOTCH, σ_{SCFM}, AND CORRESPONDING FAR FIELD APPLIED STRESS, σ_M

FIGURE G-12. AXIAL AND TRANSVERSE FATIGUE BEHAVIOR OF BORON/EPOXY [0_2/±45] NOTCHED LAMINATE. NOTCH SIZE = 0.64 CM

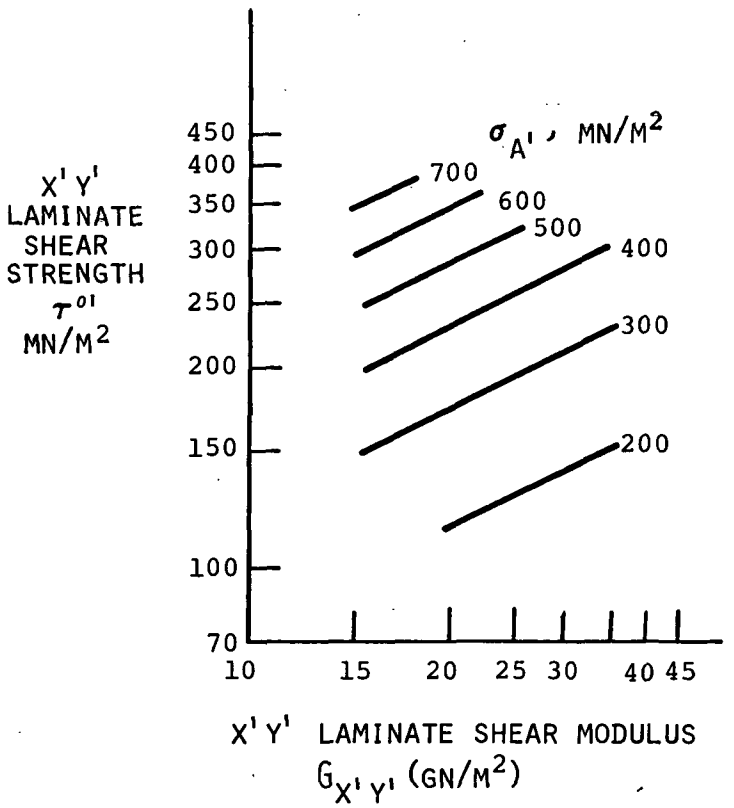

FIGURE G-13. OFF-AXIS FATIGUE BEHAVIOR OF BORON/EPOXY $[0_2/\pm45]$ LAMINATE WITH SLIT NOTCH. NOTCH SIZE = 0.64 CM (EQUIVALENT NOTCH IN X'Y' COORDINATE SYSTEM = 0.45 CM)

REFERENCES

1. Halpin, J. C., Jerina, K. L., and Johnson, T. A.: Characterization of Composites for the Purpose of Reliability Evaluation. Analysis of the Test Methods for High Modulus Fibers and Composites, ASTM STP521, 1973, pp. 5-64.

2. Durchlaub, E. C., and Freeman, R. B.: Design Data for Composite Structure Safelife Prediction. AFML-TR-73-225, March, 1974.

3. Wu, E. M.: Fracture Mechanics of Anisotropic Plates. Tsai, S. W., Halpin, J. C., and Pagano, N. J., eds: Composite Materials Workshop. Technomic Publication, 1968, pp. 20-43.
-see also-
Beaumont, P. W. R., and Phillips, D. C.: Tensile Strength of Notched Composites. Journal of Composite Materials, Vol. 6, 1972, pp. 32-46.
-see also-
Beaumont, P. W. R., and Tetelman, A. S.: The Fracture Strength and Toughness of Fibrous Composites. UCLA-ENG-7269, 1972.

4. Sih, G. C., and Chen, E. P.: Fracture Analysis of Unidirectional Composites. Journal of Composite Materials, Vol. 7, 1973, pp. 230-244.

5. Marcus, L. A., and Stinchcomb, W. W.: Measurement of Fatigue Damage in Composite Materials. Experimental Mechanics, February, 1975, pp. 55-60.

6. Kulkarni, S. V., and Rosen, B. Walter: Design Data for Composite Structure Safelife Prediction: Analysis Evaluation. TFR/2221, Materials Sciences Corporation, August, 1973. see also Reference 2.

7. Tsai, S. W., and Wu, E. M.: A General Theory of Strength for Anisotropic Materials. Journal of Composite Materials, Vol. 5, 1971, p. 58.

8. McLaughlin, P. V., Jr., and Rosen, B. Walter: Combined Stress Effects upon Failure of Fiber Composites. Final Report, Contract No. N62269-73-C-0800, NADC. Materials Sciences Corporation, April, 1974.

9. Hashin, Z., and Rotem, A.: A Fatigue Failure Criterion for Fiber Reinforced Materials. Journal of Composite Materials, Vol. 7, 1973, pp. 448-464.

10. Advanced Composites Design Guide, AFML, January, 1974.

LIBRARY-CARD ABSTRACT

This report describes the development of a semi-empirical analysis for prediction and correlation of fatigue crack growth, residual strength, and fatigue lifetime for fiber composite laminates containing notches. The analysis is based upon experimentally observed failure modes and predicts notched laminate failure from unidirectional layer tensile and shear fatigue properties. Examples are given for [0] and multidirectional laminates which illustrate application of the method.